

# Anatomy of $F_D$ -Term Hybrid Inflation

BJÖRN GARBRECHT<sup>a</sup>, CONSTANTINOS PALLIS<sup>a</sup> AND APOSTOLOS PILAFTSIS<sup>a,b</sup>

<sup>a</sup>*School of Physics and Astronomy, University of Manchester,  
Manchester M13 9PL, United Kingdom*

<sup>b</sup>*CERN, Physics Department, Theory Division, CH-1211 Geneva 23, Switzerland*

## ABSTRACT

We analyze the cosmological implications of  $F$ -term hybrid inflation with a subdominant Fayet–Iliopoulos  $D$ -term whose presence explicitly breaks a  $D$ -parity in the inflaton-waterfall sector. This scenario of inflation, which is called  $F_D$ -term hybrid model for brevity, can naturally predict lepton number violation at the electroweak scale, by tying the  $\mu$ -parameter of the MSSM to an  $SO(3)$ -symmetric Majorana mass  $m_N$ , via the vacuum expectation value of the inflaton field. We show how a negative Hubble-induced mass term in a next-to-minimal extension of supergravity helps to accommodate the present CMB data and considerably weaken the strict constraints on the theoretical parameters, resulting from cosmic string effects on the power spectrum  $P_{\mathcal{R}}$ . The usual gravitino overabundance constraint may be significantly relaxed in this model, once the enormous entropy release from the late decays of the ultraheavy waterfall gauge particles is properly considered. As the Universe enters a second thermalization phase involving a very low reheat temperature, which might be as low as about 0.3 TeV, thermal electroweak-scale resonant leptogenesis provides a viable mechanism for successful baryogenesis, while thermal right-handed sneutrinos emerge as new possible candidates for solving the cold dark matter problem. In addition, we discuss grand unified theory realizations of  $F_D$ -term hybrid inflation devoid of cosmic strings and monopoles, based on the complete breaking of an  $SU(2)_X$  subgroup. The  $F_D$ -term hybrid model offers rich particle-physics phenomenology, which could be probed at high-energy colliders, as well as in low-energy experiments of lepton flavour or number violation.

# Contents

<b>1</b>	<b>Introduction</b>	<b>1</b>
<b>2</b>	<b>General Setup</b>	<b>5</b>
2.1	The Model . . . . .	5
2.2	Radiative Lifting of MSSM Flat Directions . . . . .	9
2.3	Topological Defects and GUT Embeddings . . . . .	13
<b>3</b>	<b>Inflation</b>	<b>16</b>
3.1	Basic Formalism . . . . .	16
3.2	Numerical results . . . . .	19
3.2.1	The minimal SUGRA scenario . . . . .	21
3.2.2	The next-to-minimal SUGRA scenario . . . . .	24
<b>4</b>	<b>Preheating</b>	<b>27</b>
4.1	<i>D</i> -Parities and the Inflaton-Waterfall Sector . . . . .	29
4.2	Preheating and Thermalization . . . . .	36
<b>5</b>	<b>Coupled Reheating and Gravitino Abundance</b>	<b>39</b>
5.1	Boltzmann Equations . . . . .	40
5.2	Semi-analytic Approach . . . . .	43
5.3	Gravitino Abundance Constraints . . . . .	45
<b>6</b>	<b>Baryon Asymmetry and Cold Dark Matter</b>	<b>48</b>
6.1	Resonant Flavour-Leptogenesis at the Electroweak Scale . . . . .	48
6.2	Thermal Right-Handed Sneutrinos as CDM . . . . .	52
<b>7</b>	<b>Conclusions</b>	<b>54</b>
<b>A</b>	<b>Mechanisms of Explicit <i>D</i>-Parity Breaking</b>	<b>59</b>
A.1	<i>D</i> -Parity Breaking in the $U(1)_X$ Waterfall-Gauge Sector . . . . .	59
A.2	<i>D</i> -Parity Breaking in the $SU(2)_X$ Waterfall-Gauge Sector . . . . .	61

# 1 Introduction

Standard big-bang cosmology faces severe difficulties in accounting for the observed flatness and enormity of the causal horizon of today's Universe. It also leaves unexplained the origin of the nearly scale-invariant cosmic microwave background (CMB), as was found by a number of observations over the last decade [1–5]. All these pressing problems can be successfully addressed within the field-theoretic framework of inflation [6]. As a source of inflation, it is usually considered to be a scalar field, the inflaton, which is displaced from its minimum and whose slow-roll dynamics leads to an accelerated expansion of the early Universe. In this phase of accelerated expansion or inflation, the quantum fluctuations of the inflaton field are stretched on large scales and eventually get frozen when they become much bigger than the Hubble radius. These quantum fluctuations get imprinted in the form of density perturbations, when the former are crossing back inside the Hubble radius long after inflation has ended. In this way, inflation provides a causal mechanism to explain the observed nearly-scale invariant CMB spectrum.

A complete description of the CMB spectrum involves about a dozen of cosmological parameters, such as the power spectrum  $P_{\mathcal{R}}$  of curvature perturbations, the spectral index  $n_s$ , the running spectral index  $dn_s/d\ln k$ , the ratio  $r$  of tensor-to-scalar perturbations, the baryon-to-photon ratio of number densities  $\eta_B$ , the fractions of relic abundance  $\Omega_{\text{DM}}$  and dark energy  $\Omega_{\Lambda}$  and a few others. Recent WMAP data [2, 4], along with other astronomical observations [3], have improved upon the precision of almost all of the above cosmological observables. In particular, the precise values of these cosmological observables set stringent constraints on the model-building of successful models of inflation. To ensure the slow-roll dynamics of the inflaton, for example, one would need a scalar potential, which is almost flat. Moreover, one has to assure that the flatness of the inflaton potential does not get spoiled by large quantum corrections that depend quadratically on the cut-off of the theory. In this context, supersymmetry (SUSY), softly broken at the TeV scale, emerges almost as a compelling ingredient not only in the model-building of inflationary scenarios, but also for addressing technically the so-called gauge-hierarchy problem.

One of the most predictive and potentially testable scenarios of inflation is the model of hybrid inflation [7]. An advantageous feature of this model is that the inflaton  $\phi$  may start its slow-roll from field values well below the reduced Planck mass  $m_{\text{Pl}} = 2.4 \times 10^{18}$  GeV. As a consequence, cosmological observables, such as  $P_{\mathcal{R}}$  and  $n_s$ , do not generically receive significant contributions from possible higher-dimensional non-renormalizable operators, as these are suppressed by inverse powers of  $1/m_{\text{Pl}}$ . Thus, the hybrid model becomes very predictive and possibly testable, in the sense that the inflaton dynamics is mainly

governed by a few renormalizable operators which might have observable implications for laboratory experiments. In the hybrid model, inflation terminates through the so-called waterfall mechanism. This mechanism is triggered, when the inflaton field  $\phi$  passes below some critical value  $\phi_c$ . In this case, another field  $X$  different from  $\phi$ , which is called the waterfall field and is held fixed at origin initially, develops a tachyonic instability and rolls rapidly down to its true vacuum expectation value (VEV).

Hybrid inflation can be realized in supersymmetric theories in two forms. In the first form, the hybrid potential results from the  $F$ -terms of a superpotential, where the slope of the potential may come either from supergravity (SUGRA) corrections [8] and/or from radiative effects [9]. The second supersymmetric realization [10] of hybrid inflation uses a dominant Fayet–Iliopoulos (FI)  $D$ -term [11], which may originate from an anomalous local  $U(1)_Q$  symmetry within the context of string theories.

All models of inflation embedded in SUGRA have to address a serious problem. This is the so-called gravitino overabundance problem. If abundantly produced in the early Universe, gravitinos may disrupt, via their late gravitationally-mediated decays, the nucleosynthesis of the light elements. In order to prevent this from happening, gravitinos  $\tilde{G}$  must have a rather low abundance today, i.e.  $Y_{\tilde{G}} = n_{\tilde{G}}/s \lesssim 10^{-12}-10^{-15}$ , where  $n_{\tilde{G}}$  is the number density of gravitinos and  $s$  is the entropy density. The upper bound on  $Y_{\tilde{G}}$  depends on the properties of the gravitino and becomes tighter, if gravitinos decay appreciably to hadronic modes. These considerations set a strict upper bound on Universe’s reheat temperature  $T_{\text{reh}}$ , generically implying that  $T_{\text{reh}} \lesssim 10^{10}-10^7$  GeV [51,56]. This upper limit on  $T_{\text{reh}}$  severely restricts the size of any renormalizable superpotential coupling of the inflaton to particles of the Standard Model (SM). All these couplings must be rather suppressed. Typically, they have to be smaller than about  $10^{-5}$  [12].

The aforementioned gravitino constraint may be considerably relaxed, if there is a mechanism that could cause late entropy release in the evolution of the early Universe. Such a mechanism could then dilute the gravitinos to a level that would not upset the limits derived from Big Bang nucleosynthesis (BBN). This possibility might arise even within the context of  $F$ -term hybrid inflation, if a subdominant FI  $D$ -tadpole associated with the gauge group  $U(1)_X$  of the waterfall sector were added to the model. Such a scenario was recently discussed in [13]. It has been observed that the presence of a FI  $D$ -term breaks explicitly an exact discrete symmetry acting on the gauged waterfall sector, i.e. a kind of  $D$ -parity, which would have remained otherwise unbroken even after the spontaneous symmetry breaking (SSB) of  $U(1)_X$ . As a consequence, the ultraheavy  $U(1)_X$ -gauge-sector bosons and fermions, which would have been otherwise stable, can now decay with rates controlled by the size of the FI  $D$ -term. Since these particles could be abundantly produced

during the preheating epoch, their late decays could give rise to a second reheat phase in the evolution of the early Universe. Depending on the actual size of the FI  $D$ -term, this second reheat temperature may be as low as 0.5–1 TeV, resulting in an enormous entropy release. This could be sufficient to render the gravitinos underabundant, which might be copiously produced during the first reheating from the perturbative inflaton decays.

In this paper we present a detailed analysis of  $F$ -term hybrid inflation with a subdominant FI  $D$ -tadpole. As mentioned above, the presence of the FI  $D$ -tadpole is essential for explicitly breaking an exact discrete symmetry, a  $D$ -parity, which was acting on the gauged waterfall sector. In [13], we termed this inflationary scenario, in short,  $F_D$ -term hybrid inflation. As the inflaton chiral superfield  $\hat{S}$  couples to the Higgs-doublet chiral superfields  $\hat{H}_{u,d}$ , through  $\lambda \hat{S} \hat{H}_u \hat{H}_d$ , the model generates an effective  $\mu$ -parameter for the Minimal Supersymmetric Standard Model (MSSM), through the VEV  $\langle S \rangle$  [14]. The same mechanism may also generate an effective Majorana mass matrix for the singlet neutrino superfields  $\hat{N}_{1,2,3}$  [15], through the operator  $\frac{1}{2} \rho_{ij} \hat{S} \hat{N}_i \hat{N}_j$  [13, 16]. Assuming that this last operator is  $\text{SO}(3)$ -symmetric or very close to it, i.e.  $\rho_{ij} \approx \rho \mathbf{1}_3$ , the resulting lepton-number-violating Majorana mass,  $m_N = \rho \langle S \rangle$ , will be closely tied to the  $\mu$ -parameter of the MSSM. If  $\lambda \sim \rho$ , the  $F_D$ -term hybrid model will then give rise to 3 nearly degenerate heavy Majorana neutrinos  $\nu_{1,2,3R}$ , as well as to 3 complex right-handed sneutrinos  $\tilde{N}_{1,2,3}$ , with electroweak-scale masses. Such a mass spectrum opens up the possibility to explain the baryon asymmetry in the Universe (BAU)  $\eta_B$  [17, 18] by thermal electroweak-scale resonant leptogenesis [16, 19, 20], almost independently of the initial baryon-number composition of the primordial plasma. Moreover, since the  $F_D$ -term hybrid model conserves  $R$ -parity [13], the lightest supersymmetric particle (LSP) is stable. Here, we examine the possibility that *thermal* right-handed sneutrinos are responsible for solving the cold dark matter (CDM) problem of the Universe.

In this paper we also improve an earlier approach [13], concerning the production of the quasi-stable  $\text{U}(1)_X$  gauge-sector particles during the preheating epoch. In addition, we present a numerical analysis that properly takes into account the combined effect on the reheat temperature  $T_{\text{reh}}$  from the inflaton and gauge-sector particle decays and their annihilations. We call this two-states' mechanism of reheating the Universe, *coupled reheating*. After solving numerically a network of Boltzmann equations (BEs) that appropriately treat coupled reheating, we obtain estimates for the present abundance of gravitinos in the Universe. We show explicitly, how a small breaking of  $D$ -parity sourced by a subdominant FI  $D$ -tadpole helps to relax the strict gravitino overproduction constraint.

In addition to gravitinos, one might have to worry that topologically stable cosmic strings do not contribute significantly to the CMB power spectrum  $P_{\mathcal{R}}$ . Cosmic strings,

global or local, are topological defects and usually form after the SSB of some global or local  $U(1)$  symmetry [21–23]. According to recent analyses [24], cosmic strings, if any, should make up no more than about 10% of the power spectrum  $P_{\mathcal{R}}$ . This last requirement puts severe limits on the allowed parameter space of models of inflation. There have already been some suggestions [25] on how to get rid of cosmic strings, based on modified versions of hybrid inflation. Here, we follow a different approach to solving this problem. We consider models, for which the waterfall sector possesses an  $SU(2)_X$  gauge symmetry which breaks completely, i.e.  $SU(2)_X \rightarrow \mathbf{I}$ , such that neither cosmic strings nor monopoles are produced at the end of inflation. In this case, gauge invariance forbids the existence of an  $SU(2)_X$   $D$ -tadpole  $D^a$ . However, Planck-mass suppressed non-renormalizable operators that originate from the superpotential or the Kähler potential can give rise to explicit breaking of  $D$ -parity. The latter may manifest itself by the generation of effective  $D^a$ -tadpole terms that arise after the SSB of  $SU(2)_X$ . In this way, all the  $SU(2)_X$  gauge-sector particles can be made unstable.

The organization of the paper is as follows: in Section 2, we describe the  $F_D$ -term hybrid model and calculate the 1-loop effective potential relevant to inflation. In addition, we discuss the possible cosmological consequences of radiative effects on the flat directions in the MSSM. We conclude this section by outlining how the  $F_D$ -term hybrid model could generally be embedded into a grand unified theory (GUT), including possible realizations of a GUT without cosmic strings and monopoles. Technical details concerning mechanisms of explicit  $D$ -parity breaking in SUGRA, e.g. via an effective subdominant  $D$ -tadpole or non-renormalizable operators in Kähler potential, are given in Appendix A. Section 3 analyzes the constraints on the theoretical parameters, which are mainly derived from considerations of the power spectrum  $P_{\mathcal{R}}$  and a strongly red-tilted spectral index  $n_s$ , with  $n_s \approx 0.95$ , as observed most recently by WMAP [4, 5]. We show how a negative Hubble-induced mass term in a next-to-minimal extension of supergravity helps to account for the present CMB data, as well as to substantially weaken the strict constraints on the model parameters, originating from cosmic string effects on  $P_{\mathcal{R}}$ , within a  $U(1)_X$  realization of the  $F_D$ -term hybrid model.

In Section 4, we analyze the mass spectrum of the inflaton-waterfall sector in the post-inflationary era and present naive estimates of the reheat temperature  $T_{\text{reh}}$  as obtained from perturbative inflaton decays. We then make use of an improved approach to preheating and compute the energy density of the quasi-stable waterfall gauge particles. In Section 5, we solve numerically the BEs relevant to coupled reheating and present estimates for the gravitino abundance in the present Universe. In Section 6, we demonstrate, how thermal electroweak-scale resonant leptogenesis can be realized within the  $F_D$ -term hybrid model

and discuss the possibility of solving the CDM problem, if thermal right-handed sneutrinos are considered to be the LSPs in the spectrum. In Section 7, we present our conclusions, including a summary of possible particle-physics implications of the  $F_D$ -term hybrid model for high-energy colliders and for low-energy experiments of lepton flavour and/or number violation.

## 2 General Setup

In this section we first present the general setup of the  $F_D$ -term hybrid model within the minimal SUGRA framework and compute the renormalized 1-loop effective potential relevant to inflation. We then discuss the cosmological implications of radiative effects on the MSSM flat directions for  $F_D$ -term hybrid inflation and for SUSY inflationary models in general. Finally, we analyze the prospects of embedding the  $F_D$ -term hybrid model into a GUT.

### 2.1 The Model

The renormalizable superpotential of the  $F_D$ -term hybrid model is given by

$$W = \kappa \hat{S} \left( \hat{X}_1 \hat{X}_2 - M^2 \right) + \lambda \hat{S} \hat{H}_u \hat{H}_d + \frac{\rho_{ij}}{2} \hat{S} \hat{N}_i \hat{N}_j + h_{ij}^\nu \hat{L}_i \hat{H}_u \hat{N}_j + W_{\text{MSSM}}^{(\mu=0)}, \quad (2.1)$$

where  $W_{\text{MSSM}}^{(\mu=0)}$  denotes the MSSM superpotential without the  $\mu$ -term:

$$W_{\text{MSSM}}^{(\mu=0)} = h_{ij}^u \hat{Q}_i \hat{H}_u \hat{U}_j + h_{ij}^d \hat{H}_d \hat{Q}_i \hat{D}_j + h_l \hat{H}_d \hat{L}_l \hat{E}_l. \quad (2.2)$$

The first term in (2.1) describes the inflaton-waterfall (IW) sector. Specifically,  $\hat{S}$  is the SM-singlet inflaton superfield, and  $\hat{X}_{1,2}$  is a chiral multiplet pair of the waterfall fields with opposite charges under the  $U(1)_X$  gauge group, i.e.  $Q(\hat{X}_1) = -Q(\hat{X}_2) = 1$ . In addition, the corresponding inflationary soft SUSY-breaking sector obtained from (2.1) reads:

$$-\mathcal{L}_{\text{soft}} = M_S^2 S^* S + \left( \kappa A_\kappa S X_1 X_2 + \lambda A_\lambda S H_u H_d + \frac{\rho}{2} A_\rho S \tilde{N}_i \tilde{N}_i - \kappa a_S M^2 S + \text{H.c.} \right), \quad (2.3)$$

where  $M_S$ ,  $A_{\kappa, \lambda, \rho}$  and  $a_S$  are soft SUSY-breaking mass parameters of order  $M_{\text{SUSY}} \sim 1$  TeV.

The second term in (2.1),  $\lambda \hat{S} \hat{H}_u \hat{H}_d$ , induces an effective  $\mu$ -parameter, when the scalar component of  $\hat{S}$ ,  $S$ , acquires a VEV, i.e.

$$\mu = \lambda \langle S \rangle \approx \frac{\lambda}{2\kappa} |A_\kappa - a_S|. \quad (2.4)$$

In obtaining the last approximate equality in (2.4), we neglected the VEVs of  $H_{u,d}$  and considered the fact that the VEVs of the waterfall fields  $X_{1,2}$  after inflation are:  $\langle X_{1,2} \rangle = M$  [14]. For  $\lambda \sim \kappa$ , the size of  $\mu$ -parameter turns out to be of the order of the soft-SUSY breaking scale  $M_{\text{SUSY}}$ , as required for a successful electroweak Higgs mechanism. By analogy, the third term in (2.1),  $\frac{1}{2} \rho_{ij} \hat{S} \hat{N}_i \hat{N}_j$ , gives rise to an effective lepton-number-violating Majorana mass matrix, i.e.  $M_S = \rho_{ij} v_S$ . Assuming that  $\rho_{ij}$  is approximately SO(3) symmetric, viz.  $\rho_{ij} \approx \rho \mathbf{1}_3$ , one obtains 3 nearly degenerate right-handed neutrinos  $\nu_{1,2,3R}$ , with mass

$$m_N = \rho v_S. \quad (2.5)$$

If  $\lambda$  and  $\rho$  are comparable in magnitude, then the  $\mu$ -parameter and the SO(3)-symmetric Majorana mass  $m_N$  are tied together, i.e.  $m_N \sim \mu$ , thus leading to a scenario where the singlet neutrinos  $\nu_{1,2,3R}$  can naturally have TeV or electroweak-scale masses [13, 16].

The renormalizable superpotential (2.1) of the model may be uniquely determined by imposing the continuous  $R$  symmetry:

$$\hat{S} \rightarrow e^{i\alpha} \hat{S}, \quad \hat{L} \rightarrow e^{i\alpha} \hat{L}, \quad \hat{Q} \rightarrow e^{i\alpha} \hat{Q}, \quad (2.6)$$

with  $W \rightarrow e^{i\alpha} W$ , whereas all other fields remain invariant under an  $R$  transformation. Notice that the  $R$  symmetry (2.6) forbids the presence of higher-dimensional operators of the form  $\hat{X}_1 \hat{X}_2 \hat{N}_i \hat{N}_j / m_{\text{Pl}}$ . This fact ensures that the electroweak-scale Majorana mass  $m_N$  does not get destabilized by Planck-scale SUGRA effects.

One may now observe that the superpotential (2.1) is symmetric under the permutation of the waterfall fields, i.e.  $\hat{X}_1 \leftrightarrow \hat{X}_2$ . This permutation symmetry persists, even after the SSB of  $U(1)_X$ , since the ground state,  $\langle X_1 \rangle = \langle X_2 \rangle = M$ , is invariant under the same symmetry as well. Hence, there is an exact discrete symmetry acting on the gauged waterfall sector, a kind of  $D$ -parity. As a consequence of  $D$ -parity conservation, the ultraheavy particles of mass  $gM$ , which are related to the  $U(1)_X$  gauge sector, are stable. Such a possibility is not very desirable, as these particles, if abundantly produced, may overclose the Universe at late times. In order to break this unwanted  $D$ -parity, a subdominant FI  $D$ -term,  $-\frac{1}{2} g m_{\text{FI}}^2 D$ , is added to the model [13], giving rise to the  $D$ -term potential <sup>1</sup>

$$V_D = \frac{g^2}{8} \left( |X_1|^2 - |X_2|^2 - m_{\text{FI}}^2 \right)^2. \quad (2.7)$$

---

<sup>1</sup>The  $D$ -parity is an accidental discrete symmetry and it should not be confused with the  $U(1)_X$  charge conjugation symmetry realized by the transformations:  $X_1 \leftrightarrow X_1^*$  and  $X_2 \leftrightarrow X_2^*$ . Although both discrete symmetries have the same effect when acting on the  $U(1)_X$  scalar current  $j_X^\mu = i(X_1^* \overset{\leftrightarrow}{\partial}^\mu X_1 - X_2^* \overset{\leftrightarrow}{\partial}^\mu X_2)$ , i.e.  $j_X^\mu \leftrightarrow -j_X^\mu$ , they crucially differ when they are applied on the FI  $D$ -term:  $-\frac{g}{2} m_{\text{FI}}^2 (|X_1|^2 - |X_2|^2)$ . This term is even under charge conjugation, but odd under a  $D$ -parity conjugation.



The FI  $D$ -term will not affect the inflationary dynamics, as long as  $gm_{\text{FI}} \ll \kappa M$ . Technically, a subdominant  $D$ -term can be generated radiatively after integrating out Planck-scale heavy degrees of freedom. Further discussion is given in Section 4.1 and in Appendix A, where we also discuss the possibility of breaking explicitly  $D$ -parity by non-renormalizable Kähler potential terms. The post-inflationary implications of the FI  $D$ -term,  $m_{\text{FI}}$ , for the reheat temperature  $T_{\text{reh}}$  and the gravitino abundance  $Y_{\tilde{G}}$  will be analyzed in Section 5.

The inflationary potential  $V_{\text{inf}}$  may be represented by the sum

$$V_{\text{inf}} = V_{\text{inf}}^{(0)} + V_{\text{inf}}^{(1)} + V_{\text{SUGRA}} , \quad (2.8)$$

where  $V_{\text{inf}}^{(0)}$  and  $V_{\text{inf}}^{(1)}$  are the tree-level potential and the 1-loop effective potential, respectively and  $V_{\text{SUGRA}}$  contains the SUGRA contribution. Including soft-SUSY breaking terms related to  $S$ , the tree-level contribution to the inflationary potential is

$$V_{\text{inf}}^{(0)} = \mathcal{Z}_S \kappa^2 M^4 + M_S^2 S^* S - \left( \kappa a_S M^2 S + \text{H.c.} \right) , \quad (2.9)$$

where  $\mathcal{Z}_S^{1/2}$  is the wave-function renormalization of the inflaton field which is needed to renormalize the 1-loop effective potential given below in the SUSY limit of the theory. The counter-term,  $\delta\mathcal{Z}_S = \mathcal{Z}_S - 1$ , due to  $S$  wave-function renormalization may be obtained from the inflaton self-energy  $\Pi_{SS}(p^2)$ , through the relation

$$\delta\mathcal{Z}_S = - \left. \frac{d \text{Re} \Pi_{SS}(p^2)}{dp^2} \right|_{p^2=0} . \quad (2.10)$$

Calculating the UV part of  $\delta\mathcal{Z}_S$  from this very last relation, we find

$$\delta\mathcal{Z}_S = - \frac{1}{32\pi^2} \left[ 2\mathcal{N}\kappa^2 \ln \left( \frac{\kappa^2 M^2}{Q^2} \right) + 4\lambda^2 \ln \left( \frac{\lambda^2 M^2}{Q^2} \right) + 3\rho^2 \ln \left( \frac{\rho^2 M^2}{Q^2} \right) \right] , \quad (2.11)$$

where  $Q^2$  is the renormalization scale and the inflaton field value  $|S_R| = M$  is taken as a common mass renormalization point. In addition, the parameter  $\mathcal{N}$  in (2.11) represents the dimensionality of the waterfall sector. For example, it is  $\mathcal{N} = 1$  for an  $U(1)_X$  waterfall sector, whilst it is  $\mathcal{N} = N$ , if  $\hat{X}_1$  ( $\hat{X}_2$ ) belongs to the fundamental (anti-fundamental) representation of an  $SU(N)$  theory. Observe, finally, that only the fermionic components of the superfields,  $\hat{X}_{1,2}$ ,  $\hat{H}_{u,d}$ ,  $\hat{N}_{1,2,3}$ , contribute to  $\delta\mathcal{Z}_S$ .

Ignoring soft SUSY-breaking terms, the 1-loop effective potential relevant to inflation is calculated to be

$$V_{\text{inf}}^{(1)} = \frac{1}{32\pi^2} \left\{ \mathcal{N}\kappa^4 \left[ |S^2 + M^2|^2 \ln \left( \frac{\kappa^2(|S|^2 + M^2)}{Q^2} \right) + |S^2 - M^2|^2 \ln \left( \frac{\kappa^2(|S|^2 - M^2)}{Q^2} \right) \right] \right. \\ \left. + 2\lambda^4 \left[ |S^2 + \frac{\kappa}{\lambda} M^2|^2 \ln \left( \frac{\lambda^2(|S|^2 + \frac{\kappa}{\lambda} M^2)}{Q^2} \right) + |S^2 - \frac{\kappa}{\lambda} M^2|^2 \ln \left( \frac{\lambda^2(|S|^2 - \frac{\kappa}{\lambda} M^2)}{Q^2} \right) \right] \right\}$$

$$\begin{aligned}
& + \frac{3\rho^4}{2} \left[ |S^2 + \frac{\kappa}{\rho} M^2|^2 \ln \left( \frac{\rho^2(|S|^2 + \frac{\kappa}{\rho} M^2)}{Q^2} \right) + |S^2 - \frac{\kappa}{\rho} M^2|^2 \ln \left( \frac{\rho^2(|S|^2 - \frac{\kappa}{\rho} M^2)}{Q^2} \right) \right] \\
& - |S|^4 \left[ 2\mathcal{N}\kappa^4 \ln \left( \frac{\kappa^2 |S|^2}{Q^2} \right) + 4\lambda^4 \ln \left( \frac{\lambda^2 |S|^2}{Q^2} \right) + 3\rho^4 \ln \left( \frac{\rho^2 |S|^2}{Q^2} \right) \right] \Big\}. \quad (2.12)
\end{aligned}$$

Given (2.11) and (2.12), it can be checked that the expression  $V_{\text{inf}}^{(0)} + V_{\text{inf}}^{(1)}$  is independent of  $\ln Q^2$ , as it should be.

Finally, the SUGRA contribution  $V_{\text{SUGRA}}$  to  $V_{\text{inf}}$  in (2.8) is highly model-dependent. In general, one expects an infinite series of non-renormalizable operators to occur in  $V_{\text{SUGRA}}$ , i.e. [8, 26, 27]

$$V_{\text{SUGRA}} = -c_H^2 H^2 |S|^2 + \kappa^2 M^4 \frac{|S|^4}{2m_{\text{Pl}}^4} + \mathcal{O}(|S|^6). \quad (2.13)$$

where  $H^2 = \kappa^2 M^4 / (3m_{\text{Pl}}^2)$  is the squared Hubble rate during inflation. The first term in (2.13) represents a Hubble-induced mass term, which is preferably defined to be negative for observational reasons to be discussed in Section 3. In a model with a minimal Kähler potential, the parameter  $c_H$  vanishes identically.<sup>2</sup> In fact, if  $|c_H| \lesssim 10^{-2}$ , its influence on the CMB data [29] gets marginalized. In our analysis in Section 3, we present results for two representative models: (i) the scenario with a minimal Kähler potential ( $c_H = 0$ ); (ii) a next-to-minimal Kähler potential scenario with  $c_H \lesssim 0.2$ , where only the effect of the term  $(\hat{S}^\dagger \hat{S})^2 / m_{\text{Pl}}^2$  is considered and all higher order non-renormalizable operators are ignored in the Kähler manifold. Moreover, we neglect possible 1-loop contributions to  $V_{\text{inf}}$  from  $A_{\kappa, \lambda, \rho}$ -terms, which are insignificant for values  $M \gtrsim 10^{15}$  GeV. We only include the tadpole term  $\kappa a_S M^2 S$ , which may become relevant for values of  $\kappa \lesssim 10^{-4}$ , but ignore all other soft SUSY-breaking terms, since they are negligible during inflation [12].

The stability of the inflationary trajectory in the presence of the Higgs doublets  $H_{u,d}$  and the right-handed scalar neutrinos  $\tilde{N}_{1,2,3}$  provides further restrictions on the couplings  $\lambda$  and  $\rho$ . In order to successfully trigger hybrid inflation, the fields at the start of inflation should obey the following conditions:

$$\text{Re } S^{\text{in}} = |S^{\text{in}}| \gtrsim M, \quad X_{1,2}^{\text{in}} = 0, \quad H_{u,d}^{\text{in}} = 0, \quad \tilde{N}_{1,2,3}^{\text{in}} = 0. \quad (2.14)$$

The precise start values of the inflaton  $\text{Re } S^{\text{in}}$  are determined by the number of  $e$ -folds  $\mathcal{N}_e$ , which is a measure of Universe's expansion during inflation (see also our discussion in

---

<sup>2</sup>Strictly speaking, curvature effects related to an expanding de Sitter background will contribute to the potential a term given by  $-\frac{3}{16\pi^2} (2\mathcal{N}\kappa^2 + 4\lambda^2 + 3\rho^2) H^2 |S|^2 \ln(|S|^2/Q^2)$ , even in the minimal Kähler potential case [28]. Such a term, however, turns out to be negligible to affect the inflation dynamics in the  $F_D$ -term hybrid model. Finally, this term may be partially absorbed into the RG running of  $c_H^2(Q^2)$ .

Section 3). After inflation and the waterfall transition mechanism have been completed, it is important to ensure that the waterfall fields acquire a high VEV, i.e.  $X_{1,2}^{\text{end}} = M$ , while all other fields have small electroweak-scale VEVs. This can be achieved by requiring that the Higgs-doublet and the sneutrino mass matrices stay positive definite throughout the inflationary trajectory up to a critical value  $|S_c| \approx M$ . Instead, the corresponding mass matrix of  $X_{1,2}$  will be the first to develop a negative eigenvalue and tachyonic instability close to  $|S_c|$ . As a consequence, the fields  $X_{1,2}$  will be the first to start moving away from 0 and set in to the ‘good’ vacuum  $X_1^{\text{end}} = X_2^{\text{end}} = M$ , well before the other fields, e.g.  $H_{1,2}^{\text{in}}$  and  $\tilde{N}_{1,2,3}^{\text{in}}$ , go to a ‘bad’ vacuum where  $X_{1,2}^{\text{end}} = 0$ ,  $H_{1,2}^{\text{end}} = \frac{\kappa}{\lambda} M$  and  $\tilde{N}_{1,2,3}^{\text{end}} = \frac{\kappa}{\rho} M$ . To better understand this point, let us write down the mass matrix in the weak field basis  $(H_d, H_u^*)$ :

$$M_{\text{Higgs}}^2 = \begin{pmatrix} \lambda^2 |S|^2 & -\kappa \lambda (M^2 - X_1 X_2) \\ -\kappa \lambda (M^2 - X_1^* X_2^*) & \lambda^2 |S|^2 \end{pmatrix}. \quad (2.15)$$

Then, positive definiteness of  $M_{\text{Higgs}}^2$  implies that

$$\lambda |S|^2 \geq \kappa |M^2 - X_1 X_2|. \quad (2.16)$$

From (2.16), it is evident that the condition  $\lambda \gtrsim \kappa$  is sufficient for ending hybrid inflation to the ‘good’ vacuum. Finally, one obtains a condition analogous to (2.16) from the sneutrino mass matrix, which is equivalent to having  $\rho \gtrsim \kappa$ . The above two constraints on  $\lambda$  and  $\rho$ , i.e.  $\lambda, \rho > \kappa$ , will be imposed in the analysis presented in Section 3.

## 2.2 Radiative Lifting of MSSM Flat Directions

Flat directions in supersymmetric theories, e.g. in the MSSM [30], play an important role in cosmology [31, 32]. As we will demonstrate in this section, however, their influence on  $F_D$ -term hybrid inflation is minimal under rather realistic assumptions.

One possible consequence of flat directions could be the generation of a primordial baryon asymmetry  $\eta_B^{\text{in}}$  through the Affleck–Dine mechanism [31]. However, if this initial baryon asymmetry  $\eta_B^{\text{in}}$  is generated at temperatures  $T > m_N$ , it will rapidly be erased by the strong  $(B - L)$ -violating interactions mediated by electroweak-scale heavy Majorana neutrinos at  $T \sim m_N$ . The BAU will then reach the present observed value by means of the thermal resonant leptogenesis mechanism and will only depend on the basic theoretical parameters of the  $F_D$ -term hybrid model [16, 20]. More details are given in Section 6.

In addition, one might argue that large VEVs associated with quasi-flat directions in the MSSM would make all MSSM particles so heavy after inflation, such that all perturbative decays of the inflaton would be kinematically blocked and hence the Universe

would never thermalize [33]. The system may fall into a false vacuum with a large VEV at the start of inflation, which could, for example, be triggered by a negative Hubble-induced squared mass term of order  $H^2$  [34], along the flat direction. In the  $F_D$ -term hybrid model, however, spontaneous SUSY breaking due to a non-zero  $\langle S \rangle$  is communicated radiatively to the MSSM sector, via the renormalizable operators  $\lambda \widehat{S} \widehat{H}_u \widehat{H}_d$  and  $\rho \widehat{S} \widehat{N}_i \widehat{N}_i$ . Consequently, their effects on the MSSM flat directions can be large and so affect the inflaton decays which proceed via the same renormalizable operators. In the following, we will present a careful treatment of this radiative lifting of MSSM flat directions, and examine the conditions, under which the directions would remain sufficiently flat so as to prohibit the Universe from thermal equilibration, shortly after inflation.

To obtain a flat direction in supersymmetric theories, one has to impose the conditions of  $D$ - and  $F$ -flatness on the scalar potential  $V$ , namely the vanishing of all  $F$ - and  $D$ -terms for a specific field configuration  $\sigma$ .  $D$ -flatness is automatic for any flat direction associated with a gauge-invariant operator, which is absent in the MSSM, e.g.  $\widehat{D}_i \widehat{D}_j \widehat{U}_k$ . Based on this observation, let us therefore consider here the gauge-covariant field configuration

$$\sigma = \frac{1}{\sqrt{3}} \left( \frac{\tilde{u}_{Rk}^*}{|\tilde{u}_{Rk}|} \tilde{d}_{Ri}^* + \frac{\tilde{u}_{Rk}^*}{|\tilde{u}_{Rk}|} \tilde{d}_{Rj}^* + \tilde{u}_{Rk} \right), \quad (2.17)$$

where  $i \neq j$ . It can be straightforwardly checked that the field configuration  $\sigma$ , with the constraint

$$\frac{\tilde{u}_{Rk}^*}{|\tilde{u}_{Rk}|} \tilde{d}_{Ri}^* = \frac{\tilde{u}_{Rk}^*}{|\tilde{u}_{Rk}|} \tilde{d}_{Rj}^* = \tilde{u}_{Rk} \neq 0 \quad (2.18)$$

and all remaining fields being set to zero, is a flat direction, with vanishing  $F$ - and  $D$ -terms. It is then easy to verify that the scalar potential  $V(\sigma)$  is truly flat, i.e.  $dV/d\sigma = 0$ . Although we will consider here the case of  $\sigma = \tilde{u}_{Rk}$ , the discussion of other squark and slepton flat directions is completely analogous. For notational convenience, we drop all generation indices from the fields, and denote the flat direction simply by  $\tilde{u}_R$ .

Because of the spontaneous SUSY breaking induced by the non-zero VEV of  $S$ , the flatness of the potential along the  $\tilde{u}_R$ -direction gets lifted, once radiative corrections are taken into account. The non-renormalization theorem related to theories of SUSY is still applicable and entails that this radiative lifting should be UV finite and therefore calculable. We start our calculation by considering the pertinent mass spectrum in the background of a non-zero  $S$  and  $\tilde{u}_R$ . The fermionic sector consists of 2 Dirac higgsino doublets, with squared masses  $m_h^2 = \lambda^2 |S|^2 + h^2 |\tilde{u}_R|^2$ , while the mass spectrum of the bosonic sector may be deduced by the mass matrix

$$\mathcal{M}_H^2 = \begin{pmatrix} \lambda^2 |S|^2 & -\kappa \lambda M^2 & h \lambda S \tilde{u}_R^* \\ -\kappa \lambda M^2 & \lambda^2 |S|^2 + h^2 |\tilde{u}_R|^2 & 0 \\ h \lambda S \tilde{u}_R & 0 & h^2 |\tilde{u}_R|^2 \end{pmatrix}, \quad (2.19)$$

which is defined in the weak basis ( $H_d$ ,  $H_u^*$ ,  $\tilde{Q}$ ). The coupling  $h$  in (2.19) represents a generic up-type quark Yukawa coupling.

In the renormalization scheme of dimensional reduction with minimal subtraction  $\overline{\text{DR}}$  [35], the 1-loop effective potential  $V^{(1)}$  related to  $\tilde{u}_R$  is given by

$$V^{(1)}(\tilde{u}_R) = \frac{2Q^2}{16\pi^2} \text{STr } \mathcal{M}^2 + \frac{2}{32\pi^2} \text{STr } \left\{ \mathcal{M}^4 \left[ \ln \left( \frac{\mathcal{M}^2}{Q^2} \right) - \frac{3}{2} \right] \right\}, \quad (2.20)$$

where  $\text{STr}$  denotes the usual supertrace, e.g.  $\text{STr } \mathcal{M}^2 = \text{Tr } \mathcal{M}_H^2 - 2m_h^2$ ,  $\text{STr } \mathcal{M}^4 = \text{Tr } \mathcal{M}_H^4 - 2m_h^4$  etc. In the absence of soft SUSY-breaking terms, one finds that  $\text{STr } \mathcal{M}^2 = 0$  and  $\text{STr } \mathcal{M}^4 = 2\kappa^2\lambda^2 M^4$ . The first condition implies the absence of quadratic UV divergences in SUSY theories, whereas the first together with the second one ensure the UV finiteness along the  $\tilde{u}_R$  direction, namely the fact that  $dV^{(1)}(\tilde{u}_R)/d\tilde{u}_R$  is  $Q^2$  independent.

It would be more illuminating to compute the 1-loop effective potential in (2.20) in a Taylor series expansion with respect to  $h^2|\tilde{u}_R|^2$ . To order  $h^4|\tilde{u}_R|^4$ , the 3 mass eigenvalues of  $\mathcal{M}_H^2$  are approximately given by

$$\begin{aligned} M_\pm^2 &= \lambda^2|S|^2 \pm \kappa\lambda M^2 + \frac{\kappa M^2 \pm 2\lambda|S|^2}{2(\kappa M^2 \pm \lambda|S|^2)} h^2|\tilde{u}_R|^2 \pm \frac{\kappa M^2(\kappa M^2 \pm 3\lambda|S|^2)}{8\lambda(\kappa M^2 \pm \lambda|S|^2)^3} h^4|\tilde{u}_R|^4, \\ M_0^2 &= \frac{\kappa^2 M^4}{\kappa^2 M^4 - \lambda^2|S|^4} h^2|\tilde{u}_R|^2 - \frac{2\kappa^2\lambda^2 M^4|S|^6}{(\kappa^2 M^4 - \lambda^2|S|^4)^3} h^4|\tilde{u}_R|^4. \end{aligned} \quad (2.21)$$

Notice that in the limit  $\tilde{u}_R \rightarrow 0$ , one obtains:  $m_h^2 = \lambda^2|S|^2$ ,  $M_\pm^2 = \lambda|S|^2 \pm \kappa\lambda M^2$  and  $M_0^2 = 0$ , as expected. Moreover, it is not difficult to check that  $\text{STr } \mathcal{M}^2 = \mathcal{O}(h^6|\tilde{u}_R|^6)$  and  $\text{STr } \mathcal{M}^4 = 2\kappa^2\lambda^2 M^4 + \mathcal{O}(h^6|\tilde{u}_R|^6)$ , in accordance with our discussion given above.

Employing the fact that  $|S|^2 \gg \frac{\kappa}{\lambda} M^2$  at the start of inflation, the 1-loop effective potential  $V^{(1)}(\tilde{u}_R)$  may further be approximated as follows:

$$\begin{aligned} V^{(1)}(\tilde{u}_R) &= \frac{\kappa^2\lambda^2 M^4}{8\pi^2} \left[ \ln \left( \frac{\lambda^2|S|^2}{Q^2} \right) - \frac{3}{2} \right] - \frac{1}{48\pi^2} \frac{h^2\kappa^4 M^8}{\lambda^2|S|^6} |\tilde{u}_R|^2 + \frac{1}{16\pi^2} \frac{h^4\kappa^2 M^4}{\lambda^2|S|^4} |\tilde{u}_R|^4 \\ &\quad + \frac{1}{16\pi^2} \left( \frac{h^2\kappa^2 M^4}{\lambda^2|S|^4} |\tilde{u}_R|^2 \right)^2 \ln \left( \frac{h^2\kappa^2 M^4}{\lambda^4|S|^6} |\tilde{u}_R|^2 \right) + \mathcal{O}(h^6|\tilde{u}_R|^6). \end{aligned} \quad (2.22)$$

The first term in (2.22) contributes to the 1-loop inflationary potential (2.12), while the remaining  $Q^2$ -independent terms lift the flatness of the  $\tilde{u}_R$ -direction. Assuming that  $\kappa^2 \ll \lambda^2$  and  $M \simeq |S|$  towards the end of inflation, we find the well-defined minimum

$$\langle \tilde{u}_R \rangle = \frac{\kappa}{\sqrt{6}h} M. \quad (2.23)$$

We should remark here that the above minimum would remain unaltered, even if the flat direction were a squark or slepton doublet. In this case, only the overall normalization of

the  $Q^2$ -independent part of  $V^{(1)}(\tilde{u}_R)$  would have changed by a factor 1/2. The loop-induced VEV of  $\tilde{u}_R$  generates a squared mass  $M_{\tilde{u}_R}^2$  via the Higgs mechanism, which is given by

$$M_{\tilde{u}_R}^2 = \frac{1}{24\pi^2} \frac{h^2 \kappa^4}{\lambda^2} M^2. \quad (2.24)$$

This squared mass  $M_{\tilde{u}_R}^2$  should be compared with the size of possible negative Hubble-induced squared mass terms of order  $H^2 = \kappa^2 M^4 / (3m_{\text{Pl}}^2)$ , e.g. terms of the form  $-c_{\tilde{u}}^2 H^2 |\tilde{u}_R|^2$  that may occur in  $V^{(1)}(\tilde{u}_R)$  and originate from SUGRA effects. These terms may play some role in our model, unless  $c_{\tilde{u}}^2 H^2 < M_{\tilde{u}_R}^2$ . The latter condition may be translated into the inequality

$$c_{\tilde{u}} < \frac{1}{2\sqrt{2}\pi} \frac{h \kappa}{\lambda} \frac{m_{\text{Pl}}}{M}. \quad (2.25)$$

As a typical example, let us consider an inflationary scenario, with  $\lambda = 2\kappa$ ,  $\kappa = 10^{-3}$  and  $M = 10^{16}$  GeV. In this case, (2.25) implies that  $c_{\tilde{u}} < 0.87 h$ . Hence, although the required tuning of the coefficient  $c_{\tilde{u}}$  to fulfill this last inequality may not be significant for the third generation squarks and sleptons, it becomes excessive for the first generation, unless a minimal Kähler potential is assumed. It should be stressed here, however, that the deepest and hence most energetically favoured minimum for all squark and slepton directions is the one related to  $\tilde{t}_R$ . In other words, given chaotic initial conditions, the fields are most likely to settle to minima of quasi-flat directions involving large Yukawa couplings. In this case, radiative effects play an important role in the dynamics of flat directions<sup>3</sup>.

Let us finally assume that we are in a situation where the Hubble-induced mass terms can be neglected, i.e.  $c_{\tilde{u}} = 0$  as is the case for a minimal Kähler potential, for example. Suppose that the loop-induced VEV of the quasi-flat direction persists throughout the coherent oscillatory regime. In this case, the VEV (2.23) gives rise to masses  $h\langle\tilde{u}_R\rangle = \kappa M/\sqrt{6}$  in the  $\hat{Q}\hat{H}_u$ -sector, which do not depend on the Yukawa coupling  $h$ . Consequently, the inflaton-related fields of mass  $\sqrt{2}\kappa M$  (see Table 3) will have a large decay rate to those massive particles, thus creating a non-thermal distribution. This non-thermal distribution will in turn induce  $T$ -dependent mass terms which can be larger than the expansion rate  $H(T)$  at some temperature  $T$  soon after inflation, such that  $\langle\tilde{u}_R\rangle$  will rapidly relax to zero. Of course, one might think of contemplating configurations where multiple flat directions have VEVs which contribute constructively to the masses of both  $H_u$  and  $H_d$ , such that all inflaton and waterfall particle decays would be kinematically forbidden. However, we

---

<sup>3</sup>We should note that the evolution of flat directions during the waterfall and coherent oscillation periods is a non-equilibrium dynamics problem. Moreover, no theoretical methods yet exist that would lead to a practical solution to this problem, even though effective potential corrections to the flat directions as the ones considered here are expected to be relevant during the above cosmological periods.

consider such a possibility as a bit contrived. It is therefore reasonable to assume that, provided (2.25) is fulfilled, reheating and equilibration of all MSSM degrees of freedom will take place in the  $F_D$ -term hybrid model and in all supersymmetric models of inflation that include an unsuppressed renormalizable operator of the form  $\widehat{S}\widehat{H}_u\widehat{H}_d$ .

## 2.3 Topological Defects and GUT Embeddings

As we mentioned in the Introduction, topological defects, such as domain walls, cosmic strings or monopoles, may be created at the end of inflation, when a symmetry group  $G$ , local, global or discrete, breaks down into a subgroup  $H$ , in a way such that the vacuum manifold  $M = G/H$  is not trivial. Specifically, the topological properties of the vacuum manifold  $M$  under its homotopy groups,  $\pi_n(M)$ , determine the nature of the topological defects [22, 23]. Thus, one generally has the formation of domain walls for  $\pi_0(M) \neq \mathbf{I}$ , cosmic strings for  $\pi_1(M) \neq \mathbf{I}$ , monopoles if  $\pi_2(M) \neq \mathbf{I}$ , or textures if  $\pi_{n>2}(M) \neq \mathbf{I}$  [22]. For example, for the SSB breaking pattern  $U(1)_X \rightarrow \mathbf{I}$  in the waterfall sector, the first homotopy group of the vacuum manifold is not trivial, i.e.  $\pi_1(U(1)/\mathbf{I}) = \mathbf{Z}$ . In this case, cosmic strings will be produced at the end of inflation. In general, the non-observation of any cosmic string contribution to the power spectrum  $P_{\mathcal{R}}$  at the 10% level introduces serious constraints on the theoretical parameters of hybrid inflation models.

A potentially interesting inflationary scenario arises if the waterfall sector possesses an  $SU(2)_X$  gauge symmetry. In this case, the SSB breaking pattern is:  $SU(2)_X \rightarrow \mathbf{I}$ , i.e. the group  $SU(2)_X$  breaks completely. It is worth stressing here that this is a unique property of the  $SU(2)$  group, since the breaking of higher  $SU(N)$  groups, with  $N > 2$ , into the identity  $\mathbf{I}$  is not possible. Moreover, an homotopy group analysis gives that  $\pi_{0,1,2}(SU(2)_X/\mathbf{I}) = \mathbf{I}$ , implying the complete absence of domain walls, cosmic strings and monopoles. The only non-trivial homotopy group is  $\pi_3(SU(2)_X/\mathbf{I}) = \mathbf{Z}$ , thus signifying the formation of textures, in case the  $SU(2)_X$  group is global. If the  $SU(2)_X$  group is local, however, observable textures do not occur. Since their corresponding field configurations never leave the vacuum manifold, the would-be textures can always be compensated by local  $SU(2)_X$  gauge transformations [22]. It is therefore essential that the  $X$ -symmetry of the waterfall sector is local in the  $F_D$ -term hybrid model.

It is now interesting to explore whether generic scenarios exist, for which the waterfall gauge groups  $U(1)_X$  or  $SU(2)_X$  of the  $F_D$ -term hybrid model may, partially or completely, be embedded into a GUT. As a key element for such a model-building, we identify the maintenance of  $D$ -parity conservation in the  $X$ -gauged waterfall sector, which is discussed in detail in Section 4.1. In order to preserve  $D$ -parity, the waterfall sector should be

somehow ‘hidden’ from the perspective of the SM gauge group  $G_{\text{SM}}$ . This means that the SM fields must be neutral under  $X$  and vice versa, the  $X$ -gauge and waterfall sector fields should not be charged under  $G_{\text{SM}}$ . Consequently, we have to require, as a GUT breaking route, that the waterfall  $X$ -gauge group and the GUT-subgroup that contains  $G_{\text{SM}}$  factor out into a product of two independent groups without overlapping charges.

It is reasonable to assume that the GUT-subgroup is broken to  $G_{\text{SM}}$  before or while inflation takes place. Then, possible unwanted topological defects due to the various stages of symmetry breaking from the GUT-subgroup down to the SM will be inflated away. Notice that we do not have to require that the GUT-subgroup breaking scale is higher than the respective  $X$ -symmetry breaking scale, but only that the reheat temperature  $T_{\text{reh}}$  is low enough such that no symmetries of the GUT-subgroup are restored during reheating. A related discussion within the context of  $\text{SO}(10)$  may be found in [36].

Let us first investigate whether a ‘hidden’ gauge group  $\text{U}(1)_X$  related to the waterfall sector can be embedded into a GUT. Although ‘hidden’  $\text{U}(1)$ ’s naturally arise in models of string compactification [37], our interest here is to identify possible  $\text{U}(1)_X$  factors that can be embedded into a simple GUT. Given the above criterion, the frequently discussed GUT based on  $\text{SO}(10)$  should be excluded, since it does not contain ‘hidden’  $\text{U}(1)_X$  groups [38]. As a next candidate theory, we may consider the exceptional group  $\text{E}(6)$ , with the SSB breaking path  $\text{E}(6) \rightarrow \text{U}(1) \times \text{SO}(10)$ . The fundamental representation of  $\text{E}(6)$  is the chiral  $\mathbf{27}_F$  representation, which branches under  $\text{U}(1) \times \text{SO}(10)$  as follows:

$$\mathbf{27}_F = (4, \mathbf{1}) + (-2, \mathbf{10}) + (1, \mathbf{16}) . \quad (2.26)$$

Although the SM particles may fit into  $\mathbf{16}$ , they are not neutral under the extra  $\text{U}(1)$ . Higher representations, such as  $(0, \mathbf{45})$  stemming from  $\mathbf{78}$  of  $\text{E}(6)$ , are neutral under the  $\text{U}(1)$  factor, but they are not suitable to properly accommodate all the SM particles.

We therefore turn our attention to possible breaking patterns of maximal groups that contain a ‘hidden’  $\text{SU}(2)_X$  factor. A promising example is  $\text{E}(6) \supset \text{SU}(2)_X \times \text{SU}(6)$ , where the fundamental representation  $\mathbf{27}_F$  follows the branching:

$$\mathbf{27}_F = (\mathbf{2}, \bar{\mathbf{6}}) + (\mathbf{1}, \mathbf{15}) . \quad (2.27)$$

Under  $\text{SU}(6) \supset \text{SU}(5) \times \text{U}(1)$ ,  $\mathbf{15}$  is an antisymmetric representation of  $\text{SU}(6)$  and one of its branching rules is

$$\mathbf{15} = (\mathbf{5}, -4) + (\mathbf{10}, 2) . \quad (2.28)$$

However, we need a  $\bar{\mathbf{5}}$  of  $\text{SU}(5)$ , together with  $\mathbf{10}$  in (2.28), in order to appropriately describe all SM fermions. This shortcoming may be circumvented by adding an extra  $\bar{\mathbf{27}}_F$  of  $\text{E}(6)$  to



the spectrum, where the missing  $\bar{\mathbf{5}}$  may be obtained from the complex conjugate branching of (2.28). Such an extension of the particle spectrum may even be welcome to resolve the proton stability problem, through a kind of split multiplet mechanism [39]. Within the framework of SUSY, the quark and lepton Yukawa interactions may be generated via the introduction of a pair of the multiplets  $\mathbf{27}_H, \bar{\mathbf{27}}_H$ . Finally, in such an E(6) unified scenario, the 3 right-handed neutrinos can only appear as singlets.

Another possible GUT scenario that complies with our criterion of a hidden  $SU(2)_X$  is  $E(7) \supset SU(2)_X \times SO(12)$ . The fundamental representation is  $\mathbf{56}_F$  and branches under  $SU(2)_X \times SO(12)$  as follows:

$$\mathbf{56}_F = (\mathbf{2}, \bar{\mathbf{12}}) + (\mathbf{1}, \mathbf{32}) . \quad (2.29)$$

Subsequently,  $SO(12)$  breaks spontaneously into  $SO(10) \times U(1)$ , where  $\mathbf{32} = (\mathbf{16}, 1) + (\bar{\mathbf{16}}, -1)$  is a vector-like representation. However, one may well envisage a string-theoretic framework, in which orbifold compactification projects out the undesirable anti-chiral states. Then, all SM particles, including right-handed neutrinos, will be contained in one of the  $\mathbf{16}$ 's of  $\mathbf{32}$ . Related discussion of missing or incomplete multiplets due to orbifold compactification may be found in [40].

Building a realistic GUT model from the blocks stated above lies beyond the scope of this paper. We have demonstrated here, however, that the embedding of an  $SU(2)_X$  gauge group into a GUT, which is hidden but nevertheless takes part in the gauge coupling unification, appears feasible within E(6) and E(7) unified theories.

We conclude this section by observing that the presence of the singlet inflaton field  $S$  offers alternative options, for suppressing the heavy Majorana neutrino masses within SUSY GUTs. As an example, we mention the breaking scenario, where  $SO(10) \rightarrow SU(5)$  via the VEV of a  $\mathbf{126}_H$  Higgs representation and the usual superpotential term  $\mathbf{16}_F \langle \mathbf{126}_H \rangle \mathbf{16}_F$  induces heavy Majorana masses of the GUT scale  $M_{\text{GUT}}$ . Given that the above renormalizable operator is forbidden by some  $R$ -symmetry, the presence of an  $R$ -charged inflaton  $S$  may give rise to a drastic suppression of the GUT-scale Majorana mass, through a superpotential term of the form  $\hat{S} \mathbf{16}_F \langle \mathbf{126}_H \rangle \mathbf{16}_F / m_{\text{Pl}}$ . Since  $S$  receives a VEV of order  $M_{\text{SUSY}}/\kappa$  in general  $F$ -term hybrid models [cf. (2.4)], one naturally obtains heavy Majorana neutrino masses of order  $M_{\text{SUSY}}$ , if  $\kappa \sim \langle \mathbf{126}_H \rangle / m_{\text{Pl}} \sim 10^{-3}$ . Such values of  $\kappa$  do satisfy the current inflationary constraints which we discuss in the next section.

### 3 Inflation

Here, we first briefly review in Section 3.1 the basic formalism of inflation, including the constraints from the non-observation of cosmic strings in the power spectrum  $P_{\mathcal{R}}$  of the CMB data. Then, in Section 3.2, we present our numerical results for two scenarios: (i) the minimal SUGRA (mSUGRA) scenario and (ii) the next-to-minimal SUGRA (nmSUGRA) scenario. In particular, we exhibit numerical predictions for the spectral index  $n_s$  and discuss its possible reduction in the nmSUGRA scenario. Finally, we analyze the combined constraints on the fundamental theoretical parameters  $\kappa$ ,  $\lambda$ ,  $\rho$ , and  $M$ , which result from the recent CMB observations and inflation.

#### 3.1 Basic Formalism

According to the inflationary paradigm [6], the horizon and flatness problems of the standard Big-Bang Cosmology can be technically addressed, if our observable Universe has undergone an accelerated expansion of a number 50–60 of  $e$ -folds during inflation. In the slow-roll approximation, the number of  $e$ -folds,  $\mathcal{N}_e$ , is related to the inflationary potential through:

$$\mathcal{N}_e = \frac{1}{m_{\text{Pl}}^2} \int_{\phi_{\text{end}}}^{\phi_{\text{exit}}} d\phi \frac{V_{\text{inf}}}{V'_{\text{inf}}} \simeq 55. \quad (3.1)$$

Hereafter, a prime on  $V_{\text{inf}}$  will denote differentiation with respect to the inflaton field  $\phi = \sqrt{2} \text{Re } S$ . In addition,  $\phi_{\text{exit}}$  is the value of  $\phi$ , when our present horizon scale crossed outside inflation's horizon and  $\phi_{\text{end}}$  is the value of  $\phi$  at the end of inflation. In the slow-roll approximation, the field value  $\phi_{\text{end}}$  is determined from the condition:

$$\max\{\epsilon(\phi_{\text{end}}), |\eta(\phi_{\text{end}})|\} = 1, \quad (3.2)$$

where

$$\epsilon = \frac{m_{\text{Pl}}^2}{2} \left( \frac{V'_{\text{inf}}}{V_{\text{inf}}} \right)^2, \quad \eta = m_{\text{Pl}}^2 \frac{V''_{\text{inf}}}{V_{\text{inf}}}. \quad (3.3)$$

We have checked that the slow-roll condition (3.2) is well satisfied up to the critical point  $\phi_{\text{end}} = \sqrt{2}M$ , beyond which the waterfall mechanism takes place. We also find that the slow-roll condition remains valid, even within the nmSUGRA scenario with  $c_H \neq 0$  and with appreciable non-renormalizable SUGRA effects. Finally, we note that the assumed value of  $\mathcal{N}_e \simeq 55$  in (3.1) is slightly higher than the one computed consistently from (5.17), which is about 50 for our low-reheat cosmological scenario. However, our numerical results concerning  $P_{\mathcal{R}}$  and  $n_s$  do not depend on such a 10% variation of  $\mathcal{N}_e$  in any essential way.

The power spectrum  $P_{\mathcal{R}}$  is a cosmological observable of the curvature perturbations, which sensitively depends on the theoretical parameters of the inflationary potential. The square root of the power spectrum,  $P_{\mathcal{R}}^{1/2}$ , may be conveniently written down as

$$P_{\mathcal{R}}^{1/2} = \frac{1}{2\sqrt{3}\pi m_{\text{Pl}}^3} \frac{V_{\text{inf}}^{3/2}(\phi_{\text{exit}})}{|V'_{\text{inf}}(\phi_{\text{exit}})|}. \quad (3.4)$$

The recent WMAP [2, 4] results, which are compatible with the ones suggested for the COBE normalization [1], require that

$$P_{\mathcal{R}}^{1/2} \simeq 4.86 \times 10^{-5}. \quad (3.5)$$

In addition to scalar curvature perturbations, tensor gravity waves and cosmic string effects may also contribute to  $P_{\mathcal{R}}$ . In the  $F_D$ -term hybrid model with an Abelian  $U(1)_X$  waterfall sector, cosmic strings arise after the SSB of the gauge symmetry (see also our discussion in Section 2.3). In this case, additional constraints are obtained from the non-observation of cosmic string effects on  $P_{\mathcal{R}}$  [41, 42]. The evaluation of such effects involves a certain degree of uncertainty in the numerical simulations of string networks [43]. Nevertheless, the common approach taken to cosmic string effects [29, 44] is to require that their contribution  $(P_{\mathcal{R}})_{\text{cs}}$  to the power spectrum  $P_{\mathcal{R}}$  does not exceed the 10% level, i.e.  $(P_{\mathcal{R}})_{\text{cs}}/P_{\mathcal{R}} \lesssim 0.1$ . In detail, we require that

$$(P_{\mathcal{R}}^{1/2})_{\text{cs}} \leq 1.54 \times 10^{-5}. \quad (3.6)$$

The cosmic string contribution  $(P_{\mathcal{R}})_{\text{cs}}$  to the power spectrum may be computed by

$$(P_{\mathcal{R}}^{1/2})_{\text{cs}} = \frac{\sqrt{15}}{4\pi} \frac{\mu_{\text{cs}}}{m_{\text{Pl}}^2} y_{\text{cs}}, \quad (3.7)$$

where the tension of the cosmic strings,  $\mu_{\text{cs}}$ , is calculated using the formulae:

$$\mu_{\text{cs}} = 2\pi M^2 \epsilon_{\text{cs}}(\beta), \quad \epsilon_{\text{cs}}(\beta) \simeq \begin{cases} 1.04 \beta^{0.195}, & \text{for } \beta > 10^{-2}, \\ 2.4 / \ln(2/\beta), & \text{for } \beta \leq 10^{-2}. \end{cases} \quad (3.8)$$

In (3.8) the argument  $\beta$  is given by  $\beta = \kappa^2/(2g^2)$ , while the  $U(1)_X$  gauge coupling constant  $g$  is considered to assume the value  $g \simeq 0.7$  as is the case in GUT models. The central value of the parameter  $y_{\text{cs}}$  is 8.9 and its error margin lies in the interval [6.7, 11.6], according to the analysis in [42].

The recently announced three-years results of WMAP [4] improved upon the precision of a number of other cosmological observables. The merits of an inflationary model can be judged by comparing its predictions for the scalar spectral index,  $n_{\text{s}}$ , the tensor to scalar

ratio,  $r$ , and the running of  $n_s$ ,  $dn_s/d\ln\kappa$ , with the CMB data. In the  $F_D$ -term hybrid model,  $r = 16\epsilon(\phi_{\text{exit}})$  is much lower than the WMAP bound, i.e. well below  $10^{-2}$ , and  $dn_s/d\ln\kappa$  is always smaller than  $10^{-3}$  and so unobservable. In addition, the spectral index  $n_s$  in our model may well be approximated as follows: [6]

$$n_s = 1 - 6\epsilon(\phi_{\text{exit}}) + 2\eta(\phi_{\text{exit}}) \simeq 1 + 2\eta(\phi_{\text{exit}}), \quad (3.9)$$

since  $\epsilon$  is negligible. The predicted value needs to be compared with the recent WMAP results [4]:

$$n_s = 0.951^{+0.015}_{-0.019}. \quad (3.10)$$

The latter is translated into the double inequality,

$$0.913 \lesssim n_s \lesssim 0.981, \quad (3.11)$$

at the 95% confidence level (CL).

The result (3.11) brings under considerable stress minimal  $F$ -term hybrid inflation models [9]. This is due to the fact that these models predict  $n_s$  extremely close to unity without much running. To be precise, when the radiative corrections dominate the slope of the potential, we obtain

$$n_s \simeq 1 - 1/\mathcal{N}_e \simeq 0.98, \quad (3.12)$$

for  $\mathcal{N}_e = 55$ . On the other hand, if the non-renormalizable operator  $|S|^4$  in  $V_{\text{SUGRA}}$  of (2.13) dominates the slope of the potential of a mSUGRA model with  $c_H = 0$  [12], we obtain a blue-tilted spectrum, with

$$n_s \simeq 1 + \frac{6M^2}{m_{\text{Pl}}^2 - 2M^2\mathcal{N}_e} \gtrsim 1. \quad (3.13)$$

A possible Hubble-induced positive term  $+c_H^2 H^2 |S|^2$  in  $V_{\text{SUGRA}}$  [27, 29] implies an even more pronounced blue spectrum and is therefore excluded by the current WMAP data.

As noticed earlier in [45] and elaborated further in Ref. [46], agreement of theory's prediction for  $n_s$  with observation strongly suggests the presence of a negative Hubble-induced mass term  $-c_H^2 H^2 |S|^2$  in  $V_{\text{SUGRA}}$ , thereby clearly disfavouring the minimal Kähler potential. In our analysis, we therefore consider the following next-to-minimal form for the Kähler manifold [27]:

$$K_S = |S|^2 + k_S \frac{|S|^4}{4m_{\text{Pl}}^2}, \quad (3.14)$$

where the constant  $k_S$  can be either positive or negative. Substituting (3.14) into the general formula for the  $F$ -term type contributions to the SUGRA potential (see, e.g. [8]),

$$V_F = e^{K_S/m_{\text{Pl}}^2} \left[ F^i (K_S^{-1})_i^j F_j - 3 \frac{|W|^2}{m_{\text{Pl}}^2} \right], \quad (3.15)$$

we arrive at the result (2.13) with  $c_H^2 = 3k_S$ , after neglecting higher-order terms that are small for  $|c_H| \lesssim 0.2$ . In (3.15),  $F^i$  are the SUGRA-generalized  $F$ -terms and  $(K_S^{-1})_i^j$  is the so-called inverse metric of the Kähler manifold, where a superscript (subscript) index  $i$  or  $j$  on  $K_S$  denotes differentiation with respect to  $S$  ( $S^*$ ).

The aforementioned nmSUGRA inflationary potential, with a negative Hubble-induced mass term, reaches a local minimum and maximum at the points  $\phi_{\min}$  and  $\phi_{\max}$ , respectively. These points can be estimated by

$$\phi_{\max} \simeq \frac{m_{\text{Pl}}}{4\pi c_H} \left( 6\kappa^2 \mathcal{N} + 12\lambda^2 + 9\rho^2 \right)^{1/2}, \quad \phi_{\min} \simeq \sqrt{\frac{2}{3}} c_H m_{\text{Pl}}. \quad (3.16)$$

For relevant parameter values, for which  $\phi_{\max} < \phi_{\min}$ , and under convenient initial conditions, the so-called hilltop inflation [45] can take place, where  $\phi$  rolls from  $\phi_{\max}$  down to smaller values, such that  $\phi_{\text{exit}} < \phi_{\max}$ . In this nmSUGRA scenario, the value of  $n_s$  can be significantly lowered and can be approximately given by

$$n_s \simeq 1 - \frac{1}{\mathcal{N}_e} - c_H^2. \quad (3.17)$$

As we will show more explicitly in the next section, the spectral index  $n_s$  can be easily driven into the range of (3.11), for values of  $c_H \sim 0.1$ . The presence of the second next-to-minimal term proportional to  $k_S$  in (3.14) modifies the analytic expressions of (3.1), (3.3) and (3.5) [46]. However, these modifications turn out to be numerically insignificant for the predicted values of  $\mathcal{N}_e$  and  $P_{\mathcal{R}}$ , if  $c_H$  is not very large, e.g.  $c_H \lesssim 0.2$ .

## 3.2 Numerical results

In our numerical estimates, we use the full expression for the inflationary potential  $V_{\text{inf}}$  given in (2.8), which consists of the tree-level, 1-loop and SUGRA contributions, given in (2.9), (2.12) and (2.13), respectively. We will ignore all soft SUSY-breaking terms, but the tadpole term  $a_S$ . To facilitate our numerical analysis, we introduce the real tadpole parameter  $a_S$ , which is defined, in terms of the Lagrangian parameter  $a_S$ , by the relation:

$$a_S = -2|a_S| \cos(\arg a_S + \arg S). \quad (3.18)$$

For any given value of  $\kappa$ ,  $\lambda$ ,  $\rho$ ,  $a_S$  and  $c_H$ , we determine  $\phi_{\text{exit}}$  and  $M$ , by imposing the conditions (3.1) and (3.5) for the number  $\mathcal{N}_e$  of  $e$ -folds and the power spectrum  $P_{\mathcal{R}}^{1/2}$ , respectively. In addition, we compute  $n_s$  by means of (3.9). Our results are presented in Fig. 1 for the mSUGRA scenario and in Fig. 3 for the nmSUGRA scenario. They will be analyzed in more detail in the following two subsections.

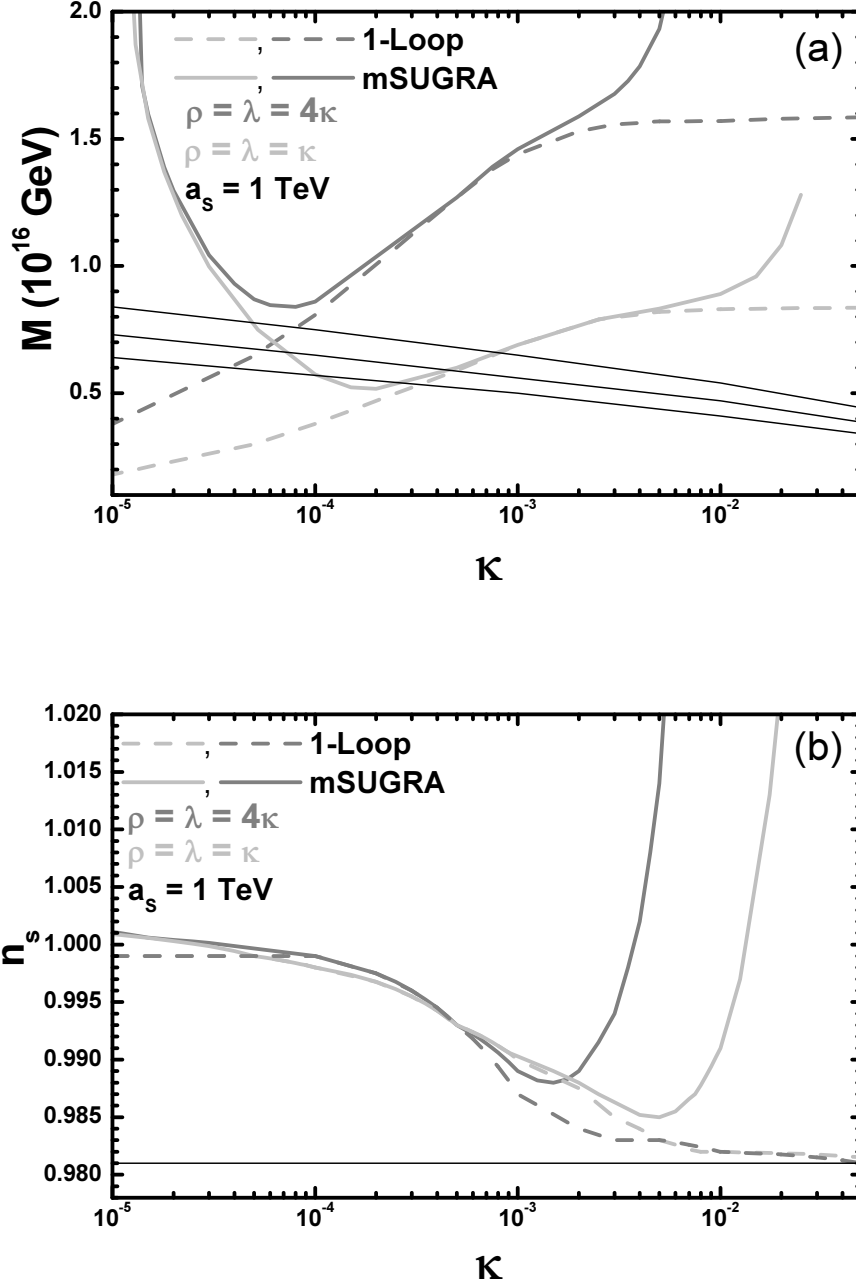


FIGURE 1: The values of the inflationary scale  $M$  allowed by (3.1) and (3.5) (a) and the predicted values of the spectral index  $n_s$  (b) as a function of  $\kappa$  for  $\mathcal{N} = 1$  and  $\rho = \lambda = \kappa$  (light grey lines) or  $\rho = \lambda = 4\kappa$  (grey lines), including the one-loop radiative corrections (dashed lines) or the mSUGRA ( $c_H = 0$ ) contributions with  $a_s = 1$  TeV (solid lines). The upper bound of (3.6) for  $y_{cs} = 6.7, 8.9, 11.6$  (from top to bottom) [cf. (3.10)] is also shown by thin lines (a) [(b)].

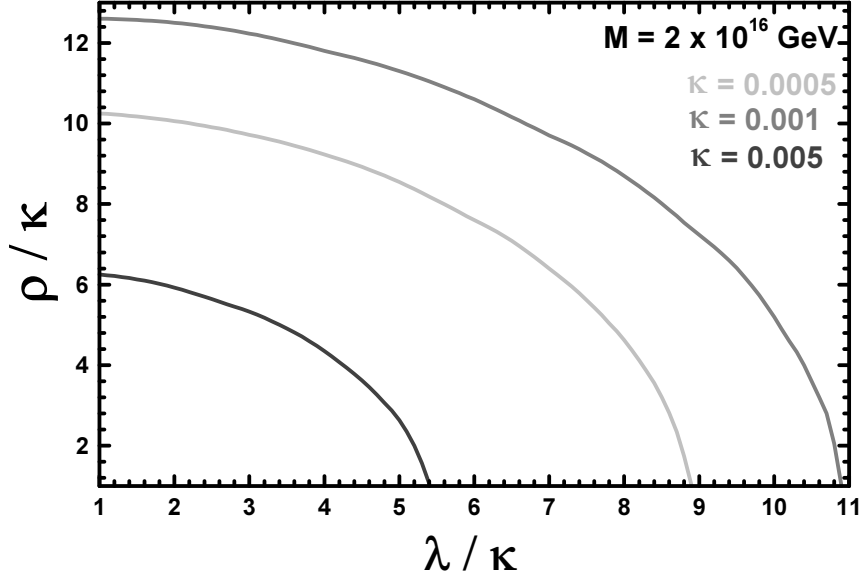


FIGURE 2: The allowed values of  $\lambda/\kappa$  versus  $\rho/\kappa$  for the mSUGRA scenario with  $M = 2 \times 10^{16}$  GeV and  $\kappa = 0.05$  (dark grey line),  $\kappa = 0.01$  (grey line) or  $\kappa = 0.005$  (light grey line).

### 3.2.1 The minimal SUGRA scenario

Here, we present numerical results for the mSUGRA scenario. The values of the inflationary scale  $M$  allowed by (3.1) and (3.5) and the predicted values of  $n_s$ , as functions of  $\kappa$ , for  $\rho = \lambda = \kappa$  (light grey lines) and  $\rho = \lambda = 4\kappa$  (grey lines), are displayed in Fig. 1(a) and 1(b), respectively. Dashed lines indicate results obtained, when only the 1-loop contribution to  $V_{\text{inf}}$  is considered and  $a_S$  is set to zero, whilst solid lines represent numerical values obtained, if the remaining contributions are included, namely those coming from (2.9) with  $a_S = 1$  TeV and (2.13) with  $c_H = 0$ . In Fig. 1, we observe that as the common value for  $\rho$ ,  $\lambda$  and  $\kappa$  increases,  $M$  and  $n_s$  increase as well. In particular,  $M$  gets closer to the GUT-scale value  $2 \times 10^{16}$  GeV for  $\kappa \sim 10^{-3}$ , unlike the case  $\lambda = \rho = 0$ , where  $M$  takes on much smaller values at this point [9, 12, 29].

It is now not difficult to identify in Fig. 1 the regimes, in which the different contributions to  $V_{\text{inf}}$  dominate. More explicitly, for  $\kappa \gtrsim 4 \times 10^{-3}$  and  $\rho = \lambda = \kappa$  or  $\kappa \gtrsim 10^{-3}$  and  $\rho = \lambda = 4\kappa$ , the non-renormalizable SUGRA term of (2.13) dominates and drives  $n_s$  to values close to or larger than 1 [cf. Fig. 1(b)]. On the other hand, for  $4 \times 10^{-4} \lesssim \kappa \lesssim 4 \times 10^{-3}$  and  $\rho = \lambda = \kappa$  or  $4 \times 10^{-4} \lesssim \kappa \lesssim 10^{-3}$  and  $\rho = \lambda = 4\kappa$ , the 1-loop corrections (2.12) dominate, in which case the spectral index  $n_s$  takes on the predicted value  $\sim 0.98$  given

Fig. 2			Fig. 5				
$M = 2 \times 10^{16}$ GeV			$\kappa = 0.005$ , $M = 10^{16}$ GeV				
$\kappa$	$\phi_{\text{exit}}$	$n_s$	$c_H$	$\phi_{\text{min}}$	$\phi_{\text{max}}$	$\phi_{\text{exit}}$	$n_s$
0.005	6.28	1.017	0.07	8.4	—	5.1	0.978
0.001	2.14	0.99	0.14	16.5	10.5	8.1	0.955
0.0005	1.51	0.99	0.18	21.7	12.8	11.2	0.941

TABLE 1: The values of  $\phi_{\text{exit}}$  (in units  $\sqrt{2}M$ ) and  $n_s$  for several  $\kappa$ 's along the curves in Fig. 2 and the values of  $\phi_{\text{min}}$ ,  $\phi_{\text{max}}$ ,  $\phi_{\text{exit}}$  (in units  $\sqrt{2}M$ ) and  $n_s$  for several  $c_H$ 's along the curves in Fig. 5.

in (3.12). Finally, for  $\kappa \lesssim 4 \times 10^{-3}$  and  $\rho = \lambda = \kappa$  or  $\rho = \lambda = 4\kappa$ , the tadpole term in (2.9) starts playing an important role. As  $M$  increases, the non-renormalizable SUGRA term of (2.13) becomes again important [12, 29]. In this case, the prediction for  $P_{\mathcal{R}}^{1/2}$  and  $n_s$  is almost independent of  $\rho$  and  $\lambda$ , as expected. For lower values of  $a_S$ , the solid lines in the latter regime would eventually approach the dashed lines [29]. In Fig. 1(b), we also indicate with a thin line the 95% CL upper limit on  $n_s$  stated in (3.11). Clearly, a mSUGRA version of the  $F_D$ -term hybrid model appears to be disfavoured by the most recent WMAP results.

In addition, we show in Fig. 1(a) upper limits due to cosmic string effects based on (3.6), for  $y_{\text{cs}} = 6.7, 8.9, 11.6$  (from top to bottom). Such constraints are only relevant for an Abelian realization of the waterfall-gauge sector. We observe that the presence of cosmic strings severely restrict the available parameter space of the  $U(1)_X$   $F_D$ -term hybrid model. As we discussed in Section 2.3, however, these constraints do no longer apply, if the waterfall-gauge sector realizes an  $SU(2)_X$  gauge symmetry. Since the dimensionality of the representation is  $\mathcal{N} = 2$  in this case, the allowed range of  $M$  as a function of  $\kappa$  slightly changes. In fact, the allowed values of  $M$  become marginally larger than the ones already shown in Fig. 1(a) by up to 12%, for  $\rho = \lambda = \kappa$ , while they stay at the 1% level, for  $\rho = \lambda = 4\kappa$ . Likewise, the predicted values of  $n_s$  remain almost unaffected at the 2% level, from those presented in Fig. 1(b). Obviously, as  $\rho$  and  $\lambda$  gets larger than  $\kappa$ , the difference between the  $\mathcal{N} = 1$  and  $\mathcal{N} = 2$  cases becomes practically unobservable.

Finally, in Fig. 2 we plot the allowed values of  $\lambda/\kappa$  versus  $\rho/\kappa$ , subject to the constraints (3.1) and (3.5), for  $M = 2 \times 10^{16}$  GeV (close to the GUT scale) and for different values of  $\kappa$ :  $\kappa = 0.005$  (dark grey line),  $\kappa = 0.001$  (grey line) or  $\kappa = 0.0005$  (light grey line). Along these contour lines,  $\phi_{\text{exit}}$  and  $n_s$  remain constant and equal to the values presented in Table 1. We observe that as  $\kappa$  increases,  $\phi_{\text{exit}}$  and  $n_s$  increase as well.



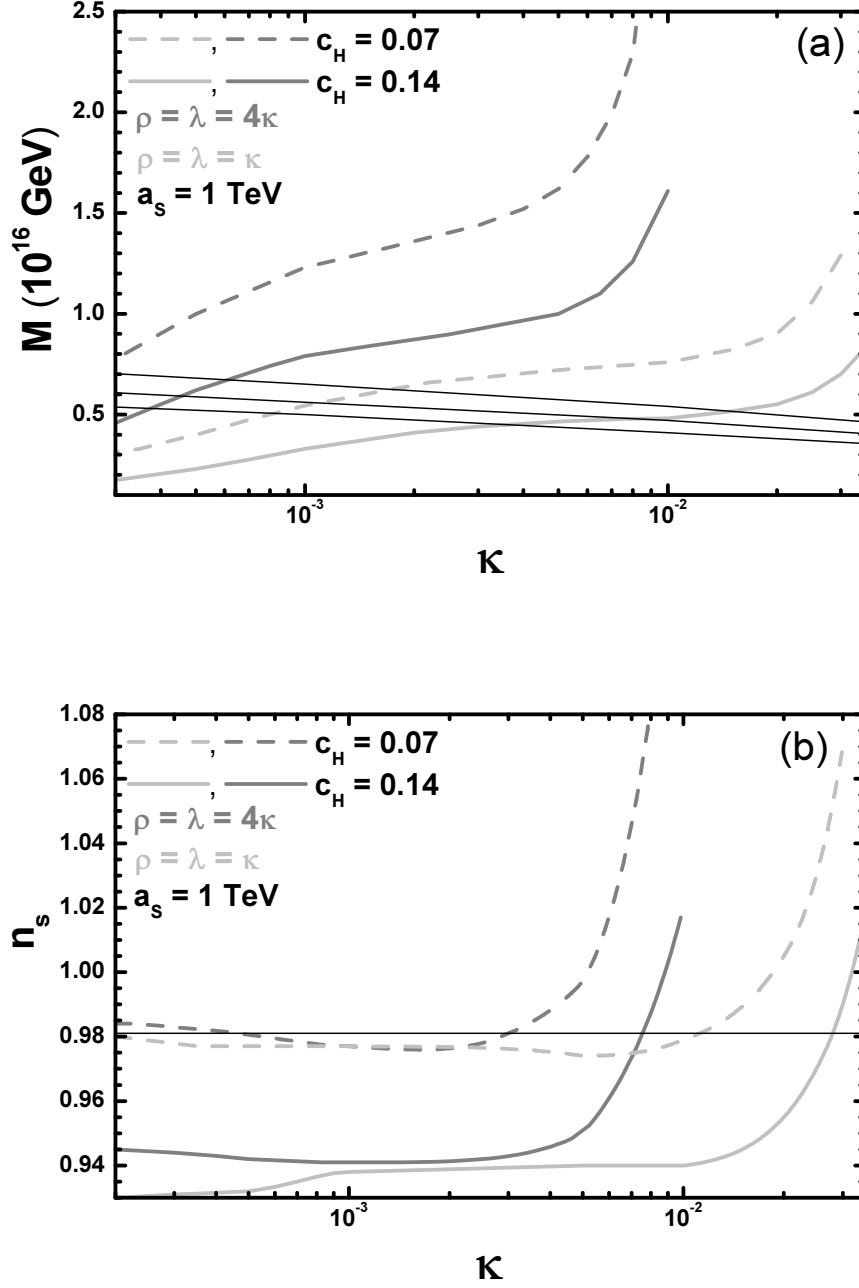


FIGURE 3: The values of the inflationary scale  $M$  allowed by (3.1) and (3.5) (a) and the predicted values of the spectral index  $n_s$  (b) as a function of  $\kappa$  for  $\mathcal{N} = 1$  and  $\rho = \lambda = \kappa$  (light grey lines) or  $\rho = \lambda = 4\kappa$  (grey lines), for the nmSUGRA scenario with  $c_H = 0.07$  (dashed lines) or  $c_H = 0.14$  (solid lines). In both cases we take  $a_s = 1$  TeV. The upper bound given in (3.6) (for  $y_{cs} = 6.7, 8.9, 11.6$  from top to bottom) [cf. (3.10)] is also depicted by thin lines (a) [(b)].

### 3.2.2 The next-to-minimal SUGRA scenario

We now turn our attention to the nmSUGRA scenario. Although we take the tadpole term to be  $a_S = 1$  TeV, its impact on our results turns out to be insignificant for the whole range of parameters we have scanned. The values of the inflationary scale  $M$  allowed by (3.1) and (3.5) and the predicted  $n_s$  as a function of  $\kappa$  are presented in Fig. 3(a) and 3(b), respectively, for  $\rho = \lambda = \kappa$  (light grey lines) and  $\rho = \lambda = 4\kappa$  (grey lines). We consider the two cases:  $c_H = 0.07$  (dashed lines) and  $c_H = 0.14$  (solid lines). As in the case of mSUGRA,  $M$  and  $n_s$  increase, with increasing  $\rho, \lambda$  and  $\kappa$ . Moreover, as  $\kappa$  decreases, the non-renormalizable SUGRA contribution in (2.13) becomes subdominant and  $n_s$  decreases. Such a reduction becomes even more drastic with increasing  $c_H$ , as can be easily inferred from Fig. 3(a), where the 95% CL upper bound on  $n_s$  [cf. (3.11)] is indicated with a thin horizontal line on the same plot. In stark contrast to the mSUGRA scenario, we observe that our model can become perfectly consistent with the recent WMAP result for  $0.04 \lesssim c_H \lesssim 0.22$ . Note that the various lines terminate at large values of  $\kappa$ , for which the two restrictions (3.1) and (3.5) cannot be simultaneously met.

It is interesting to further investigate the inflationary dynamics described by  $V_{\text{inf}}$  in the presence of a negative Hubble-induced mass term. To this end, we exhibit in Table 2 the values of  $c_H$ ,  $\phi_{\text{min}}$ ,  $\phi_{\text{max}}$ ,  $\phi_{\text{exit}}$  (in units  $\sqrt{2}M$ ) and the inflationary scale  $M$  (in units of  $10^{16}$  GeV) which are obtained for different values of  $\kappa$ , assuming that  $\lambda = \rho = \kappa$  or  $\lambda = \rho = 4\kappa$ , and for fixed values of  $n_s$ , i.e.  $n_s = 0.913, 0.951, 0.981$ , compatible with the 95% CL limits given in (3.11). In addition, we present values for the parameter  $\Delta_{\text{exit}} = (\phi_{\text{max}} - \phi_{\text{exit}})/\phi_{\text{exit}}$ , which somehow quantifies the degree of tuning required in the initial conditions of inflation. The entries without a value assigned (in Tables 1 and 2) mean that the respective inflationary potential  $V_{\text{inf}}$  has no distinguishable nearby local maximum  $\phi_{\text{max}}$ . We notice from Table 2, that as  $n_s$  decreases with fixed values of  $\kappa$ ,  $c_H$  increases while  $M$  and  $\Delta_{\text{exit}}$  decrease. Moreover, for fixed values of  $n_s$  and decreasing  $\kappa$ ,  $c_H$  and  $M$  decrease and  $\phi_{\text{exit}}$  approaches  $\phi_{\text{max}}$ . On the contrary, with increasing  $\kappa$ ,  $\lambda$  and  $\rho$ , the inflationary scale  $M$  increases and the parameter  $\Delta_{\text{exit}}$  becomes larger. We have checked that the inequality  $\phi_{\text{max}} > \phi_{\text{exit}}$  is fulfilled along the lines presented in Fig. 3. In this respect, we also note that  $\phi_{\text{min}}$  is in general much larger than  $\phi_{\text{max}}$  especially for low values of  $n_s$ .

It is important to observe from Table 2 that there is a degree of tuning required for the values  $\phi_{\text{exit}}$  with respect to  $\phi_{\text{max}}$ . For values of  $\kappa \gtrsim 10^{-3}$ , we find that the degree of tuning required is not very serious, i.e.  $\Delta_{\text{exit}} \gtrsim 10\%$ . However, the situation becomes rather delicate as  $\kappa$  gets smaller than  $10^{-3}$ , for  $n_s \lesssim 0.97$ . In this case, we find that  $\phi_{\text{max}} \approx \phi_{\text{exit}}$ ,

$\kappa$	$c_H$	$M$	$\phi_{\min}$	$\phi_{\max}$	$\phi_{\text{exit}}$	$\Delta_{\text{exit}}$	$c_H$	$M$	$\phi_{\min}$	$\phi_{\max}$	$\phi_{\text{exit}}$	$\Delta_{\text{exit}}$	$c_H$	$M$	$\phi_{\min}$	$\phi_{\max}$	$\phi_{\text{exit}}$	$\Delta_{\text{exit}}$
	$n_s = 0.913$						$n_s = 0.951$						$n_s = 0.981$					
$\lambda = \rho = \kappa$																		
0.01	0.179	0.34	73.6	11.9	11.3	0.050	0.130	0.53	32.0	10.8	8.75	0.19	0.065	0.78	16.7	—	7.50	—
0.005	0.176	0.34	73.1	6.0	5.7	0.053	0.120	0.53	32.2	6.2	4.48	0.18	0.040	0.78	8.20	—	3.90	—
0.001	0.173	0.25	95.6	1.64	1.6	0.028	0.120	0.38	45.0	1.55	1.42	0.09	0.060	0.58	19.0	2.10	1.36	0.34
0.0005	0.165	0.19	121	1.23	1.21	0.014	0.116	0.28	58.8	1.19	1.15	0.04	0.060	0.43	20.0	1.37	1.13	0.17
$\lambda = \rho = 4\kappa$																		
0.01	0.216	0.56	49	23.0	22.0	0.046	0.190	0.83	23.0	21.9	17.0	0.22	0.169	1.12	26.0	—	14.3	—
0.005	0.188	0.61	41	11.4	10.8	0.050	0.146	0.96	26.0	9.1	8.30	0.19	0.103	1.36	8.6	—	7.05	—
0.001	0.177	0.57	43	2.48	2.38	0.043	0.125	0.89	24.6	2.28	1.96	0.14	0.058	1.30	4.7	—	1.82	—
0.0005	0.178	0.46	54	1.53	1.49	0.028	0.129	0.68	26	1.45	1.33	0.08	0.070	1.00	9.6	1.83	1.30	0.29

TABLE 2: The values of  $c_H$ ,  $M$  (in units  $10^{16}$  GeV)  $\phi_{\min}$ ,  $\phi_{\max}$ ,  $\phi_{\text{exit}}$  (in units  $\sqrt{2}M$ ) and  $\Delta_{\text{exit}} = (\phi_{\max} - \phi_{\text{exit}})/\phi_{\max}$ , for selected values of  $\kappa$ ,  $\lambda$  and  $\rho$ , and for fixed values of the spectral index  $n_s$ .

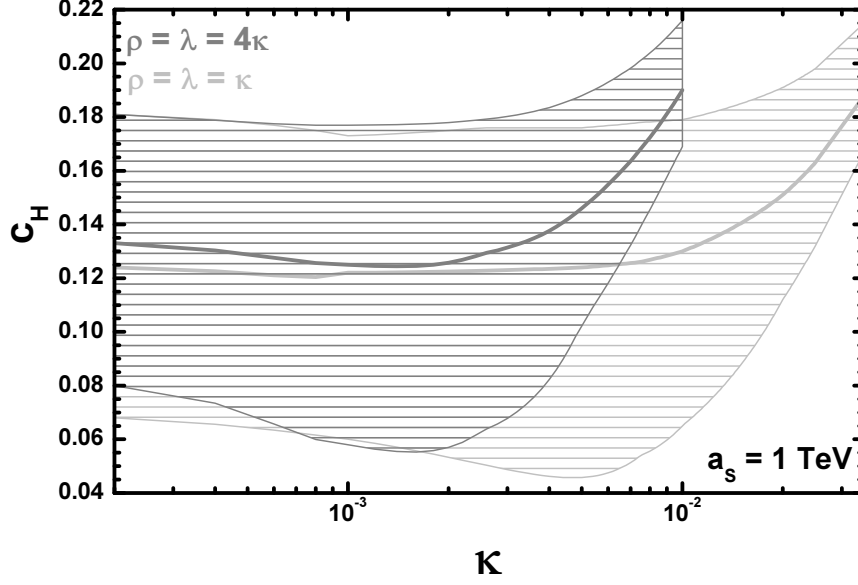


FIGURE 4: The parameter values  $(\kappa, c_H)$  allowed by (3.1), (3.5) and (3.10) in the nmSUGRA scenario, for  $\rho = \lambda = \kappa$  (light grey hatched area) and  $\rho = \lambda = 4\kappa$  (grey hatched area). The grey (light grey) line has been obtained by fixing  $n_s$  to its central value given in (3.10), for  $\rho = \lambda = 4\kappa$  ( $\rho = \lambda = \kappa$ ).

leading to a substantial tuning at the few per cent level in the initial conditions of inflation.

As in the mSUGRA case, we also show in Fig. 3(a) the upper bounds resulting from cosmic-string effects [cf. (3.6)], for  $y_{cs} = 6.7, 8.9, 11.6$  (from top to bottom). As mentioned above, these constraints are only relevant for an Abelian waterfall-gauge sector with dimensionality  $\mathcal{N} = 1$ . However, unlike in the mSUGRA case, these restrictions appear less harmful, since the inflationary scale  $M$  assumes smaller values (see also Table 2) and the tadpole term becomes unimportant. Thus, larger values of  $\kappa$  up to order  $10^{-2}$  can be tolerated in this case. For the non-Abelian  $SU(2)_X$   $F_D$ -term hybrid model, the restrictions from considerations of cosmic-string effects are totally lifted and the lines depicted in Fig. 3 only vary within the few per cent level. Such a variation becomes even smaller if  $\rho > \kappa$  and/or  $\lambda > \kappa$ .

In Fig. 4, we present the parameter space  $(\kappa, c_H)$  which is allowed by the conditions (3.1), (3.5) and (3.10) in the nmSUGRA scenario. The light grey (grey) hatched area indicates the allowed region for  $\rho = \lambda = 4\kappa$  ( $\rho = \lambda = \kappa$ ). The lower (upper) boundaries of the allowed regions correspond to the upper (lower) bound on  $n_s$ , cf. (3.11), while the solid lines correspond to the central value of  $n_s$ , cf. (3.10). We find that values of  $c_H \sim 0.2$  and

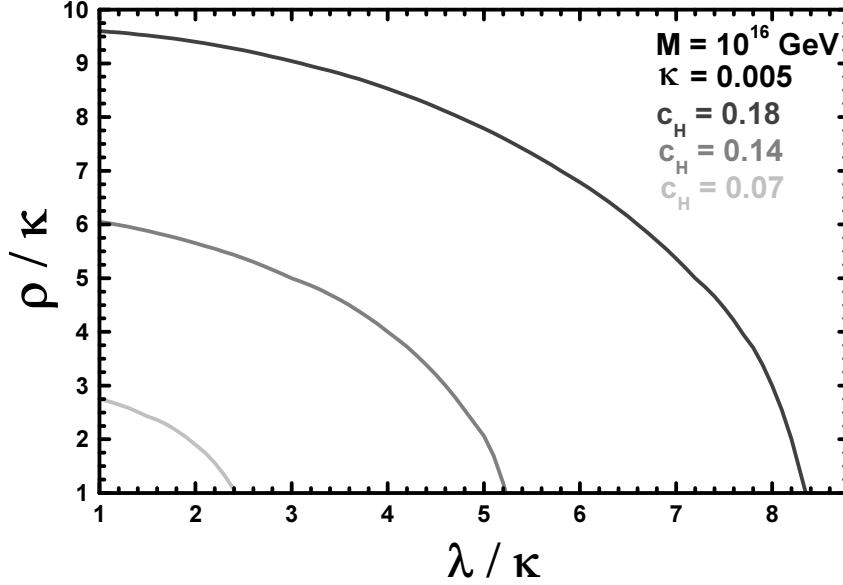


FIGURE 5: *The allowed values of  $\rho/\kappa$  versus  $\lambda/\kappa$  for the nmSUGRA scenario with  $\kappa = 0.005$ ,  $M = 10^{16}$  GeV and  $c_H = 0.18$  (dark grey line),  $c_H = 0.14$  (grey line) or  $c_H = 0.07$  (light grey line).*

$\kappa \sim 0.05$  are still possible in a nmSUGRA extension of the  $F_D$ -term hybrid model.

Finally, we plot in Fig. 5 the allowed values of  $\lambda/\kappa$  versus  $\rho/\kappa$ , on account of the inflationary constraints (3.1) and (3.5), for  $\kappa = 0.005$ ,  $M = 10^{16}$  GeV, and for  $c_H = 0.18$  (dark grey line),  $c_H = 0.14$  (grey line) and  $c_H = 0.07$  (light grey line). We have selected a slightly lower value for  $M$ , because no viable nmSUGRA scenarios seem to exist with acceptable values for  $n_s$ , if  $M = 2 \times 10^{16}$  GeV and  $c_H \geq 0.07$ . Along the contour lines in Fig. 5,  $\phi_{\min}$ ,  $\phi_{\max}$ ,  $\phi_{\text{exit}}$  and  $n_s$  remain constant and equal to the values presented in Table 1. We observe that as  $c_H$  increases,  $\phi_{\text{exit}}$  approaches  $\phi_{\max}$ ,  $\phi_{\min}$  increases, while  $n_s$  decreases. This kinematic behaviour is in agreement with our discussion related to (3.16) and (3.17).

## 4 Preheating

As stated in the Introduction, gravitinos, if thermally produced during the early stages of the evolution of the Universe, will spoil the successful predictions of BBN [47]. Their disastrous consequences may be avoided, if the reheat temperature  $T_{\text{reh}}$  of the Universe is not very high. In fact, depending on the decay properties of the gravitino, it should be

$T_{\text{reh}} \lesssim 10^7\text{--}10^{10}$  GeV [51, 56]. This fact leads to a tension between the allowed range of  $T_{\text{reh}}$  and the natural scale of hybrid inflation  $M$ , which is of order  $\sim 10^{16}$  GeV. The traditional way taken to get around this problem is to consider scenarios where the decay rate of the inflaton to SM particles is extremely suppressed, e.g. by suppressing all possible couplings of the inflaton to the SM fields.

In this and next sections, we present in detail an alternative solution to the above gravitino overabundance problem [13]. Our solution relies on the huge entropy release caused from the late out-of-equilibrium decays of the supermassive waterfall particles. The entropy produced through this mechanism is sufficient to reduce the gravitino abundance  $Y_{\tilde{G}}$  to levels compatible with BBN limits discussed in detail in Section 5. Figure 6 gives a schematic representation of the post-inflationary dynamics of the early Universe, as is predicted by the  $F_D$ -term hybrid model. Shortly after inflation ends, the energy density  $\rho_\kappa$  of the Universe is predominantly stored to coherently oscillating inflaton condensates which scale as  $a^{-3}$ , where  $a$  is the usual cosmological scale factor describing the expansion of the Universe. The coherent oscillations of the inflaton-related condensates also give rise to another non-perturbative mechanism called preheating. During preheating, waterfall gauge particles of energy density  $\rho_g$  are produced almost instantaneously, which are absolutely stable if a  $D$ -parity, an analogue of the usual  $R$ -parity in the MSSM, is conserved. Then, the following scenario visualized in Fig. 6 emerges. First,  $\rho_g/\rho_\kappa$  remains constant during the epoch of coherent oscillations, since both  $\rho_g$  and  $\rho_\kappa$  behave as matter energy densities and scale as  $a^{-3}$  during this period. The constancy of  $\rho_g/\rho_\kappa$  ceases to hold, when the coherently oscillating inflaton condensates decay and their energy density  $\rho_\kappa$  gets distributed among light relativistic degrees of freedom. As a consequence of the latter,  $\rho_\kappa$  will be  $\propto a^{-4}$ , whilst  $\rho_g$  will still be  $\propto a^{-3}$ . If the initial value of  $\rho_g/\rho_\kappa$  is not very suppressed, e.g. it is of order  $10^{-4}\text{--}10^{-5}$ , the waterfall gauge particles will eventually dominate the energy density of the Universe, leading to a second matter dominated epoch which will last until these particles decay via  $D$ -parity violating couplings. This is expected to produce an enormous entropy release and so reduce the gravitino-to-entropy ratio  $Y_{\tilde{G}}$  to values compatible with BBN constraints.

The discussion in this section is organized as follows: in Section 4.1, we pay special attention to  $D$ -parity and derive the particle spectrum of the combined inflaton-waterfall sector in the supersymmetric limit of the theory. In addition, we compute the decay rates of all inflaton-related and waterfall gauge particles. Finally, in Section 4.2, we discuss how the waterfall gauge particles are instantaneously produced through preheating and calculate the resulting energy density  $\rho_g$  carried by these particles.

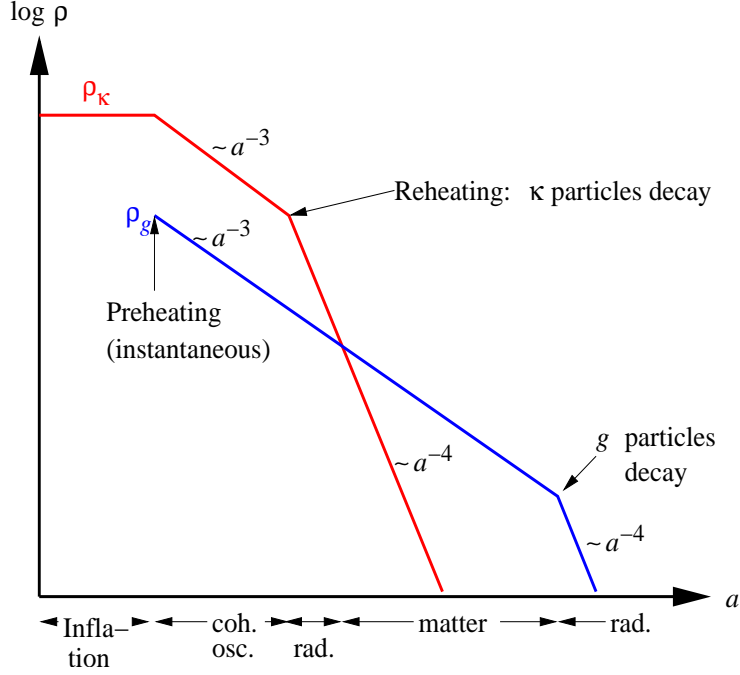


FIGURE 6: Schematic representation of the thermal history of the Universe in the  $F_D$ -term hybrid model.

## 4.1 $D$ -Parities and the Inflaton-Waterfall Sector

Let us first consider a model with a  $U(1)_X$  gauge-symmetric waterfall sector. The case of a waterfall sector realizing a non-Abelian  $SU(2)_X$  gauge symmetry is analogous and will be discussed later. In terms of superfields, the minimal gauge-kinetic Lagrangian of the  $U(1)_X$  model reads:

$$\mathcal{L}_{\text{kin}} = \int d^4\theta \left( \frac{1}{2} W^\alpha W_\alpha \delta^{(2)}(\bar{\theta}) + \frac{1}{2} \bar{W}_{\dot{\alpha}} \bar{W}^{\dot{\alpha}} \delta^{(2)}(\theta) + \hat{X}_1^\dagger e^{2g\hat{V}_X} \hat{X}_1 + \hat{X}_2^\dagger e^{-2g\hat{V}_X} \hat{X}_2 \right), \quad (4.1)$$

where  $\hat{V}_X$  is the  $U(1)_X$  vector superfield and  $W_\alpha$  ( $\bar{W}_{\dot{\alpha}}$ ) are their respective chiral (anti-chiral) field strengths. The latter are given by

$$W_\alpha = -\frac{1}{8g} \bar{D}^2 (e^{-2g\hat{V}_X} D_\alpha e^{2g\hat{V}_X}), \quad \bar{W}_{\dot{\alpha}} = \frac{1}{8g} D^2 (e^{2g\hat{V}_X} \bar{D}_{\dot{\alpha}} e^{-2g\hat{V}_X}), \quad (4.2)$$

where  $D_\alpha$  and  $\bar{D}_{\dot{\alpha}}$  are the usual SUSY-covariant derivatives which are irrelevant for our discussion here. The minimal gauge-kinetic Lagrangian (4.1) possesses the discrete symmetry

$$D: \quad \hat{X}_1 \leftrightarrow \hat{X}_2, \quad \hat{V}_X \rightarrow -\hat{V}_X, \quad (4.3)$$

whereas all other superfields do not transform. It is not difficult to verify that the complete  $F_D$ -term hybrid model, including the superpotential (2.1) and its associated soft SUSY-breaking sector, is invariant under the discrete symmetry (4.3) in the unbroken phase of the theory. After the SSB of  $U(1)_X$ , the waterfall fields receive the VEVs:  $\langle X_1 \rangle = \langle X_2 \rangle = M$ . Thus, the above discrete symmetry survives even in the spontaneously broken phase of the theory. Since the discrete symmetry acts on a gauged waterfall sector, it manifests itself as a kind of parity, which we call  $D$ -parity.

It therefore proves convenient to choose a weak basis where the fields are eigenstates of  $D$ -parity. To this end, we define the linear combinations in terms of the waterfall superfields

$$\hat{X}_\pm = \frac{1}{\sqrt{2}} \left( \hat{X}_1 \pm \hat{X}_2 \right). \quad (4.4)$$

Evidently, the superfield  $\hat{X}_+$  ( $\hat{X}_-$ ) has even (odd)  $D$ -parity; its  $D$ -parity quantum number is  $+1$  ( $-1$ ). The vector superfield  $\hat{V}_X$ , which is already a  $D$ -parity eigenstate, has odd  $D$ -parity. All remaining fields, including the inflaton superfield  $\hat{S}$  and the other MSSM superfields, have positive  $D$ -parity.

As a consequence of  $D$ -parity conservation, all  $D$ -odd particles will be stable, in as much the same way as the usual  $R$ -parity guarantees that the LSP of the MSSM is stable. As we explicitly mentioned in Section 2.1, the simplest way to break  $D$ -parity is to add a FI  $D$ -term to the model, e.g.

$$\mathcal{L}_{\text{FI}} = -\frac{g}{2} m_{\text{FI}}^2 \int d^4\theta \hat{V}_X = -\frac{g}{2} m_{\text{FI}}^2 D, \quad (4.5)$$

where  $D$  is the auxiliary component of the vector superfield  $\hat{V}_X$ . It is obvious that  $\mathcal{L}_{\text{FI}}$  flips sign under the discrete symmetry (4.3). Other mechanisms of explicitly breaking  $D$ -parity are discussed in Appendix A.

We now calculate the particle spectrum of the inflaton-waterfall sector in the presence of a subdominant FI  $D$ -term  $m_{\text{FI}}$  and in the supersymmetric limit of the theory. With this aim, we expand the scalar  $D$ -parity eigenstates  $X_\pm$  about their VEVs:

$$X_\pm = \langle X_\pm \rangle + \frac{1}{\sqrt{2}} \left( R_\pm + iI_\pm \right). \quad (4.6)$$

The VEVs  $\langle X_\pm \rangle$  are determined from the minimization conditions of the combined  $F$ - and  $D$ -term scalar potential

$$V_{FD} = F_S^* F_S + \frac{1}{2} D^2, \quad (4.7)$$



where

$$F_S = \frac{\kappa}{2} \left( X_+^2 - X_-^2 - 2M^2 \right), \quad D = \frac{g}{2} \left( X_+^* X_- + X_-^* X_+ - m_{\text{FI}}^2 \right). \quad (4.8)$$

Since SUSY is preserved after the SSB of  $U(1)_X$ , the scalar potential  $V_{FD}$  will vanish at its ground state, i.e.  $\langle V_{FD} \rangle = 0$ . Consequently, to leading order in  $m_{\text{FI}}/M$ , the VEVs of the scalar inflaton-waterfall fields are

$$\langle S \rangle = 0, \quad \langle X_+ \rangle = \sqrt{2}M, \quad \langle X_- \rangle = \frac{v}{\sqrt{2}}, \quad (4.9)$$

where  $v = m_{\text{FI}}^2/(2M)$ . Notice that the VEVs of the  $F$ - and  $D$ -terms vanish through order  $m_{\text{FI}}/M$  considered, i.e.  $\langle D \rangle = 0$  and  $\langle F_S \rangle = \mathcal{O}(m_{\text{FI}}^4/M^2)$ .

To derive the mass spectrum, we expand the potential about its ground state up to terms quadratic in all the fields involved. We first consider the  $F$ -terms. To order  $v/M$  ( $= m_{\text{FI}}^2/M^2$ ), we find the approximate mass eigenstates:

$$S = \frac{1}{\sqrt{2}} \left( \phi + ia \right), \quad R_+ - \frac{v}{2M} R_-, \quad I_+ - \frac{v}{2M} I_- . \quad (4.10)$$

All the above fields, consisting of 4 bosonic degrees of freedom in total, share the common mass

$$m_\kappa = \sqrt{2} \kappa M . \quad (4.11)$$

As a consequence of SUSY, the corresponding 4 fermionic degrees of freedom form a Dirac spinor  $\psi_\kappa$ , which also has the same mass (4.11). We refer to these particles as inflaton-related or  $\kappa$ -sector particles.

The remaining scalar fields receive their masses from the  $D$ -term of the scalar potential  $V_{FD}$  in (4.7). Performing an analogous calculation as outlined above, we obtain to order  $v/M$  the scalar mass eigenstates:

$$I_- + \frac{v}{2M} I_+, \quad R_- + \frac{v}{2M} R_+ . \quad (4.12)$$

The first field is absorbed by the longitudinal component of the  $U(1)_X$  gauge field  $V_\mu$ , via the Higgs mechanism. In the supersymmetric limit, all these fields, which mediate 4 bosonic degrees of freedom, are degenerate and characterized by the common mass

$$m_g = g M . \quad (4.13)$$

Like in the  $\kappa$ -sector case, the respective 4 fermionic degrees of freedom will make up a 4-component Dirac spinor of mass  $m_g$ . We refer to this group of particles as waterfall gauge or  $g$ -sector particles. In Table 3, we present a summary of all the inflaton-related ( $\kappa$ -sector)

Sector	Boson	Fermion	Mass
Inflaton ( $\kappa$ -sector) $D$ -parity: +1	$S$ , $R_+ - \frac{v}{2M}R_-$ , $I_+ - \frac{v}{2M}I_-$	$\psi_\kappa = \begin{pmatrix} \psi_{X_+} - \frac{v}{2M}\psi_{X_-} \\ \psi_S^\dagger \end{pmatrix}$	$\sqrt{2}\kappa M$
$U(1)_X$ Waterfall Gauge ( $g$ -sector) $D$ -parity: -1	$V_\mu [I_- + \frac{v}{2M}I_+]$ , $R_- + \frac{v}{2M}R_+$	$\psi_g = \begin{pmatrix} \psi_{X_-} + \frac{v}{2M}\psi_{X_+} \\ -i\lambda^\dagger \end{pmatrix}$	$gM$

TABLE 3: Particle spectrum of the inflaton and the  $U(1)_X$  waterfall-gauge sectors after inflation, where the approximate  $D$ -parity for each sector is displayed. The field  $V_\mu$  denotes the  $U(1)_X$  gauge boson and  $\lambda$  its associate gaugino. The would-be Goldstone boson related to the longitudinal degree of  $V_\mu$  appears in the square brackets.

and waterfall-gauge ( $g$ -sector) particles. As can also be seen from the same Table 3,  $\kappa$ -sector particles are predominantly  $D$ -even, whereas the  $g$ -sector ones have approximately  $D$ -odd parity.

It is now interesting to calculate the decay rates of the  $\kappa$ - and  $g$ -sector particles and analyze their implications for the reheat temperature of the Universe. Starting with the singlet field  $S$ , it decays predominantly into pairs of charged and neutral higgsinos,  $\tilde{h}_{u,d}^\pm$ ,  $\tilde{h}_{u,d}^0$ ,  $\tilde{\bar{h}}_{u,d}^0$ , and into pairs of right-handed Majorana neutrinos  $\nu_{1,2,3R}$ . On the other hand, the scalars  $R_+$  and  $I_+$  decay into the SUSY-conjugate partners of the aforementioned fields at the same rate. In fact, we find a common decay rate for each of the  $\kappa$ -sector particles:

$$\Gamma_\kappa = \frac{1}{32\pi} \left( 4\lambda^2 + 3\rho^2 \right) m_\kappa. \quad (4.14)$$

The reheat temperature  $T_\kappa$  resulting from these perturbative decays of the  $\kappa$ -sector particles may be estimated using the relation  $\Gamma_\kappa = H(T_\kappa)$ , where the Hubble parameter  $H(T)$  is given in the radiation dominated era of the Universe. In this way, we obtain

$$T_\kappa = \left( \frac{90}{\pi^2 g_*} \right)^{1/4} \sqrt{\Gamma_\kappa m_{\text{Pl}}}, \quad (4.15)$$

where  $g_* = 240$  is the number of the relativistic degrees of freedom in the  $F_D$ -term hybrid model. Substituting (4.14) and (4.11) into (4.15), we arrive at the expression:

$$T_\kappa = 8.1 \cdot 10^{15} \text{ GeV} \times \left[ \kappa(4\lambda^2 + 3\rho^2) \right]^{1/2} \left( \frac{M}{10^{16} \text{ GeV}} \right)^{1/2}. \quad (4.16)$$

Assuming that no relevant amount of entropy is released during the subsequent thermal history of the Universe, the gravitino constraint on the reheat temperature  $T_\kappa \lesssim 10^9$  GeV requires that each individual coupling  $\kappa$ ,  $\lambda$  and  $\rho$  must be smaller than about  $10^{-5}$ , if  $M \sim 10^{16}$  GeV. Further details are given in Section 5.

The above unnatural tuning of all inflaton couplings to SM fields may be avoided, if the large entropy release from the late decays of the  $g$ -sector particles is properly considered. An extensive discussion of this issue is given in Section 5. Here, we simply compute the decay rates of the  $g$ -sector particles which are induced by a non-vanishing FI term  $m_{\text{FI}}$ . In fact, the relevant interaction Lagrangian is given by

$$\mathcal{L}_{\text{int}} = \frac{g^2 m_{\text{FI}}^2}{8M} R_- (R_+^2 + I_+^2). \quad (4.17)$$

As mentioned above, this induces a decay width for the  $D$ -odd particle  $R_-$ , which is easily calculated to be

$$\Gamma_g = \frac{g^3}{128\pi} \frac{m_{\text{FI}}^4}{M^3}. \quad (4.18)$$

In close analogy with the  $\kappa$ -sector, each  $g$ -sector particle decay rate is equal to  $\Gamma_g$ .

Let us now consider a model with a waterfall sector based on the  $\text{SU}(2)_X$  gauge group. As was mentioned in Section 2.1, the waterfall superfields  $\hat{X}_1$  and  $\hat{X}_2$  are chosen to belong in this case to the 2-component fundamental and anti-fundamental representations of  $\text{SU}(2)_X$ , respectively. Although the two representations are equivalent for the  $\text{SU}(2)$  case, we nevertheless use this convention, such that its generalization to  $\text{SU}(N)$  theories, with  $N > 2$ , is straightforward. The superpotential is almost identical to the one given in (2.1), with the obvious substitution:  $\hat{X}_1 \hat{X}_2 \rightarrow \hat{X}_1^T \hat{X}_2$ . Extending (4.1) to the  $\text{SU}(2)_X$  case, the minimal gauge-kinetic Lagrangian is written down

$$\begin{aligned} \mathcal{L}_{\text{kin}} = \int d^4\theta \left[ \frac{1}{2} \text{Tr} (W^\alpha W_\alpha) \delta^{(2)}(\bar{\theta}) + \frac{1}{2} \text{Tr} (\bar{W}_{\dot{\alpha}} \bar{W}^{\dot{\alpha}}) \delta^{(2)}(\theta) \right. \\ \left. + \hat{X}_1^\dagger e^{2g\hat{V}_X} \hat{X}_1 + \hat{X}_2^\dagger e^{-2g\hat{V}_X^T} \hat{X}_2 \right]. \end{aligned} \quad (4.19)$$

In the above,  $\hat{V}_X = \hat{V}_X^a T^a$  is the  $\text{SU}(2)_X$  vector superfield and  $W_\alpha = W_\alpha^a T^a$  ( $\bar{W}_{\dot{\alpha}} = \bar{W}_{\dot{\alpha}}^a T^a$ ) are the corresponding non-Abelian chiral (anti-chiral) field strengths in the so-called Wess–Zumino (WZ) gauge. The superscript ‘ $T$ ’ on  $\hat{V}_X$ , i.e.  $\hat{V}_X^T$ , indicates transposition that acts on the generators  $T^a = \frac{1}{2}\tau^a$  of the  $\text{SU}(2)$  group, where  $\tau^{1,2,3}$  are the usual Pauli matrices. Finally, the trace in (4.19) is understood to be taken over the group space.

The minimal  $\text{SU}(2)_X$  gauge-kinetic Lagrangian is invariant under the discrete transformations

$$D_1 : \quad \hat{X}_1 \leftrightarrow \hat{X}_2, \quad \hat{V}_X \rightarrow -\hat{V}_X^T. \quad (4.20)$$

Notice that under the action of  $D_1$  in (4.20), the field strengths transform as:  $W_\alpha \rightarrow -(W_\alpha)^T$  and  $\overline{W}_{\dot{\alpha}} \rightarrow -(\overline{W}_{\dot{\alpha}})^T$  in *any* SUSY gauge, including the WZ gauge. If all other superfields do not transform, the complete Lagrangian of the non-Abelian  $F_D$ -term hybrid model will be invariant under the discrete transformation (4.20) in the unbroken phase of the theory.

Our discussion so far has made no reference to the specific properties of  $SU(2)_X$  and so applies equally well to any  $SU(N > 2)$  theory. However, in the  $SU(2)_X$  case, the  $F_D$ -term hybrid model exhibits an additional Abelian or diagonal discrete symmetry. This may be defined by

$$D_2 : \quad \widehat{X}_1 \rightarrow \tau^3 \widehat{X}_1, \quad \widehat{X}_2 \rightarrow \tau^3 \widehat{X}_2, \quad \widehat{V}_X \rightarrow \tau^3 \widehat{V}_X \tau^3, \quad (4.21)$$

whereas all other superfields do not transform. It is then easy to see that (4.21) implies:  $W_\alpha \rightarrow \tau^3 W_\alpha \tau^3$  in any SUSY gauge and likewise for  $\overline{W}_{\dot{\alpha}}$ . Since  $\tau^3 = (\tau^3)^T$  and  $(\tau^3)^2 = \mathbf{1}_2$ , the invariance of the Lagrangian (4.19) and of the whole model under the action of  $D_2$  is evident.<sup>4</sup>

We now proceed to compute the particle spectrum of the non-Abelian  $F_D$ -term hybrid model after the SSB of  $SU(2)_X$ . For this purpose, it is useful to introduce the notation

$$Z = \begin{pmatrix} +Z \\ -Z \end{pmatrix}, \quad (4.22)$$

where  $Z$  is a generic  $SU(2)_X$ -doublet or anti-doublet (conjugate) field. The left superscripts  $\pm$  on  $Z$  denote the eigenvalues of the discrete symmetry transformation operator  $D_2 = \tau^3$  defined in (4.21), and they should not be confused with the corresponding eigenvalues of the isospin operator  $T^3$  of the  $SU(2)_X$  group. In the unitary gauge, the minimum of the scalar potential occurs for the field values

$$+X_1 = +X_2 = M, \quad -X_1 = -X_2 = 0. \quad (4.23)$$

Consequently, the discrete symmetries  $D_1$  and  $D_2$  given in (4.20) and (4.21) remain intact after the SSB of the  $SU(2)_X$  gauge group. Since they act on a gauged waterfall sector, they are actually parities. We refer to them as  $D_1$ - and  $D_2$ -parities, or collectively as  $D$ -parities.

---

<sup>4</sup>In general, for a waterfall-gauge sector based on an  $SU(N > 2)$  group, there are  $N$  distinct discrete symmetries. The first is given by (4.20), while the remaining  $N - 1$  symmetries result from replacing  $\tau^3$  with  $D_n = \text{diag}(1, 1, \dots, 1, -1, 1, \dots, 1)$ . The entry  $-1$  occurs at the  $n$  position of the  $N$ -dimensional diagonal matrix  $D_n$ , with the restriction  $1 < n \leq N$ . Obviously, it is  $D_n = D_n^T$  and  $D_n^2 = \mathbf{1}_N$ . These discrete symmetries are non-Abelian in the adjoint group space, in the sense that the eigenvalue matrix  $c^{ab}$ , determined by means of the relation  $D_n T^a D_n = c^{ab} T^b$ , is not diagonal.

Sector	Boson	Fermion	Mass	$D_1$ -parity	$D_2$ -parity
Inflaton ( $\kappa$ -sector)	$S, {}^+R_+, {}^+I_+$	$\psi_\kappa = \begin{pmatrix} \psi_{+X_+} \\ \psi_S^\dagger \end{pmatrix}$	$\sqrt{2}\kappa M$	+	+
SU(2) $_X$ Waterfall Gauge ( $g$ -sector)	$V_\mu^1[-I_-],$ $-R_-;$	$\psi_g^1 = \begin{pmatrix} \psi_{-X_-} \\ -i\lambda^{1\dagger} \end{pmatrix}$	$gM$	-	-
	$V_\mu^2[-R_+],$ $-I_+;$	$\psi_g^2 = \begin{pmatrix} i\psi_{-X_+} \\ -i\lambda^{2\dagger} \end{pmatrix}$	$gM$	+	-
	$V_\mu^3[+I_-],$ $+R_-$	$\psi_g^3 = \begin{pmatrix} \psi_{+X_-} \\ -i\lambda^{3\dagger} \end{pmatrix}$	$gM$	-	+

TABLE 4: *Particle spectrum of the inflaton and an SU(2) $_X$ -gauged waterfall sectors after inflation. The would-be Goldstone bosons of the respective SU(2) $_X$  gauge fields are given in the square brackets*

Analogously to the U(1) $_X$  case, we express the SU(2) $_X$  doublets  $X_{1,2}$  in terms of eigenstates of the  $D_{1,2}$ -parities [cf. (4.4)]. In terms of their components, these fields may be conveniently expressed as follows:

$${}^\pm X_\pm = \langle X_\pm \rangle + \frac{1}{\sqrt{2}} \left( {}^\pm R_\pm + i {}^\pm I_\pm \right), \quad (4.24)$$

with  $\langle X_+ \rangle = \sqrt{2}M$  and  $\langle X_- \rangle = 0$  in the absence of any  $D$ -parity violating coupling in the theory. Moreover, the SU(2) $_X$   $D$ -terms are given by

$$D^a = \frac{g}{2} \left( X_1^\dagger \tau^a X_1 - X_2^T \tau^a X_2^* \right). \quad (4.25)$$

In the  $D$ -parity eigenbasis (4.4), they take on the form

$$D^a = \frac{g}{2} \times \begin{cases} X_+^\dagger \tau^a X_- + X_-^\dagger \tau^a X_+, & \text{for } \tau^a \text{ symmetric } (a = 1, 3) \\ X_+^\dagger \tau^a X_+ + X_-^\dagger \tau^a X_-, & \text{for } \tau^a \text{ antisymmetric } (a = 2) \end{cases}. \quad (4.26)$$

Exactly as in the U(1) $_X$  case, we find that there are two groups of mass-degenerate fields,  $\kappa$ - and  $g$ -sector, with masses  $m_\kappa$  and  $m_g$  given in (4.11) and (4.13), respectively. The complete inflaton-waterfall spectrum, along with their  $D_1$  and  $D_2$  parities, is exhibited in Table 4.

The conservation of both  $D_{1,2}$ -parities enforces the stability of all  $g$ -sector particles. Instead, if only the  $D_1$ -parity, but not  $D_2$ , is conserved, then only the  $D_1$ -odd particles from Table 4 will be stable, and *vice versa*. Obviously, both  $D_1$ - and  $D_2$ -parities need be broken

to make all  $g$ -sector particles unstable. In Appendix A, we discuss possible mechanisms of explicit  $D$ -parity breaking for an  $SU(2)_X$  waterfall-gauge sector. In general, there are two mechanisms for breaking  $D$ -parity. The first one consists of including higher-order non-renormalizable operators in the Kähler potential whose presence explicitly breaks  $D$ -parity, whilst the second one is very analogous to the  $U(1)_X$  case. Although a bare FI  $D$ -term is not possible in non-Abelian theories, effective  $D^a$ -tadpole terms may appear after the SSB of  $SU(2)_X$ . The effective  $D^a$ -tadpole terms do not break SUSY. They get generated either from a non-renormalizable Kähler potential or are induced radiatively, after integrating out Planck-scale degrees of freedom. Thus, without excessive tuning, the effective  $D^a$ -tadpole terms can in general be small of the size required to obtain a second reheat phase in the evolution of the Universe.

Independently of the mechanism which is invoked to break  $D$ -parity, we may in general parameterize the  $g$ -sector particle decay rates through the  $D$ -parity-violating mass  $m_{\text{FI}}$ , which enters the relation (4.18). In the next section, we will discuss how these relatively long-lived  $g$ -sector particles are produced via preheating.

## 4.2 Preheating and Thermalization

After the inflaton field  $\phi$  passes below a certain critical value  $\phi_c \approx M$ , the so-called waterfall mechanism gets triggered. In this case, the inflaton  $\phi$  and all other  $\kappa$ -sector fields (see Tables 3 and 4) oscillate about their true supersymmetric minima:  $\langle S \rangle = 0$  and  $\langle X_+ \rangle = \sqrt{2} M$ . In this waterfall epoch, most of the energy density of the Universe is stored to these coherently oscillating  $\kappa$ -sector field condensates and is given initially by  $\rho_\kappa = \kappa^2 M^4$ . During the waterfall regime, however, there is an additional mechanism for particle production called *preheating*.

In general, there are two phenomena associated with the notion of preheating:

- The first effect of preheating arises from the negative curvature of the potential with respect to the  $\kappa$ -sector fields. Such a negative curvature corresponds to a negative tachyonic mass term in the potential. As a consequence, the particle number within infrared modes of momentum less than this tachyonic mass grows exponentially. This phenomenon is known as the *negative coupling instability* or *tachyonic preheating* [48]. Numerical simulations have shown that the field amplitudes suffer strong damping during the first oscillation, due to the energy transfer to the infrared modes. In the  $F_D$ -term hybrid model, only  $\kappa$ -sector particles are produced by tachyonic preheating. A full study of this process, including thermal equilibration of the  $\kappa$ -sector particles, is

a highly nontrivial matter and has so far only been achieved for very particular models of preheating. Since the fraction of the energy density transferred instantaneously to  $\kappa$ -sector particles through tachyonic preheating is rather small, compared to their initial energy density  $\rho_\kappa$ , these model-dependent details fortunately have no dramatic impact on the expansion and the thermal history of the Universe. Therefore, we do not consider the phenomenon of tachyonic preheating in the  $F_D$ -term hybrid model.

- Particle production may also occur during the coherent oscillation regime, because both the  $\kappa$ - and  $g$ -sector particles have masses that can vary very strongly with time. This effect is called *preheating via a time-varying mass* or simply *preheating* [49, 50]. As we will show below, a small but significant fraction of the total energy density of the Universe  $\rho_\kappa$  can be transferred, almost instantaneously, to the  $g$ -sector particles, e.g.  $\rho_g \sim 10^{-4} \rho_\kappa$ , for  $\kappa \sim 10^{-2}$ . As we illustrated in the beginning of this section and will show more explicitly in Section 5, this small fraction of the  $g$ -sector energy density is sufficient to alter dramatically the thermal history of the Universe.

Our interest lies therefore in computing the production energy density  $\rho_g$  of the  $g$ -sector particles via preheating. A key element in such a computation is the profile of the time-varying mass of the  $g$ -sector particles,  $m_g(t) = g X_+(t)/\sqrt{2}$ . The exact time dependence of  $m_g(t)$  depends crucially on the dynamics of tachyonic preheating. Comparative numerical studies strongly suggest that a sufficiently accurate description of the time evolution of the  $g$ -sector mass is obtained by [50]<sup>5</sup>

$$m_g(t) = \frac{gM}{2} \left[ \tanh(\kappa Mt) + 1 \right]. \quad (4.27)$$

Notice that the time-dependent function  $m_g(t)$  properly interpolates between the values  $m_g(t \rightarrow -\infty) = 0$  and  $m_g(t \rightarrow \infty) = gM$  that occur in the beginning and the end of the waterfall epoch, respectively.

Given the time-dependent mass (4.27), we may compute the occupation number of the fermionic  $g$ -sector modes by solving the Dirac equation

$$\left[ i\gamma^0 \partial_t - \boldsymbol{\gamma} \cdot \mathbf{k} - m_g(t) \right] u_h(t) = 0. \quad (4.28)$$

---

<sup>5</sup>To be specific, the mass-term time-variation studied in [50] was for a model with a single field rolling from the top of a local maximum of a quartic potential. It was found that a tanh-functional dependence accurately captures the evolution of the time-varying mass. Even though the model considered [50] is still different from our hybrid inflationary potential, the derived tanh-functional profile for the time-varying mass should be regarded as a substantial improvement over the one assumed in [13].

The solution to the above equation may be expressed by the time-dependent Dirac spinor  $u_h(t)$  in the chiral representation:

$$u_h(t) = \begin{pmatrix} L_h(t) \\ R_h(t) \end{pmatrix} \otimes \xi_h, \quad (4.29)$$

where  $\xi_h$  is the helicity two-component eigenspinor for helicity  $h = \pm$ . The occupation number of Dirac fermions produced via preheating in the true supersymmetric vacuum at  $t \rightarrow \infty$  is given by

$$n_h^F(k) = \frac{1}{2\omega(k)} \left[ hk(|R_h|^2 - |L_h|^2) - m_g(L_h R_h^* + L_h^* R_h) \right] + \frac{1}{2}, \quad (4.30)$$

where  $k = |\mathbf{k}|$  is the modulus of the 3-momentum. With the help of (4.30), the  $k$ -mode energy density is calculated by  $\rho(k) = \sum_h \omega(k) n_h^F(k)$ , where  $\omega(k) = \sqrt{k^2 + m_g^2(t \rightarrow \infty)}$ . To obtain a unique solution to the linear differential equation (4.28), we impose initial conditions that correspond to a zero occupation number, i.e.  $n_h^F(k) = 0$ . These are given at  $t \rightarrow -\infty$  by

$$L_h = \sqrt{\frac{\omega(k) + hk}{2\omega}}, \quad R_h = \sqrt{\frac{\omega(k) - hk}{2\omega}}. \quad (4.31)$$

By analogy, the occupation number of the bosonic  $g$ -sector modes are determined by solving the Klein–Gordon equation of motion

$$\left[ \partial_t^2 + \mathbf{k}^2 + m_g^2(t) \right] \varphi(t) = 0, \quad (4.32)$$

and imposing the initial conditions at  $t \rightarrow -\infty$ ,

$$\varphi = \frac{1}{2\sqrt{\omega(k)}}, \quad \frac{\partial \varphi}{\partial t} = -i\sqrt{\frac{\omega}{2}}. \quad (4.33)$$

As in the Dirac case, these initial conditions correspond to vanishing occupation numbers. The occupation number of the bosonic modes at  $t \rightarrow \infty$  is given by

$$n^B(k) = \frac{1}{2} \omega(k) |\varphi|^2 + \frac{1}{2\omega(k)} \left| \frac{d\varphi}{dt} \right|^2 - \frac{1}{2}. \quad (4.34)$$

Using the time-dependent mass-term (4.27), along with the initial conditions (4.31) and (4.34), one may obtain analytical expressions in terms of hypergeometric functions [50], for the particle production between  $t \rightarrow -\infty$  and  $t \rightarrow \infty$ . For  $\kappa \ll g$  and  $k \ll gM$ , these analytical expressions reduce to

$$n(k) = \frac{2}{\exp\left(\frac{\pi k}{\kappa M}\right) \pm 1}, \quad (4.35)$$



where the sign  $+$  applies for  $n(k) = n_h^F(k)$  and the sign  $-$  for  $n(k) = n^B(k)$ . Recalling that there are 2 helicity states for a  $g$ -sector fermion and 4 real degrees of freedom for a  $g$ -sector boson, we may calculate the occupation number of all  $g$ -sector modes as follows:

$$n_g(k) = N_b \left( \sum_{h=\pm} n_h^F(k) + 4n^B(k) \right), \quad (4.36)$$

where  $N_b$  is the number of broken generators of the waterfall gauge symmetry. In particular, it is  $N_b = 1$  for  $U(1)_X$  and  $N_b = 3$  for  $SU(2)_X$  [cf. Tables 3 and 4]. Since the produced particles are non-relativistic, i.e.  $k \ll gM$ , their occupation number distribution  $n_g(k)$  can easily be integrated to give the total energy density carried by the  $g$ -sector fields, i.e.

$$\frac{\rho_g}{\rho_\kappa} \approx \frac{gM}{\rho_\kappa 2\pi^2} \int_0^\infty k^2 dk n_g(k) \approx 2.1 \times 10^{-2} N_b \kappa g. \quad (4.37)$$

Here  $\rho_\kappa = \kappa^2 M^4$  is the energy density of the  $\kappa$ -sector particles shortly before the waterfall transition. Equation (4.37) will be a valuable input for the next section to compute the true reheat temperature  $T_{\text{reh}}$  of the Universe, which arises from the combined effect of the  $\kappa$ - and  $g$ -sector particle decays.

## 5 Coupled Reheating and Gravitino Abundance

In the previous section, we have seen that the  $g$ -sector particles, e.g.  $\psi_g$ ,  $R_-$  and  $V_\mu$ , can be abundantly produced during the preheating epoch. Assuming that they dominate the Universe at some later time, their decays induced by the small  $D$ -parity violating couplings will give rise to a second reheat temperature, which we denote here by  $T_g$ . As we will show in this section, the large entropy, which is released by the late decays of the  $g$ -sector particles, will be sufficient to dilute the gravitinos to levels compatible with BBN limits.

More explicitly, we present a detailed numerical analysis of the gravitino abundance  $Y_{\tilde{G}}$ , where the combined effect of the  $\kappa$ - and  $g$ -sector particle decays is carefully taken into account. As we mentioned in the Introduction, we call such a two-states' mechanism of reheating the Universe *coupled reheating*. In Section 5.1, we set the BEs relevant to coupled reheating and give numerical estimates of the gravitino abundance  $Y_{\tilde{G}}$  and the energy densities  $\rho_\kappa$ ,  $\rho_g$  and  $\rho_{\text{rad}}$  related to the  $\kappa$ - and  $g$ -sector particles and their radiation, respectively. In Section 5.2, we present a semi-analytic approach to BEs, where useful approximate expressions for  $Y_{\tilde{G}}$  are obtained. Finally, in Section 5.3 we derive gravitino abundance constraints on the theoretical parameters.

## 5.1 Boltzmann Equations

The number density  $n_{\tilde{G}}$  of gravitinos, the energy density  $\rho_{\kappa}$  ( $\rho_g$ ) of the  $\kappa$  ( $g$ )-sector particles and the energy density  $\rho_{\text{rad}}$  of the radiation produced by their decays satisfy the following system of BEs [53]:

$$\begin{aligned} \dot{n}_{\tilde{G}} + 3Hn_{\tilde{G}} &= C_{\tilde{G}} T^6, \\ \dot{\rho}_{\kappa} + 3H\rho_{\kappa} &= -\Gamma_{\kappa} \rho_{\kappa}, \\ \dot{\rho}_g + 3H\rho_g &= -\Gamma_g \rho_g, \\ \dot{\rho}_{\text{rad}} + 4H\rho_{\text{rad}} &= \Gamma_{\kappa} \rho_{\kappa} + \Gamma_g \rho_g, \end{aligned} \quad (5.1)$$

where a dot on  $n_{\tilde{G}}$ ,  $\rho_{\kappa,g}$  and  $\rho_{\text{rad}}$  indicates differentiation with respect to the cosmic time  $t$ . The quantity  $C_{\tilde{G}}(T)$  is a collision term for gravitino production calculated in [51, 52] and the Hubble parameter  $H$  is given by

$$H = \frac{1}{\sqrt{3} m_{\text{Pl}}} \left( m_{\tilde{G}} n_{\tilde{G}} + \rho_{\kappa} + \rho_g + \rho_{\text{rad}} \right)^{1/2}, \quad (5.2)$$

where  $m_{\tilde{G}}$  is the mass of the gravitino  $\tilde{G}$ . In addition, the temperature  $T$  and the entropy density  $s$  may be determined through the relations:

$$\rho_{\text{rad}} = \frac{\pi^2}{30} g_* T^4, \quad s = \frac{2\pi^2}{45} g_* T^3, \quad (5.3)$$

where  $g_*(T)$  is the effective number of degrees of freedom at temperature  $T$ . Since the initial temperature is  $T_{\text{in}} \ll \kappa M$ , it is  $g_* = 240$  for all  $T > M_{\text{SUSY}}$ .

Here we should note that in BEs (5.1) we have neglected the collision terms related to the self-annihilation of  $g$ -sector particles. Their thermally averaged cross section times velocity,  $\langle \sigma_{\text{ann}} v \rangle$ , is estimated to be

$$\langle \sigma_{\text{ann}} v \rangle \lesssim 10^{-35} \text{ GeV}^{-2}, \quad (5.4)$$

which is numerically negligible.

The numerical analysis of the BEs (5.1) gets simplified by absorbing the Hubble expansion terms into new variables. To this end, we define the following dimensionless quantities [54]:

$$f_{\tilde{G}} = n_{\tilde{G}} a^3, \quad f_{\kappa} = \rho_{\kappa} a^3, \quad f_g = \rho_g a^3, \quad f_{\text{rad}} = \rho_{\text{rad}} a^4. \quad (5.5)$$

where  $a$  is the usual expansion scale factor of the Universe. We also convert the time derivatives to derivatives with respect to the logarithmic time  $\ln(a/a_I)$  [55], where  $a_I$  is

some initial or reference value for the scale factor  $a$ . With the above substitutions, the BEs (5.1) may be re-written as

$$\begin{aligned} H f'_{\tilde{G}} &= C_{\tilde{G}} T^6 a^3, \\ H f'_{\kappa} &= -\Gamma_{\kappa} f_{\kappa}, \\ H f'_g &= -\Gamma_g f_g, \\ H f'_{\text{rad}} &= \Gamma_{\phi} f_{\phi} a + \Gamma_g f_g a, \end{aligned} \quad (5.6)$$

where the prime now denotes differentiation with respect to  $\ln(a/a_I)$ . Correspondingly, the Hubble parameter  $H$  and temperature  $T$  may now be expressed in terms of the newly introduced variables (5.5) as follows:

$$H = \frac{1}{\sqrt{3} a^{3/2} m_{\text{Pl}}} \left( m_{\tilde{G}} f_{\tilde{G}} + f_{\kappa} + f_g + a^{-1} f_{\text{rad}} \right)^{1/2}, \quad T = \left( \frac{30 f_{\text{rad}}}{\pi^2 g_* a^4} \right)^{1/4}. \quad (5.7)$$

The transformed system of BEs (5.6) can be numerically solved by imposing the following initial conditions:

$$f_{\kappa, \text{I}} a_{\text{I}}^3 = \kappa^2 M^4, \quad f_{g, \text{I}} a_{\text{I}}^3 = 2.1 \times 10^{-2} g \kappa^3 M^4, \quad f_{\text{rad}, \text{I}} = 0, \quad (5.8)$$

where the subscript I refers to quantities defined at  $\ln(a/a_I) = 0$ . Notice that the initial value  $f_{g, \text{I}} a_{\text{I}}^3$  is equal to the energy density  $\rho_{g, \text{I}}$  of the  $g$ -sector particles produced during preheating and is given in (4.37).

In Fig. 7(a), we present numerical estimates of the cosmological evolution of energy densities  $\rho_{\kappa, g, \text{rad}}$  as functions of the temperature  $T$  in a double  $x$ - $y$  logarithmic plot, where  $\rho_{\kappa}$  is represented by a dark grey line,  $\rho_g$  by a grey line and  $\rho_{\text{rad}}$  by a light grey line. As an example, we use  $M = 0.7 \times 10^{16}$  GeV,  $\rho = \lambda = \kappa = 10^{-3}$  and  $m_{\text{FI}}/M = 4.3 \times 10^{-7}$  (bold lines) and  $m_{\text{FI}}/M = 10^{-3}$  (thin lines). Since  $\rho_{\text{rad}}$  is affected very little for the larger value of  $m_{\text{FI}}/M$ , it has not been added to the plot. The intersection point of the  $T$ -dependent functions  $\rho_{\kappa}$  and  $\rho_{\text{rad}}$  signals the completion of the  $\kappa$ -sector particle decays. For the specific example, this point occurs at  $T_{\kappa} = 3.2 \times 10^{11}$  GeV. For  $m_{\text{FI}}/M = 4.3 \times 10^{-7}$  GeV, we obtain two more intersections: one for  $T = T_{\text{eq}} \simeq 3.9 \times 10^6$  GeV where  $\rho_g(T_{\text{eq}}) = \rho_{\text{rad}}(T_{\text{eq}})$  and another one for  $T = T_g \simeq 200$  GeV, where the  $g$ -sector particles have practically decayed away and  $\rho_g(T_g) = \rho_{\text{rad}}(T_g)$ . Thanks to the huge entropy release in this case, the gravitino abundance  $Y_{\tilde{G}} = n_{\tilde{G}}/s$  gets sharply decreased from about  $2.2 \times 10^{-11}$  to  $2.4 \times 10^{-15}$ . This dramatic reduction of  $Y_{\tilde{G}}$  is shown in Fig. 7(b). On the contrary, if  $m_{\text{FI}}/M = 10^{-3}$ , no intersection of  $\rho_g$  with  $\rho_{\text{rad}}$  takes place and, in consequence, no phase of second reheating occurs. This is also illustrated in Fig. 7(a), where the dependence of  $\rho_g$  is displayed by a thin line. As can be seen from Fig. 7(b), the gravitino abundance  $Y_{\tilde{G}}$  remains unsuppressed in this case, i.e.  $Y_{\tilde{G}} \sim 10^{-10}$ . As we will see below in Section 5.3, such large values of  $Y_{\tilde{G}}$  are in gross conflict with BBN constraints.

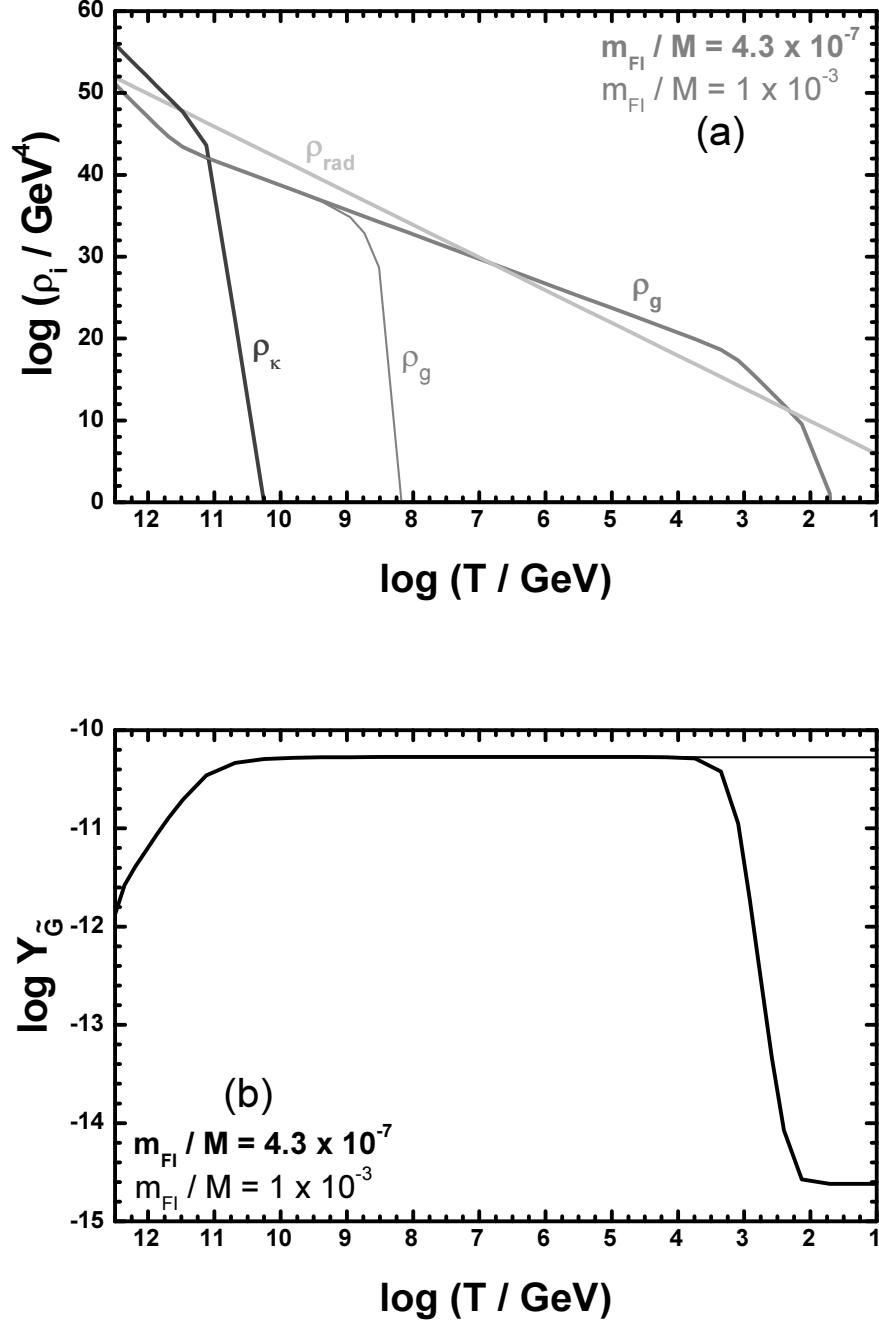


FIGURE 7: The evolution as a function of  $\log T$  of the quantities: (a)  $\log \rho_i$  with  $i = \kappa$  (dark grey line),  $i = g$  (grey line),  $i = \text{rad}$  (light grey line) (b)  $\tilde{G}$  yield,  $Y_{\tilde{G}}$ . In both cases, we take  $M = 0.7 \times 10^{16}$  GeV,  $\rho = \lambda = \kappa = 0.001$  and  $m_{\text{FI}}/M = 4.3 \times 10^{-7}$  GeV (bold lines) and  $m_{\text{FI}}/M = 1 \times 10^{-3}$  (thin lines).

## 5.2 Semi-analytic Approach

We now present a more intuitive and rather accurate approach to the dynamics of coupled reheating, and find approximate analytical expressions that describe the evolution of the energy densities  $\rho_{\kappa,g,\text{rad}}$ . In addition, we derive the conditions that ensure the existence of a second reheat phase in the evolution of the Universe. Finally, we estimate the gravitino abundance  $Y_{\tilde{G}}$  due to coupled reheating.

Shortly after inflation ends, the energy of our observable Universe is dominated by the inflaton  $S$  and the other  $\kappa$ -sector particles, with an initial energy density  $\rho_{\kappa,\text{I}} = \kappa^2 M^4$ . As we schematically illustrated in Section 4.2, the  $\kappa$ -sector particles decay into relativistic degrees of freedom, producing an energy density  $\rho_{\text{rad}}$ . The energy density  $\rho_g$  of the  $g$ -sector particles is subdominant at these early stages after the first reheating due to the  $\kappa$ -sector particle decays. In fact, for temperatures  $T > T_{\text{eq}}$ , where  $T_{\text{eq}}$  is the first intersection point of the  $T$ -dependent functions  $\rho_{\text{rad}}$  and  $\rho_g$  [see (5.10)], the evolution of all relevant energy densities may be approximately described as follows:

$$\rho_{\kappa} = \rho_{\kappa,\text{I}} (a/a_{\text{I}})^{-3}, \quad \rho_g = \rho_{g,\text{I}} (a/a_{\text{I}})^{-3}, \quad \rho_{\text{rad}} = \rho_{\text{rad}}(T_{\kappa}) (T/T_{\kappa})^4. \quad (5.9)$$

As mentioned above, the  $T$ -dependent function  $\rho_{\text{rad}}$  may first cross the corresponding  $\rho_g$  at  $T = T_{\text{eq}}$ , where

$$\rho_{\text{rad}}(T_{\text{eq}}) = \rho_g(T_{\text{eq}}). \quad (5.10)$$

Using the fact that  $\rho_{\text{rad}}(T_{\kappa}) = \rho_{\kappa}(T_{\kappa})$  and assuming that the Universe expands isentropically with  $a \propto T^{-1}$  when  $T_{\text{eq}} \leq T \leq T_{\kappa}$ , we obtain from (5.10) the approximate relation

$$T_{\text{eq}} \simeq T_{\kappa} \frac{\rho_{g,\text{I}}}{\rho_{\kappa,\text{I}}}. \quad (5.11)$$

In deriving (5.11), we have also made use of (5.9).

A second reheat phase in the evolution of the Universe takes place, only if  $T_g < T_{\text{eq}}$ , where  $T_g$  is the naive reheat temperature due to the  $g$ -sector particles decays [see (5.20) below]. To better explore the consequences of this last condition, we use the abbreviation  $g$ -DAD ( $g$ -DBD) to indicate whether the  $g$ -sector particles Decay After (Before) the Domination of their energy density. With the aid of (5.11), the following two conditions for  $g$ -DAD and  $g$ -DBD may be deduced:

$$\frac{T_g}{T_{\kappa}} < \frac{\rho_{g,\text{I}}}{\rho_{\kappa,\text{I}}} \quad (g\text{-DAD}), \quad \frac{T_g}{T_{\kappa}} \geq \frac{\rho_{g,\text{I}}}{\rho_{\kappa,\text{I}}} \quad (g\text{-DBD}). \quad (5.12)$$

These two possible scenarios are illustrated in Fig. 7 for  $m_{\text{FI}}/M = 4.3 \times 10^{-7}$  ( $m_{\text{FI}}/M = 10^{-3}$ ), where the bold (thin) lines correspond to  $g$ -DAD ( $g$ -DBD).

The gravitino abundance  $Y_{\tilde{G}}$  can be calculated by simply integrating  $f'_{\tilde{G}}$  that occurs in the first BE of (5.6) and using the fact that  $Y_{\tilde{G}} = f_{\tilde{G}}/sa^3$ . It turns out that the main contribution to  $Y_{\tilde{G}}$  comes from the integration after the commencement of the radiation dominated era, i.e. for  $T \leq T_\kappa$ . The so-derived formula reproduces rather accurately the one presented in [51] in the massless gluino limit, where

$$Y_{\tilde{G}}^\kappa = 1.6 \times 10^{-12} \left( \frac{T_\kappa}{10^{10} \text{ GeV}} \right). \quad (5.13)$$

Note that (5.13) is only valid for the  $g$ -DBD case.

The situation is different for the  $g$ -DAD case, where a drastic reduction of the gravitino abundance, caused by the huge entropy release from the  $g$ -sector particle decays, takes place. In this case, the gravitino abundance  $Y_{\tilde{G}}^g$  may be estimated in the following way. We first notice that

$$Y_{\tilde{G}}^g = Y_{\tilde{G}}^\kappa \frac{s(T_{\text{eq}}) a^3(T_{\text{eq}})}{s(T_g) a^3(T_g)}. \quad (5.14)$$

Then, with the help of (5.3) and (5.9), we may obtain the relation

$$\frac{s(T_{\text{eq}}) a^3(T_{\text{eq}})}{s(T_g) a^3(T_g)} = \left( \frac{T_{\text{eq}}}{T_g} \right)^3 \left( \frac{\rho_g(T_{\text{eq}})}{\rho_g(T_g)} \right)^{-1} = \frac{T_g}{T_{\text{eq}}}. \quad (5.15)$$

Substituting the respective expressions of (5.15), (5.13) and (5.11) into (5.14) yields

$$Y_{\tilde{G}}^g = 1.6 \times 10^{-12} \left( \frac{T_g}{10^{10} \text{ GeV}} \right) \frac{\rho_{\kappa, \text{I}}}{\rho_{g, \text{I}}} \simeq \frac{7.6 \times 10^{-11}}{\kappa g} \left( \frac{T_g}{10^{10} \text{ GeV}} \right), \quad (5.16)$$

where we have used (4.37) to derive the last approximate equality. We have checked that the semi-analytic formula (5.16) is in remarkable agreement with numerical estimates in the  $g$ -DAD regime.

Finally, we should comment on the fact that the number of  $e$ -folds,  $\mathcal{N}_e$  gets modified in the  $g$ -DAD case, because of the occurrence of a  $g$ -sector-matter dominated era. Making use of standard methods [6, 8], we are able to determine  $\mathcal{N}_e$  at the WMAP pivotal point  $k_0 = 0.002 \text{ Mpc}^{-1}$  by the following relation:

$$\mathcal{N}_e = 22.6 + \frac{1}{6} \ln(\kappa^2 M^4) + \frac{1}{3} \ln T_g + \frac{1}{3} \ln \frac{\rho_{\kappa, \text{I}}}{\rho_{g, \text{I}}}. \quad (5.17)$$

This result, however, does not crucially alter the value of  $\mathcal{N}_e$ , which remains close to 55–60 in the  $g$ -DAD case as well. Interestingly enough,  $Y_{\tilde{G}}^g$  and  $\mathcal{N}_e$  do not directly depend on  $T_\kappa$  given in (4.15). In fact, in the  $g$ -DAD case,  $Y_{\tilde{G}}^g$  and  $\mathcal{N}_e$  are fully independent of the superpotential couplings  $\lambda$  and  $\rho$ , and only have a mild linear and logarithmic dependence on  $\kappa$ , respectively. As we will discuss below, it is this last property that leads to a significant relaxation of the strict gravitino constraints on these couplings, when compared to the  $g$ -DBD case.

### 5.3 Gravitino Abundance Constraints

In order to avoid destroying the apparent success between the standard theory for BBN and observation, gravitinos must have an abundance  $Y_{\tilde{G}}$  below certain upper limits, which crucially depend on their decay properties [51, 56]. Some representative upper bounds on  $Y_{\tilde{G}}$ , obtained in a very recent analysis [51], are

$$Y_{\tilde{G}} \lesssim \begin{cases} 10^{-15}, & \text{for } m_{\tilde{G}} \simeq 360 \text{ GeV}, \\ 10^{-14}, & \text{for } m_{\tilde{G}} \simeq 600 \text{ GeV}, \\ 10^{-13}, & \text{for } m_{\tilde{G}} \simeq 7.5 \text{ TeV}, \\ 10^{-12}, & \text{for } m_{\tilde{G}} \simeq 9.3 \text{ TeV}. \end{cases} \quad (5.18)$$

The above bounds pertain to the less restrictive case of a gravitino that decays with a small branching ratio  $B_h = 0.001$  into hadronic modes. For the  $g$ -DBD case discussed above, the upper limits (5.18) imply the corresponding stringent bounds on  $T_{\text{reh}}$ :

$$T_{\text{reh}} \lesssim \begin{cases} 9 \times 10^6 \text{ GeV}, & \text{for } m_{\tilde{G}} \simeq 360 \text{ GeV}, \\ 7 \times 10^7 \text{ GeV}, & \text{for } m_{\tilde{G}} \simeq 600 \text{ GeV}, \\ 7 \times 10^8 \text{ GeV}, & \text{for } m_{\tilde{G}} \simeq 7.5 \text{ TeV}, \\ 7 \times 10^9 \text{ GeV}, & \text{for } m_{\tilde{G}} \simeq 9.3 \text{ TeV}. \end{cases} \quad (5.19)$$

The aforementioned upper limits lead to serious constraints on the basic couplings  $\kappa$ ,  $\lambda$  and  $\rho$ , usually forcing them to acquire very small values, i.e.  $\kappa, \lambda, \rho \lesssim 10^{-5}$ . For the standard  $F$ -term hybrid model within mSUGRA and with a soft SUSY-breaking tadpole parameter  $a_S = 1 \text{ TeV}$ , the requirement of accounting for the observed power spectrum  $P_{\mathcal{R}}$ , with a number of  $e$ -folds  $\mathcal{N}_e = 50\text{--}60$ , implies that  $\kappa > 10^{-4}$  and  $T_\kappa = T_{\text{reh}} \gtrsim 9 \times 10^9 \text{ GeV}$ . Such a high lower bound on  $T_{\text{reh}}$  invalidates all the limits presented in (5.19), thereby ruling out the above  $F$ -term hybrid model.

The above situation, however, changes drastically in the  $F_D$ -term hybrid model with small  $D$ -parity violation, e.g. due to the presence of a subdominant FI  $D$ -term. This corresponds to the  $g$ -DAD case described in the previous subsection, where the upper bounds (5.18) translate, by means of (5.16), into upper bounds on  $m_{\text{FI}}/M$  for  $\kappa > 8 \times 10^{-5}$ . The required size of the  $D$ -parity violating parameter  $m_{\text{FI}}$  may naively be estimated using a relation very analogous to (4.15), viz.

$$T_g = \left( \frac{90}{\pi^2 g_*} \right)^{1/4} \sqrt{\Gamma_g m_{\text{FI}}} , \quad (5.20)$$

where  $\Gamma_g$  is the decay width of a  $g$ -sector particle and is given in (4.18). If we solve (5.20) for the ratio  $m_{\text{FI}}/M$ , we obtain

$$\frac{m_{\text{FI}}}{M} \approx 8.4 \cdot 10^{-4} \times \left( \frac{0.5}{g} \right)^{3/4} \left( \frac{T_g}{10^9 \text{ GeV}} \right)^{1/2} \left( \frac{10^{16} \text{ GeV}}{M} \right)^{1/4} . \quad (5.21)$$

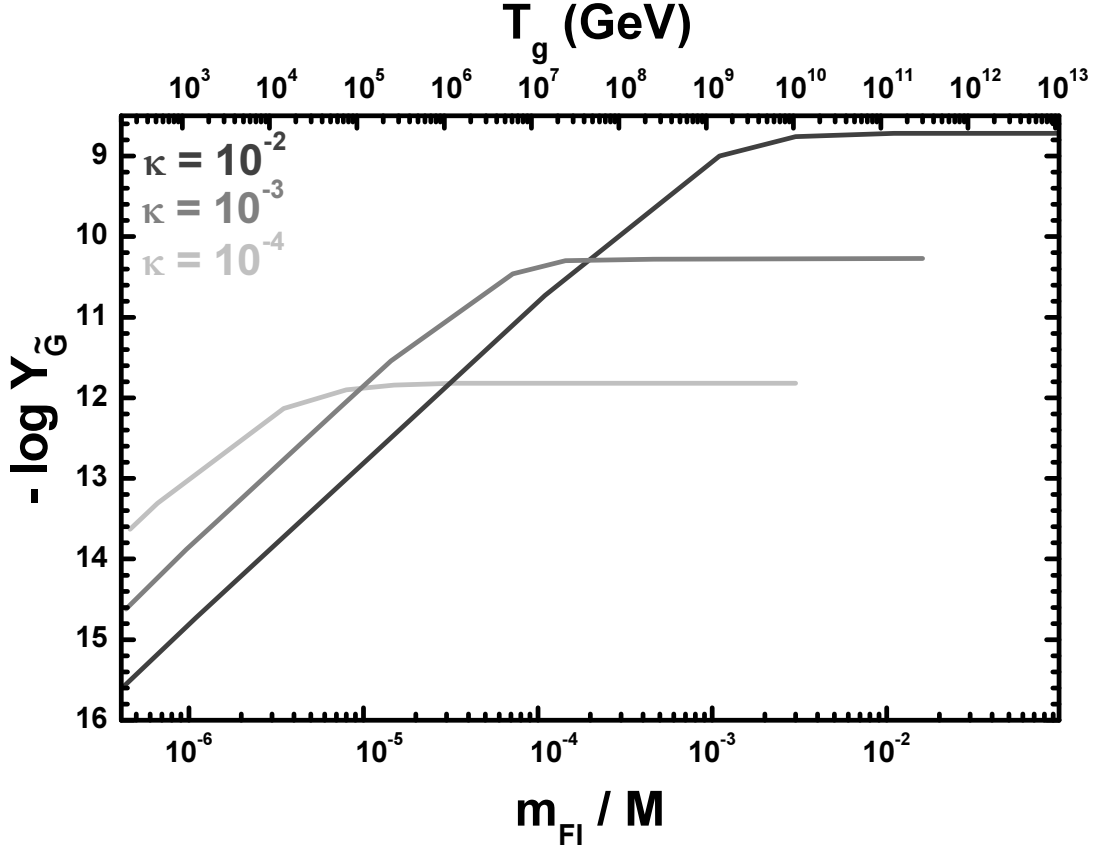


FIGURE 8: The dependence of  $\log Y_{\tilde{G}}$  on  $m_{\text{FI}}/M$ , for  $\kappa = 10^{-2}$  (dark grey line),  $\kappa = 10^{-3}$  (grey line) and  $\kappa = 10^{-4}$  (light grey line).

For second reheat temperatures  $T_g$  of cosmological interest, i.e.  $0.2 \text{ TeV} \lesssim T_g \lesssim 10^9 \text{ GeV}$ , the following double inequality for  $M = 10^{16} \text{ GeV}$  may be derived:

$$4 \times 10^{-7} \lesssim \frac{m_{\text{FI}}}{M} \lesssim 10^{-3} . \quad (5.22)$$

The lower bounds on  $T_g$  and  $m_{\text{FI}}/M$  result from the requirement that thermal electroweak-scale resonant leptogenesis be successfully realized. More details are given in Section 6.

A numerical analysis of the gravitino abundance predictions and constraints related to the  $g$ -DAD scenario has been performed in Figs. 8 and 9, respectively. Our numerical results apply equally well to both mSUGRA and nmSUGRA scenarios. In detail, Fig. 8 shows  $\log Y_{\tilde{G}}$  as a function of  $m_{\text{FI}}/M$  and  $T_g$ , for the different values of  $\kappa = 10^{-4}, 10^{-3}, 10^{-2}$ , while  $M$  is fixed by the usual inflationary constraints on  $\mathcal{N}_e$  and  $P_{\mathcal{R}}$ , for  $\kappa = \lambda = \rho$  and  $c_H = 0$ . The different lines in Fig. 8 terminate at high values of  $m_{\text{FI}}/M$ , since the inequality  $T_g < T_\kappa$  does no longer hold. The lowest value of  $m_{\text{FI}}/M$  is determined by the



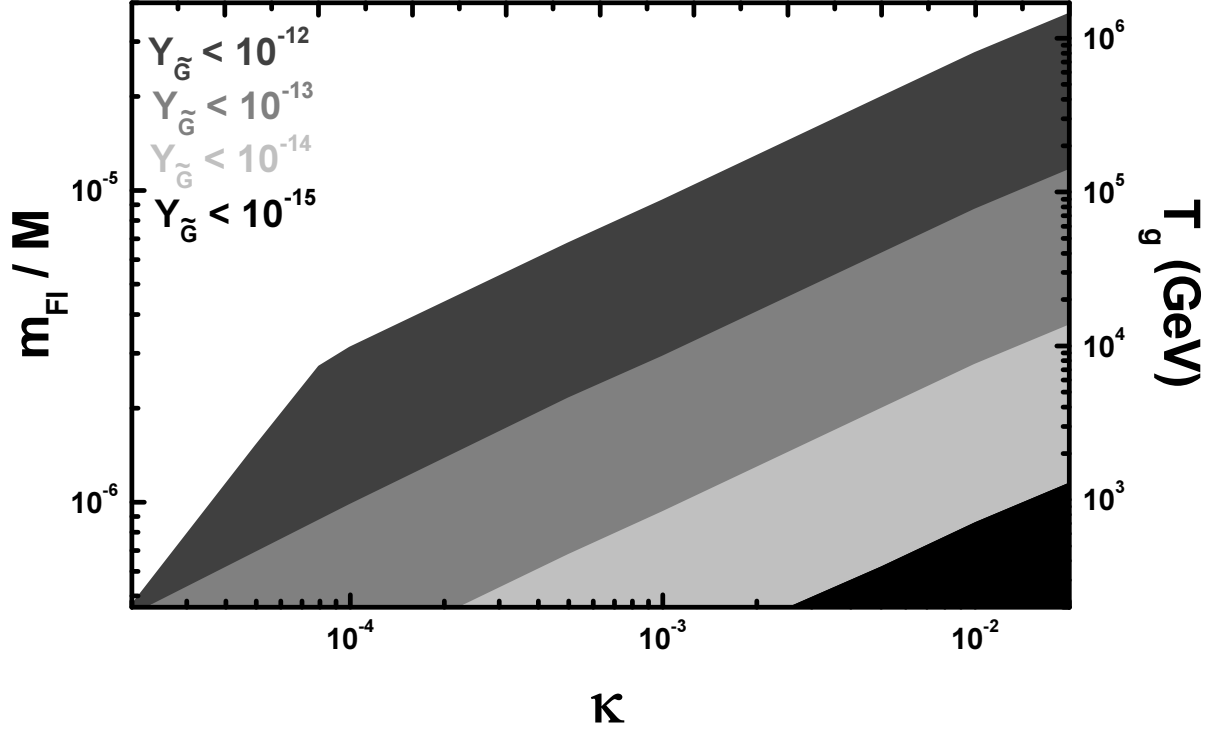


FIGURE 9: The allowed region on the  $(m_{\text{FI}}/M, \kappa)$  plane for  $Y_{\tilde{G}} < 10^{-15}$  (black area),  $Y_{\tilde{G}} < 10^{-14}$  (light grey area),  $Y_{\tilde{G}} < 10^{-13}$  (grey area) and  $Y_{\tilde{G}} < 10^{-12}$  (dark grey area).

condition  $T_g > 200$  GeV, which results from the aforementioned requirement that thermal electroweak-scale resonant leptogenesis is successfully realized [16, 19, 20].

In Fig. 8, we also observe the two regimes:  $g$ -DBD and  $g$ -DAD. In the  $g$ -DBD regime,  $\log Y_{\tilde{G}}$  remains constant for given  $\kappa$  up to some value  $m_{\text{FI}}/M$ . For example, for  $\kappa = 10^{-3}$ ,  $\log Y_{\tilde{G}}$  is constant for  $m_{\text{FI}}/M \gtrsim 10^{-4}$ . This result is consistent with (5.13). For smaller values of  $m_{\text{FI}}/M$ , one enters the  $g$ -DAD regime. In this case,  $\log Y_{\tilde{G}}$  decreases rapidly, as  $m_{\text{FI}}/M$ , or equivalently  $T_g$ , decreases. This behaviour of  $Y_{\tilde{G}}$  is expected on account of (5.16). Also, in agreement with (5.16), the reduction of  $Y_{\tilde{G}}$  becomes more drastic for larger values of  $\kappa$ .

In Fig. 9 we delineate the allowed regions on the  $(\kappa, m_{\text{FI}}/M)$  plane for the discrete values of  $Y_{\tilde{G}} = 10^{-15}, 10^{-14}, 10^{-13}, 10^{-12}$ , for  $\kappa \geq 8 \times 10^{-5}$ . The upper boundaries of the various areas are obtained using (5.16). For  $\kappa < 8 \times 10^{-5}$ , we are in the  $g$ -DBD region, where

we obtain  $10^{-13} < Y_{\tilde{G}} < 10^{-12}$ , almost independently of  $m_{\text{FI}}/M$  [cf. (5.13)]. Therefore, we only display values for  $m_{\text{FI}}/M$ , for which  $g$ -DAD becomes relevant. We observe that the most stringent limit on  $Y_{\tilde{G}}$  can still be fulfilled for  $\kappa \gtrsim 10^{-2}$  and  $m_{\text{FI}}/M \lesssim 10^{-6}$ . Such large values of  $\kappa$  would have been excluded from naive estimates of the  $\kappa$ -sector reheat temperature  $T_\kappa$  due to the  $\kappa$ -sector particle decays. According to our analysis in this section, however, these large values of  $\kappa$ ,  $\lambda$  and  $\rho$  of order  $10^{-2}$ – $10^{-1}$  are allowed within the  $F_D$ -term hybrid inflationary model. As we will see in the next section, this is a distinctive feature of the  $F_D$ -term hybrid model that opens up novel possibilities in solving the CDM problem.

At the end of this section, we wish to comment on a possible  $F_D$ -term hybrid scenario, where the  $\kappa$ -sector particles can decay directly into the  $g$ -sector ones. This can happen, for example, if  $m_\kappa > 2m_g$  or equivalently when  $\kappa > \sqrt{2}g$ . Since the gauge coupling  $g$  of the waterfall sector must be smaller than 0.1 in this case, it would be difficult to embed such a  $F_D$ -term hybrid scenario into a GUT. The energy density transferred from the  $\kappa$ -sector particles into the  $g$ -sector ones may be calculated by

$$\frac{\rho_g}{\rho_\kappa} = \frac{g}{\sqrt{2}\kappa} B_{\kappa \rightarrow g} . \quad (5.23)$$

Here  $B_{\kappa \rightarrow g}$  denotes the branching ratio of the decays of the  $\kappa$ - to  $g$ -sector particles. Assuming conservatively that  $B_{\kappa \rightarrow g} \sim 10^{-2}$  and  $\kappa = 2g$ , we obtain an estimate for the gravitino abundance  $Y_{\tilde{G}} \sim 10^{-18}$  for  $m_{\text{FI}}/M \lesssim 10^{-6}$ , thereby rendering gravitinos quite harmless.

## 6 Baryon Asymmetry and Cold Dark Matter

In this section we briefly discuss further cosmological implications of the  $F_D$ -term hybrid model for the BAU and the CDM.

### 6.1 Resonant Flavour-Leptogenesis at the Electroweak Scale

Earlier studies of the BAU in supersymmetric models of hybrid inflation have mainly been focused on scenarios of non-thermal leptogenesis [57], with an hierarchical heavy Majorana neutrino spectrum, e.g.  $m_{N_1} < m_{N_2} \ll m_{N_3}$ . The simplest model of this type is obtained by identifying the waterfall gauge group with  $U(1)_{B-L}$ , which allows the presence of the operator  $\gamma_{ij} \hat{X}_2 \hat{X}_2 \hat{N}_i \hat{N}_j / m_{\text{Pl}}$  in the superpotential. Notice that such a term is forbidden in the  $F_D$ -term hybrid model by virtue of the  $R$  symmetry (2.6). In the non-thermal

leptogenesis model, the reheat temperature consistent with the observed BAU  $\eta_B = 6.1 \times 10^{-10}$  and low-energy neutrino data is estimated to be [12]

$$T_{\text{reh}} \gtrsim 2.5 \cdot 10^7 \text{ GeV} \times \left( \frac{10^{16} \text{ GeV}}{M} \right)^{1/2} \left( \frac{\kappa}{10^{-5}} \right)^{3/4}, \quad (6.1)$$

where the superpotential couplings  $\lambda$ ,  $\rho$  are set to zero. If  $\lambda = \kappa$ , the lower bound (6.1) gets larger roughly by a factor 20. It is obvious that in this generic non-thermal leptogenesis scenario, the gravitino constraint on  $T_{\text{reh}}$  favours rather small values of  $\kappa$  and  $\lambda$ , e.g.  $\kappa, \lambda \lesssim 10^{-5}$  for  $T_{\text{reh}} \lesssim 10^8 \text{ GeV}$ . As was discussed in Section 3.2, however, such small values of  $\kappa$  introduce strong tuning at a less than 1% level to the horizon exit values of the inflaton field  $\phi_{\text{exit}}$  in a nmSUGRA scenario that accounts for the recently observed value of the spectral index  $n_s$  given by (3.10). Moreover, the success of this scenario relies heavily on the assumption that there is no other source of baryogenesis, e.g. through the Affleck–Dine mechanism, nor of entropy release, e.g. from possible late decays of moduli or flaton fields [58], between the energy scales  $m_{N_1}$  ( $\gg T_{\text{reh}}$ ) and the electroweak phase transition.

In the  $F_D$ -term hybrid model, non-thermal leptogenesis is not possible for one of the reasons mentioned above. The late decays of the  $g$ -sector ( $D$ -odd) particles generally lead to an enormous entropy release, so that not only gravitinos, but also any initial lepton-number excess will be diluted to unobservable values. However, as has already been discussed in [13], the  $F_D$ -term model can realize electroweak-scale resonant leptogenesis [16], if the coupling of the inflaton superfield  $\hat{S}$  to the respective right-handed neutrinos  $\hat{N}_i$  is very close to an  $\text{SO}(3)$ -symmetric form, i.e.  $\rho_{ij} \approx \rho \mathbf{1}_3$ . This will give rise to 3 nearly heavy Majorana neutrinos of mass  $m_N$  and so would enable a successful realization of the resonant leptogenesis mechanism at the electroweak scale. The required  $\text{SO}(3)$ -breaking may, for example, originate from renormalization-group (RG) [59] or possible GUT threshold effects [16, 60].

An order of magnitude estimate of the final BAU  $\eta_B$ , including single lepton flavour effects, may be obtained as [16, 20]

$$\eta_B \sim -10^{-2} \times r(T_g/m_N) \sum_{l=1}^3 \sum_{N_i} \delta_{N_i}^l \frac{K_{N_i}^l}{K_l K_{N_i}}, \quad (6.2)$$

where

$$K_{N_i}^l = \frac{\Gamma(N_i \rightarrow L_l \Phi) + \Gamma(N_i \rightarrow L_l^C \Phi^\dagger)}{H(T = m_N)} \quad (6.3)$$

is a lepton-flavour dependent wash-out factor, which quantifies in a way the degree of in- or out-of-equilibrium of the decay rates of the heavy Majorana neutrino mass eigenstates

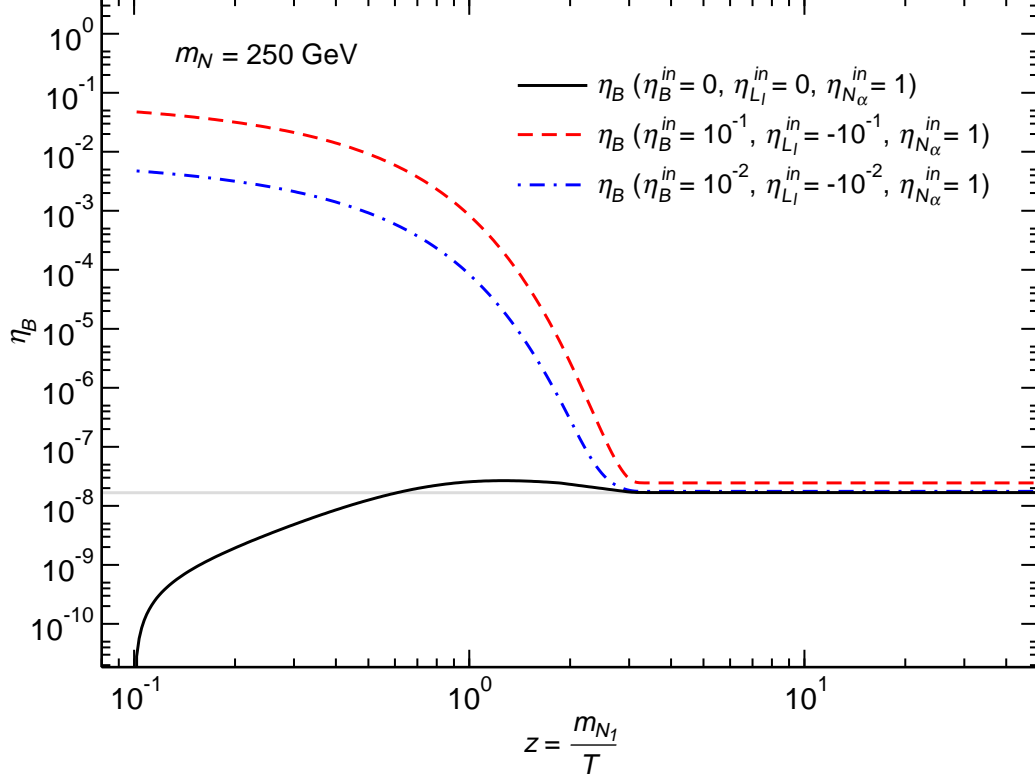


FIGURE 10: Numerical estimates of the BAU for a scenario with  $m_N = 250$  GeV and for different initial lepton- and baryon-number abundances,  $\eta_{L_l}^{\text{in}}$  and  $\eta_B^{\text{in}}$ , assuming an initial thermal distribution for the heavy Majorana neutrinos, i.e.  $\eta_{N_{1,2,3}}^{\text{in}} = 1$ . The horizontal grey line shows the BAU needed to agree with today's observed value.

$N_i$  ( $i = 1, 2, 3$ ) into the SM-like Higgs doublet  $\Phi$  and the lepton doublet  $L_l$  ( $l = e, \mu, \tau$ ). The remaining  $K$ -factors in (6.2) are defined with the help of  $K_{N_i}^l$  as follows:

$$K_{N_i} = \sum_{l=1}^3 K_{N_i}^l, \quad K_l = \sum_{N_i} K_{N_i}^l. \quad (6.4)$$

The parameters  $\delta_{N_i}^l$  denote the different lepton-flavour asymmetries related to the decays  $N_i \rightarrow L_l \Phi$  and are defined by

$$\delta_{N_i}^l = \frac{\Gamma(N_i \rightarrow L_l \Phi) - \Gamma(N_i \rightarrow L_l^C \Phi^\dagger)}{\Gamma(N_i \rightarrow L_l \Phi) + \Gamma(N_i \rightarrow L_l^C \Phi^\dagger)}. \quad (6.5)$$

Finally, the prefactor  $r(T_g/m_N)$  in (6.2) takes care of a possible dilution effect on the BAU that might be caused by the entropy release of late  $g$ -sector particle decays. This dilution

effect is only relevant, if the second reheat temperature  $T_g$  is smaller than the leptogenesis scale  $m_N$ . Employing standard arguments of thermodynamics, one may estimate that

$$r(T_g/m_N) \sim \left(\frac{T_g}{m_N}\right)^5. \quad (6.6)$$

Instead, if  $T_g \gg m_N$ , the dilution factor  $r(T_g/m_N)$  approaches 1 and can therefore be omitted.

In Fig. 10, we display numerical estimates of the BAU for a resonant leptogenesis scenario with  $m_N = 250$  GeV and an inverted hierarchical light-neutrino spectrum. For a detailed discussion of the heavy and light neutrino spectra of this model, the reader is referred to [16]. As can be seen from Fig. 10, one advantageous feature of resonant leptogenesis is that the final baryon asymmetry  $\eta_B$  does not sensitively depend on any pre-existing lepton- or baryon-number abundance,  $\eta_{L_i}^{\text{in}}$  or  $\eta_B^{\text{in}}$ . For instance, assuming an initial thermal distribution for the heavy Majorana neutrinos, i.e.  $\eta_{N_{1,2,3}}^{\text{in}} = 1$ , and primordial baryon asymmetries  $\eta_B^{\text{in}} \lesssim 10^{-2}$ , we observe that the final  $\eta_B$  is practically independent of the initial conditions, once the relevant particle-physics model parameters, such as the heavy Majorana masses and their respective Yukawa couplings, are fixed.

It is important to comment here on the fact that the above property of the independence of the BAU on the initial conditions does not necessarily get spoiled, if the second reheat temperature  $T_g$  happens to be smaller than the resonant leptogenesis scale  $m_N$ . In this case, one only needs to make sure that the entropy dilution suppression factor  $\sim (T_g/m_N)^5$  does not lead to a significant reduction of the BAU. Therefore, we have rather conservatively assumed throughout our numerical analysis in Section 5 that  $T_g \gtrsim m_N \sim 250$  GeV, even though  $T_g$  could still be somewhat smaller than the resonant leptogenesis scale  $m_N$ .

Another point that deserves to be clarified here is the physical significance of lepton-flavour effects on the BAU. In general, there are two sources of lepton flavour: (i) the charged lepton Yukawa couplings  $h_l$  and (ii) the neutrino Yukawa couplings  $h_{ij}^\nu$ . The former has been extensively discussed in the literature [61] and may affect the predictions for the BAU by up to one order of magnitude, depending on the scale of leptogenesis. For our electroweak-scale leptogenesis scenario, these effects are not significant, since all charged lepton Yukawa couplings mediate interactions that are in thermal equilibrium. The second source of flavour effects is due to neutrino-Yukawa couplings  $h_{ij}^\nu$  and has been studied only very recently in [16, 20, 62]. The effect on the BAU is most relevant when the heavy Majorana neutrinos get closer in mass. In models of resonant leptogenesis, neutrino-Yukawa coupling effects can have a dramatic impact on the predictions for the BAU, enhancing its value by many orders of magnitude [16, 20].

This last fact opens up new vistas in the model-building of scenarios that can be phenomenologically more accessible to laboratory experiments. For instance, if a certain hierarchy among the Yukawa-neutrino couplings  $h_{ij}^\nu$  is assumed, e.g.  $h_{i2}^\nu = ih_{i3}^\nu \sim 10^{-2} \sim h_\tau$  and  $h_{i1}^\nu = 10^{-6}-10^{-7} \sim h_e$ , resulting from the approximate breaking of some global  $U(1)_l$  symmetry, the required BAU can still be generated successfully from an individual lepton number asymmetry, namely  $L_\tau$  in this case. For this particular model of resonant  $\tau$ -leptogenesis, the values of the  $K$ -factors defined in (6.3) are:

$$K_{N_{1,2,3}}^\tau \sim 10, \quad K_{N_3}^{e,\mu} \sim 30, \quad K_{N_{1,2}}^{e,\mu} \sim 10^{10}. \quad (6.7)$$

Given that the leptonic asymmetry is  $\delta_{N_3}^\tau \sim 10^{-6}$ , one can estimate from (6.2) that the right amount of baryon asymmetry is produced, with  $\eta_B \sim 10^{-9}$ . This is also shown in Fig. 10. Instead, older approaches to BEs that do not appropriately treat lepton flavour effects via the neutrino Yukawa couplings  $h_{ij}^\nu$  would have predicted a value that would have been short of a huge factor  $\sim 10^{-6}$  [16, 20].

As can be seen from the above example, the lepton-flavour directions  $L_{e,\mu}$  orthogonal to  $L_\tau$  can involve large neutrino Yukawa couplings of order  $10^{-2}$ . Such couplings can give rise to distinctive signatures in the production and decay of electroweak-scale heavy Majorana neutrinos at high-energy colliders, such as the LHC [63], the International Linear  $e^+e^-$  Collider (ILC) [64] and other future colliders [65]. Moreover, electroweak-scale heavy Majorana neutrinos can give rise to phenomena of lepton flavour and/or number violation, such as the neutrinoless double-beta decay ( $0\nu\beta\beta$ ), the decays  $\mu \rightarrow e\gamma$  [66],  $\mu \rightarrow eee$ ,  $\mu \rightarrow e$  conversion in nuclei etc [67–70]. A detailed discussion of the low-energy phenomenology of resonant leptogenesis models may be found in [16].

## 6.2 Thermal Right-Handed Sneutrinos as CDM

An interesting feature of the  $F_D$ -term hybrid model is that  $R$ -parity is conserved, even though the lepton number  $L$ , as well as  $B - L$ , are explicitly broken by the Majorana operator  $\frac{1}{2}\rho\widehat{S}\widehat{N}_i\widehat{N}_i$ . In fact, in our model, all superpotential couplings either conserve the  $B - L$  number or break it by even number of units. For example, the coupling  $\rho$  breaks explicitly  $L$ , along with  $B - L$ , by 2 units. Since the  $R$ -parity of each superpotential operator is determined to be  $R = (-1)^{3(B-L)} = +1$ , the  $F_D$ -term hybrid model conserves  $R$ -parity. As a consequence, the LSP of the spectrum is stable and so becomes a viable candidate to address the CDM problem of the Universe.

In addition to the standard CDM candidates of the MSSM, e.g. a stable neutralino, it would be interesting to explore whether thermal right-handed sneutrinos as LSPs could

solve the CDM problem. Before we estimate their relic abundance, we first observe that light right-handed sneutrinos may easily appear in the spectrum. Ignoring the small neutrino-Yukawa coupling terms, the right-handed sneutrino mass matrix  $\mathcal{M}_{\tilde{N}}^2$  is written down in the weak basis  $(\tilde{N}_{1,2,3}, \tilde{N}_{1,2,3}^*)$ :

$$\mathcal{M}_{\tilde{N}}^2 = \frac{1}{2} \begin{pmatrix} \rho^2 v_S^2 + M_{\tilde{N}}^2 & \rho A_\rho v_S + \rho \lambda v_u v_d \\ \rho A_\rho^* v_S + \rho \lambda v_u v_d & \rho^2 v_S^2 + M_{\tilde{N}}^2 \end{pmatrix}, \quad (6.8)$$

where  $v_S = \langle S \rangle$ ,  $v_{u,d} = \langle H_{u,d} \rangle$  and  $M_{\tilde{N}}^2$  is the soft SUSY-breaking mass parameters associated with the sneutrino fields. The sneutrino spectrum will then consist of 3 heavy (light) right-handed sneutrinos of mass

$$\rho^2 v_S^2 + M_{\tilde{N}}^2 + (-) \left( \rho A_\rho v_S + \rho \lambda v_u v_d \right).$$

Hence, the 3 light sneutrinos can act as LSPs, which we collectively denote them by  $\tilde{N}_{\text{LSP}}$ .

Recently, the possibility that right-handed sneutrinos are the CDM was considered in [71]. This recent analysis showed that thermal right-handed sneutrinos have rather high relic abundances and will generally overclose the Universe in a supersymmetric extension of the MSSM with right-handed neutrino superfields  $\hat{N}_i$  and bare Majorana masses  $(m_M)_{ij} \hat{N}_i \hat{N}_j$ . The underlying reason is that because of the small Yukawa-neutrino couplings  $h_{ij}^\nu$ , the self- and co-annihilation interactions of the sneutrino LSP with itself and other MSSM particles are rather weak. These weak processes do not allow the sneutrino LSP to stay long enough in thermal equilibrium before its freeze-out temperature, such that its number density gets reduced to a level compatible with the CMB data, i.e.  $\Omega_{\text{DM}} h^2 \approx 0.15$ . Instead, the predicted values turn out to be many orders of magnitude larger than 1.

In the  $F_D$ -term hybrid model, however, there is a new interaction that can make the right-handed sneutrinos annihilate more efficiently. This is the quartic coupling <sup>6</sup>

$$\mathcal{L}_{\text{int}}^{\text{LSP}} = \frac{1}{2} \lambda \rho \tilde{N}_i^* \tilde{N}_i^* H_u H_d + \text{H.c.} \quad (6.9)$$

It results from the  $F$ -term of the inflaton field:  $F_S \sim \frac{1}{2} \rho \hat{N}_i \hat{N}_i + \lambda \hat{H}_u \hat{H}_d$ . To assess the significance of the interaction (6.9), we estimate the relic density of  $\tilde{N}_{\text{LSP}}$  in different kinematic regions.

---

<sup>6</sup>The implications of a generic quartic coupling of the same form for the CDM abundance and detection was studied earlier in [72, 73] within the context of a simple non-SUSY model. These studies will not be directly applicable to our more elaborate case of a supersymmetric scenario with right-handed sneutrinos. However, we have used their results to check our qualitative estimates for the CDM abundance.

We first consider the self-annihilation off-resonant process  $\tilde{N}_{\text{LSP}}\tilde{N}_{\text{LSP}} \rightarrow \langle H_u \rangle H_d \rightarrow W^+W^-$ , which occurs when  $m_{\tilde{N}_{\text{LSP}}} > M_W$ . A simple estimate yields

$$\Omega_{\text{DM}} h^2 \sim \left( \frac{10^{-4}}{\rho^2 \lambda^2} \right) \left( \frac{\tan \beta M_H}{g_w M_W} \right)^2. \quad (6.10)$$

To obtain an acceptable relic density, we need relatively large  $\rho$  and  $\lambda$  couplings, i.e.  $\rho, \lambda \gtrsim 0.1^7$ . Such values go in opposite direction with those obtained by requiring successful inflation with a red-tilted spectrum. Therefore, as far as inflation is concerned, they signify the necessity of going well beyond the minimal Kähler potential.

The above situation may slightly improve for  $m_{\tilde{N}_{\text{LSP}}} < M_W$ , in large  $\tan \beta$  scenarios with light Higgs bosons that couple appreciably to  $b$ -quarks [74]. In particular, in the kinematic region  $M_{H_d} \approx 2m_{\tilde{N}_{\text{LSP}}}$ , the self-annihilation process  $\tilde{N}_{\text{LSP}}\tilde{N}_{\text{LSP}} \rightarrow \langle H_u \rangle H_d \rightarrow b\bar{b}$  becomes resonant, and the above estimate modifies to

$$\Omega_{\text{DM}} h^2 \sim 10^{-4} \times B^{-1}(H_d \rightarrow \tilde{N}_{\text{LSP}}\tilde{N}_{\text{LSP}}) \times \left( \frac{M_H}{100 \text{ GeV}} \right)^2. \quad (6.11)$$

Consequently, if the couplings  $\lambda, \rho$  are not too small, e.g.  $\lambda, \rho \gtrsim 10^{-2}$ , the LSP right-handed sneutrinos  $\tilde{N}_{\text{LSP}}$  can efficiently annihilate via a Higgs resonance  $H_d$  into pairs of  $b$ -quarks in this kinematic region, thus obtaining a relic density compatible with the CMB data. A detailed study of the thermal right-handed sneutrino as CDM could be given elsewhere.

## 7 Conclusions

We have analyzed the cosmological implications of a novel  $F$ -term hybrid inflationary model, in which the inflaton and the gauged waterfall sectors respect an approximate discrete symmetry which we called here  $D$ -parity. The approximate breaking of  $D$ -parity occurs explicitly either through the presence of a subdominant FI  $D$ -term or through non-renormalizable operators in the Kähler potential. For brevity, this scenario of inflation was termed  $F_D$ -term hybrid inflation. One of the most interesting features of the model is that the VEV of the inflaton field closely relates the  $\mu$ -parameter of the MSSM to an  $\text{SO}(3)$  symmetric Majorana mass  $m_N$ . If  $\lambda \sim \rho$ , this implies that  $\mu \sim m_N$ , so the  $F_D$ -term hybrid model may naturally predict lepton-number violation at the electroweak scale.

---

<sup>7</sup>An upper bound on the product  $\rho\lambda$ , although somewhat model-dependent, can be derived from experimental limits on the flux of energetic upward muons that occur in the possible detection of CDM using neutrino telescopes [73]. Our initial estimates indicate that it should be  $\rho\lambda \lesssim 0.03$  for  $m_{\tilde{N}_{\text{LSP}}} \sim 50 \text{ GeV}$ , which is not a very restrictive bound.



Before summarizing the cosmological and particle-physics implications of the  $F_D$ -term hybrid model, it might be interesting to list our basic assumptions pertinent to inflation and to the model itself:

- (i) The standard assumption for successful hybrid inflation is that the inflaton field  $\phi$  should be displaced from its true minimum at the start of inflation, whereas all other scalar fields in the spectrum must have zero VEVs [c.f. (2.14)]. In a nmSUGRA scenario of hybrid inflation, however, additional tuning is required beyond the above standard assumption. The horizon exit values of the inflaton field  $\phi_{\text{exit}}$  have to be close to the value  $\phi_{\text{max}}$ , at which the inflationary potential has a maximum. Nevertheless, such a tuning is not so strong, i.e.  $(\phi_{\text{max}} - \phi_{\text{exit}})/\phi_{\text{exit}} \gtrsim 10\%$ , as long as  $\kappa \gtrsim 10^{-3}$ .
- (ii) Although there may exist several ways of breaking  $D$ -parity explicitly, we have considered here two possibilities to motivate the required small amount of  $D$ -parity violation. As discussed in Appendix A, we first considered the case where  $D$ -parity is broken by a subdominant FI  $D$ -term, which is induced radiatively after heavy degrees of freedom have been integrated out. Another minimal way would be to introduce non-renormalizable operators in the Kähler potential that break  $D$ -parity explicitly.
- (iii) In order to be able to realize thermal resonant leptogenesis at a low scale, the coupling matrix  $\rho_{ij}$  is assumed to be close to  $\text{SO}(3)$  symmetric, i.e.  $\rho_{ij} \approx \rho \mathbf{1}_3$ .

The  $F_D$ -term hybrid model has several cosmological implications that may be summarized as follows:

- The model can accommodate the currently favoured strong red-tilted spectrum with  $n_s - 1 \approx -0.05$  [4,5], if the radiative corrections dominate the slope of the inflationary potential and a next-to-minimal Kähler potential is assumed, where the parameter  $c_H$  is in the range 0.05–0.2. The radiative corrections dominate the slope of the potential, if the superpotential couplings,  $\kappa$ ,  $\lambda$ ,  $\rho$ , lie in a certain interval:  $10^{-4} \lesssim \kappa, \lambda, \rho \lesssim 10^{-2}$ . In addition, the actual value of the power spectrum  $P_{\mathcal{R}}$  and the required number of  $e$ -folds,  $\mathcal{N}_e \approx 55$ , provide further constraints on these couplings and the SSB scale  $M$  of the waterfall gauge symmetry. For example, for  $M \approx 10^{16}$  GeV, one finds the allowed parameter space:  $\kappa \lesssim \lambda$ ,  $\rho \lesssim 4\kappa$ , for  $\kappa \sim 10^{-3}$ – $10^{-2}$  and  $0.05 \lesssim c_H \lesssim 0.1$ .
- For  $F_D$ -term hybrid models with spontaneously broken  $\text{U}(1)_X$  gauge symmetry, the non-observation of a cosmic string contribution to the power spectrum at the 10% level implies an upper bound on the superpotential coupling  $\kappa$ , i.e.  $\kappa \lesssim 10^{-3}$ . This

strict upper bound on  $\kappa$  can be weakened by one order of magnitude in a nmSUGRA model of  $F_D$ -term hybrid inflation, with  $\kappa = \lambda = \rho$  and  $c_H = 0.14$ . On the other hand, this upper limit can be completely evaded, if the waterfall sector of the  $F_D$ -term hybrid model realizes an  $SU(2)_X$  local symmetry that breaks completely to the identity  $\mathbf{I}$ , i.e.  $SU(2)_X \rightarrow \mathbf{I}$ . In this case, not only cosmic strings but any other topological defects can be avoided, such as monopoles and textures. As we outlined in Section 2, GUTs, such as those based on the exceptional groups  $E(6)$  and  $E(7)$ , have breaking patterns that contain  $SU(2)_X$  subgroups uncharged under the SM gauge group and so are able to realize  $F_D$ -term hybrid inflation devoid of monopoles and cosmic strings.

- To avoid overproduction of gravitinos, one needs to impose a strict upper limit on the reheat temperature  $T_{\text{reh}}$  obtained from the perturbative inflaton decays, i.e.  $T_{\text{reh}} \lesssim 10^{10} - 10^7$  GeV. This upper bound depends on the decay properties of the gravitino and gives rise to tight constraints on the basic theoretical parameters  $\kappa$ ,  $\lambda$  and  $\rho$ , i.e.  $\kappa, \lambda, \rho \lesssim 10^{-5}$ . However, these tight limits may be significantly relaxed by considering the late decays of the so-called  $g$ -sector particles which are induced by small  $D$ -parity violating couplings that may result from either a subdominant FI  $D$ -term or non-renormalizable Kähler potential terms. These  $g$ -sector particles are produced during the preheating epoch, and if they are abundant, they will lead to a second reheating phase in the evolution of the early Universe, giving rise to a rather low reheat temperature, even as low as 0.3 TeV. In this case, the enormous entropy release from the  $g$ -sector particles may reduce the gravitino abundance  $Y_{\tilde{G}}$  below the BBN limits discussed in Section 5.
- After the inflaton  $S$  receives a VEV, one ends up with 3 nearly degenerate heavy Majorana neutrinos with masses at the electroweak scale. As we discussed in Section 6, this opens up the possibility to successfully address the BAU within the thermal electroweak-scale resonant leptogenesis framework, in a way independent of any pre-existing lepton- or baryon-number abundance.
- The  $F_D$ -term hybrid model conserves  $R$ -parity, in spite of the fact that the lepton number is explicitly broken by the Majorana operator  $\frac{1}{2} \rho \hat{S} \hat{N}_i \hat{N}_i$ . This is so, because all superpotential couplings either conserve the  $B - L$  number or break it by even number of units. The aforementioned Majorana operator breaks explicitly  $L$ , as well as  $B - L$ , by 2 units. Consequently, the LSP of the spectrum is stable and so qualifies as candidate to address the CDM problem. The new aspect of the  $F_D$ -term hybrid model is that thermal right-handed sneutrinos emerge as new candidates to solve this problem, by virtue of the quartic coupling:  $\frac{1}{2} \lambda \rho \tilde{N}_i^* \tilde{N}_i^* H_u H_d + \text{H.c.}$ . This new quartic

coupling results in the Higgs potential from the  $F$ -terms of the inflaton field, and it is not present in the more often-discussed extension of the MSSM, where right-handed neutrino superfields have bare Majorana masses. Provided that the couplings  $\lambda$  and  $\rho$  are not too small, e.g.  $\lambda, \rho \gtrsim 10^{-2}$ , the LSP right-handed sneutrinos  $\tilde{N}_{\text{LSP}}$  can efficiently annihilate via a Higgs resonance  $H_d$  into pairs of  $b$ -quarks, in the kinematic region  $M_{H_d} \approx 2m_{\tilde{N}_{\text{LSP}}}$ , and so drastically reduce its relic density to values compatible with the CMB data.

In addition to the above cosmological implications, the  $F_D$ -term hybrid model has a rich particle-physics phenomenology. The main phenomenological characteristics of the model are:

- (a) It is straightforward to embed the  $F_D$ -term hybrid model into minimal or next-to-minimal SUGRA, where the soft SUSY-breaking parameters are constrained at the gauge coupling unification point  $M_X$ . Instead, electroweak baryogenesis is not viable in a minimal SUGRA scenario of the MSSM. It requires an unconventionally large hierarchy between the left-handed and right-handed top squarks [75], which is difficult to obtain within the framework of minimal SUGRA. In addition, the CP-odd soft phases required for successful electroweak baryogenesis face severe constraints from the absence of observable 2-loop contributions to the electron and neutron electric dipole moments [76].
- (b) As has been discussed in Section 6, if one assumes that the neutrino-Yukawa couplings  $h_{ij}^\nu$  have a certain hierarchical structure controlled by the approximate breaking of global flavour symmetries, the model can have further testable implications for low-energy observables of lepton flavour and/or number violation, e.g.  $0\nu\beta\beta$  decay,  $\mu \rightarrow e\gamma$ ,  $\mu \rightarrow eee$ ,  $\mu \rightarrow e$  conversion in nuclei etc. In addition, electroweak-scale heavy Majorana neutrinos may be copiously produced at high-energy colliders, such as the LHC, the ILC and  $e^- \gamma$  colliders, whose decays give rise to distinctive signatures of lepton-number violation which are usually manifested by like-sign dileptons accompanied by hadron jets.
- (c) Since successful inflation requires small couplings, i.e.  $\kappa, \lambda, \rho \lesssim 10^{-2}$ , the inflaton field decouples effectively from the low-energy spectrum and the Higgs-sector of the model becomes identical to the one of the MSSM. In spite of the aforementioned decoupling of the inflaton, however, the  $F_D$ -term hybrid model could still point towards particular benchmark scenarios of the MSSM. For example, if  $\lambda \gg \kappa$ , the

$F_D$ -term hybrid model may explain the origin of a possible large value of the  $\mu$ -parameter. Specifically, if  $\lambda = 2\kappa$ ,  $A_\kappa = -a_S = 2M_{\text{SUSY}}$ , one gets from (2.4) the hierarchy  $\mu \approx 4M_{\text{SUSY}}$ , where  $M_{\text{SUSY}}$  is a common soft SUSY-breaking scale of all scalar fermion fields in the model. If one additionally requires  $A_t = A_b = 2M_{\text{SUSY}}$ , the low-energy limit of the  $F_D$ -term hybrid model becomes identical to the so-called CPX benchmark scenario [77] describing maximal CP violation in the MSSM Higgs sector at low and moderate values of  $\tan\beta$ . In the CPX scenario, the lightest neutral Higgs boson weighing less than 60 GeV might have escaped detection at LEP. There have been several strategies to unravel the existence of such a light CP-violating Higgs boson [78].

- (d) The possible CDM scenario with the right-handed sneutrinos as LSPs requires large  $\lambda$  and  $\rho$  couplings that could make Higgs bosons decay invisibly, e.g.  $H \rightarrow \tilde{N}_{\text{LSP}} \tilde{N}_{\text{LSP}}$ . Also, right-handed sneutrinos could be present in the cascade decays of the heavier supersymmetric particles. The collider phenomenology of such a CDM scenario lies beyond the scope of the present article.

The  $F_D$ -term hybrid model studied in this paper should be regarded as a first attempt towards the formulation of a minimal Particle-Physics and Cosmology Standard Model, which does not involve excessive fine-tuning in the fundamental parameters of the theory. As we outlined above, it might be possible to test the validity of our model by a number of laboratory experiments and further substantiate it by future astronomical observations. The  $F_D$ -term hybrid model is not plagued with the usual gauge-hierarchy problem of non-supersymmetric theories and can, in principle, be embedded within an E(6) or E(7) GUT, within the framework of SUGRA where SUSY is softly broken at the TeV scale. In the same vein, we note that a possible natural solution to the famous cosmological constant problem will shed valuable light on the model-building aspects of cosmologically viable models. It will also open up new avenues in quantitatively addressing the major energy-density component of today's Universe, the so-called Dark Energy. We hope that all these insights, along with new observational and experimental data, will help us to improve further our present bottom-up approach to formulating a more complete minimal model of particle physics and cosmology.

## Acknowledgements

We thank Richard Battye, Zurab Tavartkiladze and Thomas Underwood for illuminating discussions. This work is supported in part by the PPARC research grants: PP/D000157/1 and PP/C504286/1.

# A Mechanisms of Explicit $D$ -Parity Breaking

Here we will present mechanisms for explicitly breaking  $D$ -parity within the SUGRA framework, pointing out their possible implications for the decay rates of the  $g$ -sector particles. We separately discuss the breaking of  $D$ -parity for an Abelian  $U(1)_X$  and an non-Abelian  $SU(2)_X$  waterfall-gauge sector.

## A.1 $D$ -Parity Breaking in the $U(1)_X$ Waterfall-Gauge Sector

As already discussed in Section 4.1, the simplest way of breaking  $D$ -parity is to add a subdominant bare FI  $D$ -term  $\mathcal{L}_{\text{FI}}$  to the Lagrangian [cf. (4.5)]. As was shown in [13], however, even if such a term were absent from the tree-level Lagrangian, it could still be generated by quantum-mechanical effects in an effective manner, after integrating out Planck-scale degrees of freedom. It should be stressed here that the radiative generation of an *effective* FI  $D$ -term occurs only *after* the SSB of the  $U(1)_X$  gauge symmetry.

To elucidate this point, let us consider a simple extension of the  $F_D$ -term hybrid model, which includes a pair of superfields  $\widehat{X}_{1,2}$  of opposite  $U(1)_X$  charge, i.e.  $Q(\widehat{X}_2) = -Q(\widehat{X}_1) = Q(\widehat{X}_1) = -Q(\widehat{X}_2) = 1$ . In this case, the superpotential  $W_{\text{IW}}$  pertinent to the inflaton-waterfall sector may be extended as follows:

$$W_{\text{IW}} = \kappa \widehat{S} \left( \widehat{X}_1 \widehat{X}_2 - M^2 \right) + \xi m_{\text{Pl}} \widehat{X}_1 \widehat{X}_2 + \xi_1 \frac{(\widehat{X}_1 \widehat{X}_1)^2}{2 m_{\text{Pl}}} + \xi'_1 \frac{(\widehat{X}_2 \widehat{X}_2)^2}{2 m_{\text{Pl}}} \dots \quad (\text{A.1})$$

where the dots stand for subleading terms that multiply the leading operators by extra powers of  $(\widehat{X}_1 \widehat{X}_2)^n / m_{\text{Pl}}^{2n}$ , with  $n \geq 1$ . These subleading operators are irrelevant for our discussion here and can be ignored, within a perturbative framework of SUGRA. The leading operator form of the superpotential (A.1) may be reinforced by the  $R$  symmetry:

$$\widehat{S} \rightarrow e^{i\alpha} \widehat{S}, \quad \widehat{X}_{1,2} \rightarrow e^{i\alpha/2} \widehat{X}_{1,2}, \quad (\widehat{L}, \widehat{Q}) \rightarrow e^{i\alpha} (\widehat{L}, \widehat{Q}), \quad (\text{A.2})$$

with  $W \rightarrow e^{i\alpha} W$ . As before, all remaining fields do not transform under the  $R$  symmetry.<sup>8</sup>

We will now show that a FI  $D$ -term,  $-\frac{1}{2} g m_{\text{FI}}^2 D$ , will be generated if the ultraheavy Planck-scale superfields  $\widehat{X}_{1,2}$  are integrated out. As a starting point, we consider the  $U(1)_X$   $D$ -term Lagrangian

$$\mathcal{L}_D = \frac{1}{2} D^2 + \frac{g}{2} D \left( X_1^* X_1 - X_2^* X_2 - \overline{X}_1^* \overline{X}_1 + \overline{X}_2^* \overline{X}_2 \right). \quad (\text{A.3})$$

---

<sup>8</sup>Observe that the  $R$ -symmetry (A.2) allows for the subleading operator  $\kappa' S (\widehat{X}_1 \widehat{X}_2)^2 / m_{\text{Pl}}^2$ . This superpotential term can break the  $U(1)_X$  gauge symmetry along the inflationary trajectory, thereby inflating away unwanted topological defects [25]. This scenario is known as shifted hybrid inflation.

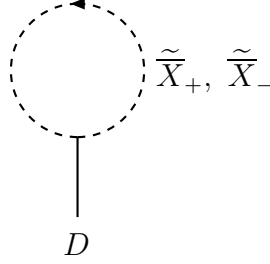


FIGURE 11: Radiative generation of an effective FI  $D$ -term,  $-\frac{g}{2} m_{\text{FI}}^2 D$ .

In order to integrate out the fields  $\overline{X}_{1,2}$ , we need their mass spectrum in the post-inflationary era, where  $\langle X_{1,2} \rangle = M$  and  $\langle \overline{X}_{1,2} \rangle = \langle S \rangle = 0$ . In the weak basis  $\overline{X}_{\pm} = \frac{1}{\sqrt{2}} (\overline{X}_1 \pm \overline{X}_2)$ , this is approximately given by the Lagrangian

$$-\mathcal{L}_{\text{mass}}^{\overline{X}_{\pm}} \approx (\overline{X}_+^*, \overline{X}_-^*) \begin{pmatrix} \xi^2 m_{\text{Pl}}^2 + \xi (\xi_1 + \xi'_1) M^2 & (\xi_1^2 - \xi_1'^2) \frac{M^4}{2 m_{\text{Pl}}^2} \\ (\xi_1^2 - \xi_1'^2) \frac{M^4}{2 m_{\text{Pl}}^2} & \xi^2 m_{\text{Pl}}^2 - \xi (\xi_1 + \xi'_1) M^2 \end{pmatrix} \begin{pmatrix} \overline{X}_+ \\ \overline{X}_- \end{pmatrix}. \quad (\text{A.4})$$

The approximate mass eigenstates derived from (A.4) are

$$\tilde{\overline{X}}_+ = \overline{X}_+ + s_{\theta} \overline{X}_-, \quad \tilde{\overline{X}}_- = \overline{X}_- - s_{\theta} \overline{X}_+, \quad (\text{A.5})$$

where  $s_{\theta} \approx (\xi_1 - \xi'_1) M^2 / (4 \xi m_{\text{Pl}}^2)$  is a mixing angle which is typically much smaller than 1. In terms of the mass-eigenstates  $\tilde{\overline{X}}_{\pm}$ , the part of the Lagrangian (A.3) linear in the  $D$ -terms associated with the Planck-scale degrees of freedom reads:

$$\begin{aligned} \mathcal{L}_D^{\overline{X}_{\pm}} &= -\frac{g}{2} D \left( \overline{X}_+^* \overline{X}_- + \overline{X}_-^* \overline{X}_+ \right) \\ &= -\frac{g}{2} D \left[ \tilde{\overline{X}}_+^* \tilde{\overline{X}}_- + \tilde{\overline{X}}_-^* \tilde{\overline{X}}_+ + 2s_{\theta} \left( \tilde{\overline{X}}_+^* \tilde{\overline{X}}_+ - \tilde{\overline{X}}_-^* \tilde{\overline{X}}_- \right) + \mathcal{O}(s_{\theta}^2) \right]. \end{aligned} \quad (\text{A.6})$$

A FI  $D$ -tadpole can only be generated from terms linear in  $s_{\theta}$  in the Lagrangian (A.6). This result should be expected on symmetry grounds, since terms linear in  $s_{\theta}$  explicitly break the  $D$ -symmetry. The  $D$ -tadpole  $m_{\text{FI}}^2$ , calculated from the one-loop graph of Fig. 11, is found to be

$$m_{\text{FI}}^2 \approx \frac{\xi_1^2 - \xi_1'^2}{8\pi^2} \frac{M^4}{m_{\text{Pl}}^2} \ln \left( \frac{m_{\text{Pl}}}{M} \right). \quad (\text{A.7})$$

Typically, one gets  $m_{\text{FI}}/M \lesssim 10^{-6}$ , for  $M = 10^{16}$  GeV and  $\xi_1, \xi_1' \lesssim 10^{-3}$ .

For later use, it is interesting to outline a short-cut derivation of the result (A.7), using the original weak basis of the fields, i.e.  $X_{1,2}$  and  $\overline{X}_{1,2}$ . We notice that, after the SSB

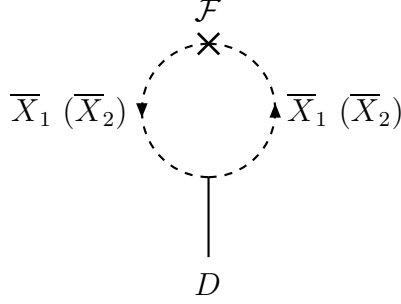


FIGURE 12: *Diagram pertinent to a short-cut derivation of the effective FI D-term.*

of  $U(1)_X$ , the  $F$ -terms of  $\overline{X}_{1,2}$  give rise to the  $D$ -odd operator,

$$\mathcal{F} = (\xi_1^2 - \xi_1'^2) \frac{M^4}{2m_{\text{Pl}}^2} \left( \overline{X}_1^* \overline{X}_1 - \overline{X}_2^* \overline{X}_2 \right), \quad (\text{A.8})$$

in the scalar potential of the extended  $F_D$ -term hybrid model. This operator induces, via the diagram shown in Fig. 12, an effective FI  $D$ -tadpole. Since the scalar fields  $\overline{X}_{1,2}$  are degenerate in mass to leading order, i.e.  $M_{\overline{X}_{1,2}} \approx \xi m_{\text{Pl}}$ , the graph in Fig. 12 is easily calculated using standard field-theoretic methods. It is logarithmically divergent, and in an effective cut-off theory it is given by (A.7). We will use this short-cut approach below to calculate effective  $D$ -tadpoles in more elaborate extensions of the inflation-waterfall sector.

The size of the FI  $D$ -term may be further suppressed, if the Planck-mass chiral superfields  $\widehat{X}_{1,2}$  possess higher  $U(1)_X$  charges. In general, one may assume that the  $U(1)_X$  charges of  $\widehat{X}_{1,2}$  are:  $Q(\widehat{X}_2) = -Q(\widehat{X}_1) = n$ , where  $n \geq 1$ . In this case, the leading operator form of the inflaton-waterfall superpotential reads:

$$W_{\text{IW}} = \kappa \widehat{S} \left( \widehat{X}_1 \widehat{X}_2 - M^2 \right) + \xi m_{\text{Pl}} \widehat{X}_1 \widehat{X}_2 + \xi_n \frac{(\widehat{X}_1)^2 (\widehat{X}_1)^{n+1}}{2m_{\text{Pl}}^n} + \xi_n' \frac{(\widehat{X}_2)^2 (\widehat{X}_2)^{n+1}}{2m_{\text{Pl}}^n}. \quad (\text{A.9})$$

Employing the short-cut method outlined above, it is straightforward to compute the loop-induced  $D$ -term, which is given by

$$m_{\text{FI}}^2 \approx \frac{\xi_n^2 - \xi_n'^2}{8\pi^2} \frac{M^{2(n+1)}}{m_{\text{Pl}}^{2n}} \ln \left( \frac{m_{\text{Pl}}}{M} \right). \quad (\text{A.10})$$

To obtain a small ratio  $m_{\text{FI}}/M \sim 10^{-6}$  with  $\xi_n, \xi_n' \sim 1$ , one would simply need  $n = 5, 6$ . Finally, we should remark that the loop-induced  $D$ -term does not lead to spontaneous breakdown of global supersymmetry.

## A.2 $D$ -Parity Breaking in the $SU(2)_X$ Waterfall-Gauge Sector

Here we outline two possible mechanisms for explicitly breaking the  $D$ -parities,  $D_1$  and  $D_2$  defined in (4.20) and (4.21), which govern the minimal inflaton-waterfall sector based on

an  $SU(2)_X$  gauge group.

The first mechanism utilizes a non-minimal Kähler waterfall-gauge sector, where the two  $D$ -parities are broken by non-renormalizable operators. To be specific, a minimal  $D_{1,2}$ -parity violating Kähler potential of the waterfall-gauge sector may be cast into the form:

$$\begin{aligned}
K_{\text{WF}} = \int d^4\theta \left( \widehat{X}_1^\dagger e^{2g\widehat{V}_X} \widehat{X}_1 + \widehat{X}_2^T e^{-2g\widehat{V}_X} \widehat{X}_2^* + \kappa_1 \frac{(\widehat{X}_1^\dagger e^{2g\widehat{V}_X} \widehat{X}_1)^2}{2m_{\text{Pl}}^2} \right. \\
+ \kappa_2 \frac{(\widehat{X}_2^T e^{-2g\widehat{V}_X} \widehat{X}_2^*)^2}{2m_{\text{Pl}}^2} + \frac{\kappa'_1 (\widehat{X}_1^\dagger e^{2g\widehat{V}_X} i\tau^2 \widehat{X}_2)(\widehat{X}_1^\dagger e^{2g\widehat{V}_X} \widehat{X}_1) + \text{H.c.}}{2m_{\text{Pl}}^2} \\
\left. + \frac{\kappa'_2 (\widehat{X}_1^\dagger e^{2g\widehat{V}_X} i\tau^2 \widehat{X}_2)(\widehat{X}_2^T e^{-2g\widehat{V}_X} \widehat{X}_2^*) + \text{H.c.}}{2m_{\text{Pl}}^2} + \dots \right), \quad (\text{A.11})
\end{aligned}$$

where the ellipses denote possible higher-order non-renormalizable operators. The couplings  $\kappa_{1,2}$  are real, whereas  $\kappa'_{1,2}$  can in general be complex. Moreover, the difference  $\kappa_- = \kappa_1 - \kappa_2$  signifies  $D_1$ -parity violation, whilst  $\kappa'_- = \kappa'_1 - \kappa'_2$  is a parameter of  $D_2$ -parity violation. Hence, non-zero values of the parameters  $\kappa_-$  and  $\kappa'_-$  will give rise to  $D_1$ - and  $D_2$ -parity violation in the waterfall-gauge Kähler potential  $K_{\text{WF}}$ . Notice that, as far as  $D_1$ -parity violation is concerned, the present mechanism applies to the Abelian case as well.

There are several sources of  $D$ -parity violation contained in  $K_{\text{WF}}$ . More explicitly,  $D$ -parity violation will first originate from the terms linear in  $D^a$ , where  $D^a$  are the auxiliary  $SU(2)_X$  components of the gauge-vector superfield  $\widehat{V}_X$ . In fact, these are the lowest dimensional  $D_{1,2}$ -odd operators that emerge after the SSB of the  $SU(2)_X$  and are given by the effective Lagrangian

$$\mathcal{L}_{\text{eff}}^{D^a-\text{tad}} = \frac{g}{2} \frac{M^4}{m_{\text{Pl}}^2} \left( \text{Re}\kappa'_- D^1 - \text{Im}\kappa'_- D^2 + \kappa_- D^3 \right). \quad (\text{A.12})$$

These effective FI  $D$ -terms can be included in the Lagrangian by adding the constants  $\frac{g}{2} (m_{\text{FI}}^a)^2$  to the on-shell constrained  $D^a$  terms, according to the scheme:  $D^a \rightarrow D^a + \frac{g}{2} (m_{\text{FI}}^a)^2$ , where

$$(m_{\text{FI}}^1)^2 = \frac{M^4}{m_{\text{Pl}}^2} \text{Re}\kappa'_-, \quad (m_{\text{FI}}^2)^2 = -\frac{M^4}{m_{\text{Pl}}^2} \text{Im}\kappa'_-, \quad (m_{\text{FI}}^3)^2 = \frac{M^4}{m_{\text{Pl}}^2} \kappa_-. \quad (\text{A.13})$$

One may obtain a fair estimate of the  $g$ -sector particle decay rates, using the formula (4.18) and identifying  $m_{\text{FI}}$  with  $m_{\text{FI}}^a$ . In this way, we obtain

$$\Gamma[-R_-, {}^-I_+, {}^+R_-] \sim [\kappa_-^2, \text{Re}^2(\kappa'_-), \text{Im}^2(\kappa'_-)] \frac{g^3}{128\pi} \frac{M^5}{m_{\text{Pl}}^4}. \quad (\text{A.14})$$

In addition to the effective  $D$ -tadpoles, higher-dimensional operators will also break the  $D$ -parities and so render the  $g$ -sector particles unstable. For example, after expanding



the superfields  $\widehat{X}_{1,2}$  about their VEVs in the Kähler potential (A.11), we find the non-renormalizable  $D$ -parity violating interactions described by the Lagrangian

$$\mathcal{L}_{\text{non-ren}} = -\frac{M}{2m_{\text{Pl}}^2}\kappa_-^+ R_- |\partial_\mu^+ X_+|^2 + \frac{M}{4\sqrt{2}m_{\text{Pl}}^2} \left( \kappa_-'^- X_- + \text{H.c.} \right) |\partial_\mu^+ X_+|^2. \quad (\text{A.15})$$

With the aid of (A.15), an order of magnitude estimate of the  $g$ -sector particle decay rates gives:  $\Gamma_g \sim (\kappa_-^2, |\kappa_-'|^2) g^3 M^5 / m_{\text{Pl}}^4$ . These are of comparable order to the ones obtained earlier in (A.14). For a typical inflationary scale,  $M = 10^{16}$  GeV (with  $g \sim 1$ ), we find the decay width  $\Gamma_g \sim (\kappa_-^2, |\kappa_-'|^2) 10^7$  GeV. The latter should be compared with the bounds:  $3.8 \times 10^{-13}$  GeV  $\lesssim \Gamma_g \lesssim 4.3$  GeV, corresponding to an upper and lower limit on the second reheat temperature  $T_g$  of cosmological interest:  $0.3$  TeV  $\lesssim T_g \lesssim 10^9$  GeV. Consequently, values ranging from  $10^{-9}$  to  $10^{-2}$  for the couplings  $\kappa_-$  and/or  $\kappa_-'$  are required for successful coupled reheating. The lower end values of order  $10^{-9}$  may possibly be seen as a strong tuning of the parameters. One way to explain the smallness of these parameters is to contemplate Kähler manifolds that break the  $D$ -parities by even higher-order non-renormalizable operators, e.g. of order  $\sim 1/m_{\text{Pl}}^4$ . In this case, the couplings  $\kappa_-$  and  $\kappa_-'$  will be multiplied by extra factors of  $M^2/m_{\text{Pl}}^2 \sim 10^{-4}$ , so these couplings can have values of order 1 and still predict a second reheat temperature  $T_g \sim 0.3$  TeV.

We now describe a second mechanism of  $D$ -parity violation which might be useful to obtain small  $D$ -parity violating interactions. Let us therefore assume that the Kähler potential respects the  $D$ -parities. In this case, we may invoke a mechanism very analogous to the Abelian case. We extend the field content of the inflaton-waterfall sector by adding a pair of Planck-mass chiral superfields  $\widehat{X}_1$  and  $\widehat{X}_2$ , which belong to the anti-fundamental and fundamental representations of  $\text{SU}(2)_X$ , respectively. As in the  $\text{U}(1)_X$  case, the superheavy superfields  $\widehat{X}_{1,2}$  are charged under the continuous  $R$ -symmetry given in (A.2). With this restriction, the leading operator form of the inflaton-waterfall superpotential is given by

$$\begin{aligned} W_{\text{IW}} = & \kappa \widehat{S} \left( \widehat{X}_1^T \widehat{X}_2 - M^2 \right) + \xi m_{\text{Pl}} \widehat{X}_1^T \widehat{X}_2 + \theta_1 \frac{(\widehat{X}_1^T \widehat{X}_1)(\widehat{X}_2^T \widehat{X}_2)}{m_{\text{Pl}}} \\ & + \theta_2 \frac{(\widehat{X}_1^T i\tau^2 \widehat{X}_2)(\widehat{X}_2^T i\tau^2 \widehat{X}_1)}{m_{\text{Pl}}} + \zeta_1 \frac{(\widehat{X}_1^T i\tau^2 \widehat{X}_2)(\widehat{X}_2^T \widehat{X}_1)}{m_{\text{Pl}}} \\ & + \zeta_2 \frac{(\widehat{X}_1^T \widehat{X}_1)(\widehat{X}_2^T i\tau^2 \widehat{X}_1)}{m_{\text{Pl}}} + \dots, \end{aligned} \quad (\text{A.16})$$

where the dots stand for additional operators that turn out to be irrelevant for the generation of effective  $D^a$ -tadpoles, and especially for those related to the  $D^1$ - and  $D^2$ -terms. The presence of these operators is only important to lift an accidental global  $\text{U}(1)_{\overline{X}}$  symmetry that governs this restricted part of the superpotential  $W_{\text{IW}}$  under consideration. Here,

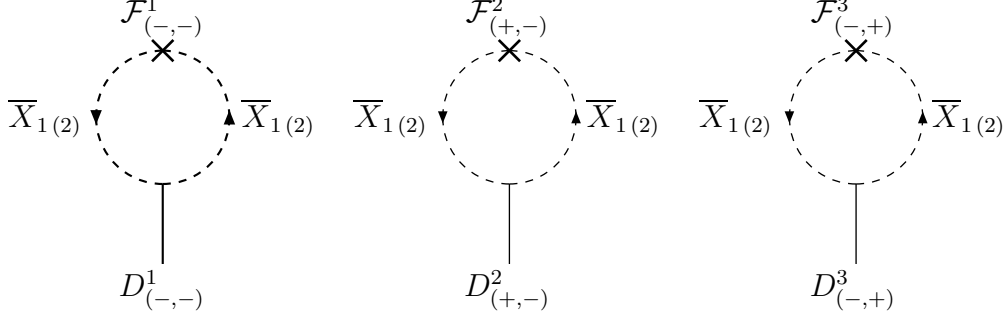


FIGURE 13: *Diagrams responsible for the generation of effective  $D^{1,2,3}$ -tadpoles for the  $SU(2)_X$  case, in the single insertion approximation of the  $D$ -odd operators  $\mathcal{F}^{1,2,3}$ . The subscripts in parentheses label the  $(D_1, D_2)$  parities of the respective operator.*

all non-renormalizable couplings  $\theta_{1,2}$  and  $\zeta_{1,2}$  can in general be complex. Extending the notion of  $D_{1,2}$  parities to the Planck-mass superfields  $\widehat{\overline{X}}_{1,2}$ , we observe that the operators related to the couplings  $\kappa$ ,  $\xi$  and  $\theta_{1,2}$  are even under  $D_1$  and  $D_2$ , whereas those related to the couplings  $\zeta_{1,2}$  are  $D_2$ -odd. Moreover, the superpotential operators proportional to the couplings  $\zeta_{+(-)} = \zeta_1 + (-)\zeta_2$  are  $D_1$ -even ( $D_1$ -odd).

To calculate the effective  $D^{1,2,3}$ -tadpoles after the SSB of the  $SU(2)_X$  gauge group, we use the short-cut approach described above in Section A.1. Thus, the  $F$ -terms of  $\widehat{\overline{X}}_{1,2}$  give rise to the following  $D$ -odd contributions to the scalar potential:

$$\begin{aligned} \mathcal{F}_{(-,-)}^1 &= \theta_1^* \zeta_- \frac{M^2}{2m_{\text{Pl}}^2} \left[ \left( \overline{X}_1^\dagger \langle X_1^* \rangle \right) \left( \overline{X}_1^T i\tau^2 \langle X_2 \rangle \right) - (1 \leftrightarrow 2) \right] \\ &\quad - \theta_2^* \zeta_- \frac{M^2}{2m_{\text{Pl}}^2} \left[ \left( \overline{X}_1^\dagger i\tau^2 \langle X_2^* \rangle \right) \left( \overline{X}_1^T \langle X_1 \rangle \right) - (1 \leftrightarrow 2) \right] + \text{H.c.}, \quad (\text{A.17}) \end{aligned}$$

$$\begin{aligned} \mathcal{F}_{(+,-)}^2 &= \theta_1^* \zeta_+ \frac{M^2}{2m_{\text{Pl}}^2} \left[ \left( \overline{X}_1^\dagger \langle X_1^* \rangle \right) \left( \overline{X}_1^T i\tau^2 \langle X_2 \rangle \right) + (1 \leftrightarrow 2) \right] \\ &\quad + \theta_2^* \zeta_+ \frac{M^2}{2m_{\text{Pl}}^2} \left[ \left( \overline{X}_1^\dagger i\tau^2 \langle X_2^* \rangle \right) \left( \overline{X}_1^T \langle X_1 \rangle \right) + (1 \leftrightarrow 2) \right] + \text{H.c.}, \quad (\text{A.18}) \end{aligned}$$

$$\begin{aligned} \mathcal{F}_{(-,+)}^3 &= -\text{Re}(\zeta_+ \zeta_-^*) \frac{M^2}{2m_{\text{Pl}}^2} \left[ \left( \overline{X}_1^\dagger i\tau^2 \langle X_2^* \rangle \right) \left( \langle X_2^T \rangle i\tau^2 \overline{X}_1 \right) + \left( \overline{X}_1^\dagger \langle X_1^* \rangle \right) \left( \langle X_1^T \rangle \overline{X}_1 \right) \right. \\ &\quad \left. - (1 \leftrightarrow 2) \right], \quad (\text{A.19}) \end{aligned}$$

where the subscripts in parentheses indicate the  $(D_1, D_2)$  parities of the above operators. Note that possible  $D$ -odd operators proportional to  $\xi\theta_{1,2}$  and  $\xi\zeta_\pm$  have not been displayed, since they do not contribute to the generation of effective  $D^a$ -tadpoles. To be specific, the effective  $D$ -tadpoles are induced radiatively via the graphs shown in Fig. 13, once the

operators  $\mathcal{F}^{1,2,3}$  are individually contracted with the  $D$ -term operator  $\mathcal{D}_{\overline{X}}^{1,2,3}$  related to the  $\overline{X}_{1,2}$  fields:

$$\mathcal{D}_{\overline{X}}^a = -\frac{g}{2} \left( \overline{X}_1^T \tau^a \overline{X}_1^* - \overline{X}_2^\dagger \tau^a \overline{X}_2 \right). \quad (\text{A.20})$$

These loop-induced effective FI  $D$ -terms can be included in the effective Lagrangian by shifting the on-shell constrained  $D^a$  terms by constants, according to the above described scheme:  $D^a \rightarrow D^a + \frac{g}{2}(m_{\text{FI}}^a)^2$ . In this scheme, the mass parameters  $(m_{\text{FI}}^a)^2$  are found to be

$$\begin{aligned} (m_{\text{FI}}^1)^2 &= -\frac{\text{Re}(\theta_-^* \zeta_-)}{4\pi^2} \frac{M^4}{m_{\text{Pl}}^2} \ln\left(\frac{m_{\text{Pl}}}{M}\right), \\ (m_{\text{FI}}^2)^2 &= \frac{\text{Im}(\theta_-^* \zeta_+)}{4\pi^2} \frac{M^4}{m_{\text{Pl}}^2} \ln\left(\frac{m_{\text{Pl}}}{M}\right), \\ (m_{\text{FI}}^3)^2 &= -\frac{\text{Re}(\zeta_+ \zeta_-^*)}{4\pi^2} \frac{M^4}{m_{\text{Pl}}^2} \ln\left(\frac{m_{\text{Pl}}}{M}\right), \end{aligned} \quad (\text{A.21})$$

where  $\theta_\pm = \theta_1 \pm \theta_2$ . It can be estimated from (A.21) that for values  $\theta_\pm, \zeta_\pm \sim 10^{-4}$ , one gets  $m_{\text{FI}}^{1,2,3}/M \lesssim 10^{-6}$ , leading to a low second reheat temperature  $T_g$ , below 1 TeV. In this context, one should notice that the size of the effective  $D$ -tadpoles is very sensitive to the cut-off scale, which we have chosen here to be the reduced Planck mass  $m_{\text{Pl}}$ . For instance, if a cut-off larger by one order of magnitude were adopted, then values of order  $10^{-2}$  for the non-renormalizable superpotential couplings would be sufficient to generate the effective  $D^a$ -tadpoles at the required size.

The violation of  $D$ -parities will also affect the particle spectrum of the  $\text{SU}(2)_X$  inflaton-waterfall sector. This will depend on the particular choice of the non-renormalizable part of the superpotential and Kähler potential. Our intention is not to pursue this issue any further here, by putting forward a specific non-minimal SUGRA scenario. Instead, our goal has been to explicitly demonstrate the existence of at least two mechanisms, which utilize the non-renormalizable part of the Kähler potential or superpotential to break the  $D$ -parities at the required order of magnitude.

## References

- [1] G.F. Smoot *et al.*, *Astrophys. J.* **396** (1992) L1.
- [2] D.N. Spergel *et al.*, *Astrophys. J. Suppl.* **148** (2003) 175.
- [3] M. Tegmark *et al.*, *Phys. Rev. D* **69** (2004) 103501.
- [4] D.N. Spergel *et al.*, astro-ph/0603449.
- [5] For a recent global analysis that includes the Ly- $\alpha$  forest power spectrum, see, U. Seljak, A. Slosar and P. McDonald, astro-ph/0604335.
- [6] For reviews, see,  
D. H. Lyth and A. Riotto, *Phys. Rept.* **314** (1999) 1;  
B.A. Bassett, S. Tsujikawa and D. Wands, astro-ph/0507632.
- [7] A. D. Linde, *Phys. Lett. B* **259** (1991) 38.
- [8] E. J. Copeland, A. R. Liddle, D. H. Lyth, E. D. Stewart and D. Wands, *Phys. Rev. D* **49** (1994) 6410.
- [9] G. R. Dvali, Q. Shafi and R. K. Schaefer, *Phys. Rev. Lett.* **73** (1994) 1886.
- [10] E. Halyo, *Phys. Lett. B* **387** (1996) 43; *Phys. Lett. B* **454** (1999) 223;  
P. Binétruy and G. Dvali, *Phys. Lett. B* **388** (1996) 241.
- [11] P. Fayet and J. Iliopoulos, *Phys. Lett. B* **51** (1974) 461.
- [12] V.N. Senoguz and Q. Shafi, *Phys. Rev. D* **71** (2005) 043514.
- [13] B. Garbrecht and A. Pilaftsis, *Phys. Lett. B* **636** (2006) 154 [hep-ph/0601080].
- [14] For a related observation in other variants of hybrid inflation, see,  
G. R. Dvali, G. Lazarides and Q. Shafi, *Phys. Lett. B* **424** (1998) 259;  
S. F. King and Q. Shafi, *Phys. Lett. B* **422** (1998) 135.
- [15] For alternative suggestions based on non-renormalizable operators that involve higher powers of  $\phi$ , see,  
F. Borzumati and Y. Nomura, *Phys. Rev. D* **64** (2001) 053005;  
N. Arkani-Hamed, L. J. Hall, H. Murayama, D. R. Smith and N. Weiner, *Phys. Rev. D* **64** (2001) 115011;  
S. Dar, S. Huber, V.N. Senoguz and Q. Shafi, *Phys. Rev. D* **69** (2004) 077701.

- [16] A. Pilaftsis and T.E.J. Underwood, Phys. Rev. D **72** (2005) 113001.
- [17] M. Fukugita and T. Yanagida, Phys. Lett. B **174** (1986) 45.
- [18] S. Davidson and A. Ibarra, Phys. Lett. B **535** (2002) 25;  
W. Buchmuller, P. Di Bari and M. Plumacher, Nucl. Phys. B **643** (2002) 367;  
G. C. Branco, R. Gonzalez Felipe, F. R. Joaquim, I. Masina, M. N. Rebelo and  
C. A. Savoy, Phys. Rev. D **67** (2003) 073035;  
G. F. Giudice, A. Notari, M. Raidal, A. Riotto and A. Strumia, Nucl. Phys. B **685**  
(2004) 89.
- [19] A. Pilaftsis, Phys. Rev. D **56** (1997) 5431;  
A. Pilaftsis and T.E.J. Underwood, Nucl. Phys. B **692** (2004) 303;  
T. Hambye, J. March-Russell and S. M. West, JHEP **0407** (2004) 070;  
E. J. Chun, Phys. Rev. D **72** (2005) 095010.
- [20] A. Pilaftsis, Phys. Rev. Lett. **95** (2005) 081602.
- [21] H. B. Nielsen and P. Olesen, Nucl. Phys. B **61** (1973) 45.
- [22] A Vilenkin and E. P. S. Shellard, "Cosmological Strings and Other Defects," Cambridge University Press, Cambridge UK (1994).
- [23] For a pedagogical review, see,  
M.B. Hindmarsh and T.W.B. Kibble, Rept. Prog. Phys. **58** (1995) 477.
- [24] L. Pogosian and T. Vachaspati, Phys. Rev. D **60** (1999) 083504;  
L. Pogosian, I. Wasserman and M. Wyman, arXiv:astro-ph/0604141.
- [25] R. Jeannerot, S. Khalil, G. Lazarides and Q. Shafi, JHEP **10** (2000) 012.
- [26] A. D. Linde and A. Riotto, Phys. Rev. D **56** (1997) 1841.
- [27] C. Panagiotakopoulos, Phys. Rev. D **55** (1997) 7335; Phys. Rev. D **71** (2005) 063516.
- [28] B. Garbrecht, hep-th/0604166.
- [29] R. Jeannerot and M. Postma, JHEP **0505** (2005) 071.
- [30] T. Gherghetta, C. F. Kolda and S. P. Martin, Nucl. Phys. B **468** (1996) 37
- [31] I. Affleck and M. Dine, Nucl. Phys. B **249** (1985) 361.
- [32] M. Dine and A. Kusenko, Rev. Mod. Phys. **76** (2004) 1.

- [33] R. Allahverdi and A. Mazumdar, hep-ph/0505050; hep-ph/0603244.
- [34] M. Dine, L. Randall and S. D. Thomas, Nucl. Phys. B **458** (1996) 291.
- [35] D. M. Capper, D. R. T. Jones and P. van Nieuwenhuizen, Nucl. Phys. B **167** (1980) 479.
- [36] B. Kyae and Q. Shafi, Phys. Rev. D **72** (2005) 063515;  
B. Garbrecht, T. Prokopec and M. G. Schmidt, Nucl. Phys. B **736** (2006) 133.
- [37] M. Cvetič and P. Langacker, Phys. Rev. D **54** (1996) 3570.
- [38] R. Slansky, Phys. Rept. **79** (1981) 1.
- [39] For related suggestions in 4- and 5-dimensional theories, see,  
Q. Shafi and Z. Tavartkiladze, Phys. Lett. B **459** (1999) 563; Phys. Lett. B **487** (2000) 145;  
G. Altarelli and F. Feruglio, Phys. Lett. B **511** (2001) 257;  
A. B. Kobakhidze, Phys. Lett. B **514** (2001) 131.
- [40] S. Forste, H. P. Nilles, P. K. S. Vaudrevange and A. Wingerter, Phys. Rev. D **70** (2004) 106008.
- [41] B. Allen, R.R. Caldwell, E.P.S. Shellard, A. Stebbins and S. Veeraraghavan, Phys. Rev. Lett. **77** (1996) 3061.
- [42] M. Landriau and E.P. S. Shellard, Phys. Rev. D **69** (2004) 023003.
- [43] D. Austin, E.J. Copeland and T.W.B Kibble, Phys. Rev. D **48** (1993) 5594.
- [44] J. Rocher and M. Sakellariadou, JCAP **0503** (2005) 004.
- [45] L. Boubekeur and D.H. Lyth, JCAP **0507** (2005) 010.
- [46] M. Bastero-Gil, S.F. King and Q. Shafi, hep-ph/0604198.
- [47] J. R. Ellis, D. V. Nanopoulos and S. Sarkar, Nucl. Phys. B **259** (1985) 175;  
J. R. Ellis, G. B. Gelmini, J. L. Lopez, D. V. Nanopoulos and S. Sarkar, Nucl. Phys. B **373** (1992) 399.
- [48] T. Prokopec and T. G. Roos, Phys. Rev. D **55** (1997) 3768;  
T. Prokopec, arXiv:hep-ph/9708428;  
G. N. Felder, J. Garcia-Bellido, P. B. Greene, L. Kofman, A. D. Linde and I. Tkachev, Phys. Rev. Lett. **87** (2001) 011601.

- [49] J. H. Traschen and R. H. Brandenberger, Phys. Rev. D **42** (1990) 2491;  
 L. Kofman, A. D. Linde and A. A. Starobinsky, Phys. Rev. D **56** (1997) 3258;  
 D. J. H. Chung, E. W. Kolb, A. Riotto and I. I. Tkachev, Phys. Rev. D **62** (2000) 043508;  
 M. Peloso and L. Sorbo, JHEP **0005** (2000) 016;  
 B. Garbrecht, T. Prokopec and M. G. Schmidt, Eur. Phys. J. C **38** (2004) 135;  
 J. Berges and J. Serreau, Phys. Rev. Lett. **91** (2003) 111601.
- [50] J. Garcia-Bellido and E. Ruiz Morales, Phys. Lett. B **536** (2002) 193.
- [51] M. Kawasaki, K. Kohri and T. Moroi, Phys. Lett. B **625** (2005) 7;  
 M. Kawasaki, K. Kohri and T. Moroi, Phys. Rev. D **71** (2005) 083502.
- [52] M. Bolz, A. Brandenburg and W. Buchmuller, Nucl. Phys. B **606** (2001) 518.
- [53] E.W. Kolb and M.S. Turner, *Redwood City, USA: Addison-Wesley (1990)*.
- [54] G.F. Giudice, E.W. Kolb, A. Riotto, Phys. Rev. D **64** (2001) 023508.
- [55] C. Pallis, Astropart. Phys. **21** (2004) 689; hep-ph/0510234.
- [56] R.H. Cyburt, J.R. Ellis, B.D. Fields and K.A. Olive, Phys. Rev. D **67** (2003) 103521;  
 J.R. Ellis, K.A. Olive and E. Vangioni, Phys. Lett. B **619** (2005) 30.
- [57] G. Lazarides and Q. Shafi, Phys. Lett. **B258** (1991) 305;  
 H. Murayama, H. Suzuki, T. Yanagida and J. Yokoyama, Phys. Rev. Lett. **70** (1993) 1912; Phys. Rev. **D50** (1994) 2356;  
 T. Asaka, K. Hamaguchi, M. Kawasaki and T. Yanagida, Phys. Lett. **B464** (1999) 12.
- [58] D.H. Lyth and E.D. Stewart, Phys. Rev. **D53** (1996) 1784.
- [59] R. Gonzalez Felipe, F. R. Joaquim and B. M. Nobre, Phys. Rev. D **70** (2004) 085009;  
 G. C. Branco, R. Gonzalez Felipe, F. R. Joaquim and B. M. Nobre, hep-ph/0507092.
- [60] For recent works on GUT flavour symmetries, see,  
 C. Hagedorn, M. Lindner and R. N. Mohapatra, hep-ph/0602244;  
 C. Hagedorn, M. Lindner and F. Plentinger, hep-ph/0604265.
- [61] R. Barbieri, P. Creminelli, A. Strumia and N. Tetradis, Nucl. Phys. B **575** (2000) 61;  
 E. Nardi, Y. Nir, J. Racker and E. Roulet, JHEP **0601** (2006) 068;  
 A. Abada, S. Davidson, F. X. Josse-Michaux, M. Losada and A. Riotto, JCAP **0604** (2006) 004;  
 E. Nardi, Y. Nir, E. Roulet and J. Racker, JHEP **0601** (2006) 164.

- [62] P. Di Bari, Nucl. Phys. B **727** (2005) 318;  
O. Vives, Phys. Rev. D **73** (2006) 073006.
- [63] A. Pilaftsis, Z. Phys. C **55** (1992) 275;  
A. Datta, M. Guchait and A. Pilaftsis, Phys. Rev. D **50** (1994) 3195;  
F. M. L. Almeida, Y. A. Coutinho, J. A. Martins Simoes and M. A. B. do Vale, Phys. Rev. D **62** (2000) 075004;  
T. Han and B. Zhang, hep-ph/0604064.
- [64] W. Buchmuller and C. Greub, Nucl. Phys. B **363** (1991) 345;  
G. Cvetič, C. S. Kim and C. W. Kim, Phys. Rev. Lett. **82** (1999) 4761;  
F. del Aguila, J. A. Aguilar-Saavedra, A. Martinez de la Ossa and D. Meloni, Phys. Lett. B **613** (2005) 170;  
F. del Aguila and J. A. Aguilar-Saavedra, JHEP **0505** (2005) 026.
- [65] S. Bray, J. S. Lee and A. Pilaftsis, Phys. Lett. B **628** (2005) 250.
- [66] T.P. Cheng and L.F. Li, Phys. Rev. Lett. **45** (1980) 1908.
- [67] A. Ilakovac and A. Pilaftsis, Nucl. Phys. B **437** (1995) 491.
- [68] G. Bhattacharya, P. Kalyniak and I. Mello, Phys. Rev. D **51** (1995) 3569;  
A. Ilakovac, B.A. Kniehl, and A. Pilaftsis, Phys. Rev. D **52** (1995) 3993;  
A. Ilakovac, Phys. Rev. D **54** (1996) 5653;  
M. Frank and H. Hamidian, Phys. Rev. D **54** (1996) 6790;  
P. Kalyniak and I. Mello, Phys. Rev. D **55** (1997) 1453;  
Z. Nagy-Palfy, A. Pilaftsis and K. Schilcher, Nucl. Phys. B **513** (1998) 517;  
S. Fajfer and A. Ilakovac, Phys. Rev. D **57** (1998) 4219;  
M. Raidal and A. Santamaria, Phys. Lett. B **421** (1998) 250;  
M. Czakon, M. Zralek and J. Gluza, Nucl. Phys. B **573** (2000) 57;  
A. Ioannisian and A. Pilaftsis, Phys. Rev. D **62** (2000) 066001;  
J. I. Illana and T. Riemann, Phys. Rev. D **63** (2001) 053004;  
G. Cvetič, C. Dib, C. S. Kim and J. D. Kim, Phys. Rev. D **66** (2002) 034008;  
hep-ph/0504126;  
A. Masiero, S. K. Vempati and O. Vives, New J. Phys. **6** (2004) 202.
- [69] For recent studies, see,  
T. Fujihara, S. K. Kang, C. S. Kim, D. Kimura and T. Morozumi, hep-ph/0512010;  
F. Deppisch, T. S. Kosmas and J. W. F. Valle, arXiv:hep-ph/0512360.



- [70] C. P. Burgess, S. Godfrey, H. Konig, D. London and I. Maksymyk, Phys. Rev. D **49** (1994) 6115;  
 E. Nardi, E. Roulet and D. Tommasini, Phys. Lett. B **327** (1994) 319;  
 D. Tommasini, G. Barenboim, J. Bernabeu and C. Jarlskog, Nucl. Phys. B **444** (1995) 451;  
 S. Bergmann and A. Kagan, Nucl. Phys. B **538** (1999) 368.
- [71] S. Gopalakrishna, A. de Gouvea and W. Porod, hep-ph/0602027.
- [72] J. McDonald, Phys. Rev. D **50** (1994) 3637.
- [73] C.P. Burgess, M. Pospelov and T. ter Veldhuis, Nucl. Phys. B **619** (2001) 709.
- [74] For recent studies within the context of the CP-violating MSSM, see,  
 M. E. Gomez, T. Ibrahim, P. Nath and S. Skadhauge, Phys. Rev. D **72** (2005) 095008;  
 G. Belanger, F. Boudjema, S. Kraml, A. Pukhov and A. Semenov, arXiv:hep-ph/0604150.
- [75] For recent analyses, see,  
 M. Carena, M. Quiros, M. Seco and C. E. M. Wagner, Nucl. Phys. B **650** (2003) 24;  
 T. Konstandin, T. Prokopec and M. G. Schmidt, Nucl. Phys. B **716** (2005) 373;  
 M. Carena, A. Megevand, M. Quiros and C. E. M. Wagner, Nucl. Phys. B **716** (2005) 319;  
 T. Konstandin, T. Prokopec, M. G. Schmidt and M. Seco, Nucl. Phys. B **738** (2006) 1.
- [76] D. Chang, W. Y. Keung and A. Pilaftsis, Phys. Rev. Lett. **82** (1999) 900;  
 A. Pilaftsis, Nucl. Phys. B **644** (2002) 263;  
 D. Chang, W. F. Chang and W. Y. Keung, Phys. Rev. D **66** (2002) 116008.
- [77] M. Carena, J. R. Ellis, A. Pilaftsis and C. E. M. Wagner, Phys. Lett. B **495** (2000) 155.
- [78] D. K. Ghosh, R. M. Godbole and D. P. Roy, Phys. Lett. B **628** (2005) 131;  
 D. K. Ghosh and S. Moretti, Eur. Phys. J. C **42** (2005) 341.